KfK 4549
März 1989

Coincidence and Pulsed Neutron Assay of Sealed α-Waste Drums

H. Würz, W. Eyrich, W. D. Klotz
Institut für Neutronenphysik und Reaktortechnik
Hauptabteilung Ingenieurtechnik
Projekt Wiederaufarbeitung und Abfallbehandlung

Kernforschungszentrum Karlsruhe

KERNFORSCHUNGSZENTRUM KARLSRUHE

Institut für Neutronenphysik und Reaktortechnik

Hauptabteilung Ingenieurtechnik

Projekt Wiederaufarbeitung und Abfallbehandlung

KfK 4549

PWA 15/89

Coincidence and pulsed neutron assay of sealed α-waste drums

H. Würz, W. Eyrich, W.D. Klotz

Kernforschungszentrum Karlsruhe GmbH, Karlsruhe

Kernforschungszentrum Karlsruhe GmbH
Postfach 3640, 7500 Karlsruhe 1

ISSN 0303-4003

Coincidence and pulsed neutron assay of sealed α-waste drums

H. Würz, W. Eyrich, W.D. Klotz

Abstract

The pulsed neutron and the neutron coincidence method have been applied to the assay of sealed 100 and 220 l α-waste drums. After completion of the measurements the Pu content of the drums became known.

The report describes the methods, the measurement systems, the correction procedures and the results obtained for sealed drums. Generally the results of the coincidence method are in better agreement with the actual values. However the Pu values are systematically overestimated. This demonstrates that the correction procedures have to be improved and that methods for matrix identification are of great importance.

For the pulsed neutron method the influence of sample self shielding was demonstrated. It turned out that the correction procedure for the influence of matrix composition as used for the data evaluation is inadequate for neutron absorbers. This becomes important if just instead of hydrogeneous matrix materials such as PE foam real waste materials with a high PVC content are used.

The measurements were done in the frame of a Round Robin Test Exercise on α-contaminated waste sponsored by the European Community (EC). The aim of the Exercise was a comparison of methods and equipment available in different laboratories in the EC for the nondestructive assay of α-waste drums. Laboratories from Cadarache, Dounray, Harwell, Ispra, Jülich, Rome and Karlsruhe participated in the Test Exercise.

The measurement program to be reported was done in close agreement with the EC and the other European laboratories involved in the test exercise. The Pu samples and the modular drums for the calibration program and the sealed α-waste drums were furnished by the EC.

Koinzidenz- und gepulste Neutronen-Messungen an versiegelten Fässern mit α-haltigen Abfällen

Zusammenfassung:

Die gepulste und die Koinzidenzmethode wurden zur Bestimmung des Spaltstoffgehaltes in versiegelten unbekannten 100 l und 220 l Fässern mit Laborabfall und Laborabfallsimulaten verwendet. Die tatsächlichen Plutoniumgehalte der Fässer wurden nach Vorliegen der Meßresultate bekanntgegeben.

Der vorliegende Bericht beschreibt die Meßmethoden, die Meßsysteme, die Datenauswertung und die erhaltenen Resultate. Generell sind die Resultate der Koinzidenzmessung in besserer Übereinstimmung mit den wahren Werten. Jedoch werden die Pu-gehalte systematisch überschätzt. Dies demonstriert die Bedeutung von Matrixeinflüssen und die Notwendigkeit einer Matrixidentifikation.

Für die gepulste Methode wird der Einfluß der Probenselbstabschirmung demonstriert. Außerdem wird gezeigt, daß das Matrixkorrekturverfahren in Gegenwart von auch schwachen Neutronenabsorbern unzureichend ist.

Die Messungen wurden im Rahmen eines von der Europäischen Gemeinschaft (EG) geförderten Round Robin Tests an α-haltigen Abfällen durchgeführt. Der Round Robin Test hatte das Ziel zerstörungsfreie Methoden und Geräte zur Spaltstoffbestimmung in Abfallgebinden EG-weit zu vergleichen. Am Test beteiligt waren Labors aus Cadarache, Harwell, Dounray, Ispra, Jülich, Rom und Karlsruhe.

Das Meßprogramm wurde in enger Übereinstimmung zwischen der EG und den beteiligten Laboratorien spezifiziert und durchgeführt. Die Pu-Proben und die modularen Fässer für das Kalibrierprogramm, sowie die versiegelten α-haltigen Abfallfässer wurden von der EG zur Verfügung gestellt.

1. Introduction

Sealed α-contaminated waste drums have been assayed using 3 different measuring techniques and systems. These have been high resolution γ-spectrocopy, pulsed neutron measurement and passive and coincidence n-counting. The results of the γ-spectrocopy measurements have been discussed elsewhere /1/ and therefore are not included explicitly in this report. However the results of the γ-spectroscopy are used to calculate the amount of total Plutonium from the measured quantities $^{240}Pu_{eq}$ and $^{239}Pu_{eq}$.

The purpose of the report is to give details on the methods and measurement systems used, to discuss error sources and correction procedures applied to the data evaluation and finally to compare the NDA results obtained with the true Pu values, which were given after completion of the evaluation.

2. Assay methods and systems

2.1 Pulsed neutron system

The principle of the method is shown in Fig.1 /2,3/. A pulsed neutron source produces 14 MeV neutrons using the d(tn) ^{4}He reaction. The source neutrons are slowed down and finally are thermalized in the moderator walls of the facility made from polyethylene and graphite (composite moderator). The thermalized neutrons are penetrating into the waste barrel and are producing fast neutrons by induced fission in the fissile material.

Fissile isotopes are ^{239}Pu, ^{241}Pu and ^{235}U. The equivalent mass of the fissile material being detected is given according to

$$m^{239}Pu_{eq} = m^{239}Pu + \frac{(\nu\sigma_f)^{241}}{(\nu\sigma_f)^{239}}\, m^{241}Pu + \frac{(\nu\sigma_f)^{235}}{(\nu\sigma_f)^{239}}\, m^{235}U \qquad (1)$$

with the weight factors for thermal neutron fission the equivalent mass of fissile material is

$$m\,^{239}Pu_{eq} = m\,^{239}Pu + 1{,}38\, m\,^{241}Pu + 0{,}68\, m\,^{235}U \qquad (2)$$

The induced fission neutrons are detected as epithermal neutrons using Cd shielded He-3 detectors. The epithermal detector countrate is given by three terms: direct source neutrons CR_{dir}, induced fission neutrons CR_{ind} (the signal countrate) and neutrons being emitted from the waste item itself CR_{ne}. The contribution of the direct source neutrons to the total countrate CR_{tot} can be made small by increasing the delay time between the source neutron pulse and the start of the measurement. That means waiting until almost complete thermalization of the source neutrons.

The signal countrate $CR_{ind}(t)$ is given according

$$CR_{ind}(t) = \varepsilon \int \sum_i \nu_i \Sigma_{f_i}^{th}(r)\, \Phi_{th}(\underline{r},t)\, T(|\underline{r}-\underline{r}'|)\, d\underline{r} \qquad (3)$$

with

ε detection sensitivity for epithermal fission neutrons

$\sum_i N_i \nu_i \sigma_{fi}(\underline{r})\, \Phi_{th}(\underline{r},t) = {}^{239}m_{eq}\,(\nu\sigma_f)^{239}\,\Phi_{th}(r,t)$ space and time dependen fission rate of the fissile isotopes i

$\Phi_{th}(\underline{r},t) = e^{-\alpha t}\,\Phi_{th}(\underline{r})$ thermal neutron flux distribution in the drum due to the thermalized source neutrons

$1/\alpha$ thermal neutron lifetime

$T(|\underline{r}-\underline{r}'|)$ leakage probability for fission neutrons

From eq.(3) it follows for a homogeneous distribution of the fissile material

$$\int CR_{ind}(t)\, dt = \varepsilon\, A\, {}^{239}m_{eq} \int \Phi_{th}(r)\, T(|\underline{r}-\underline{r}'|)\, d\underline{r} \qquad (4)$$
$$= B_1\, {}^{239}m_{eq}$$

with $^{239}m_{eq}$: equivalent mass of fissile material

$$B_1 = K \int \Phi_{th}(\underline{r})\, T\,(|\underline{r}-\underline{r}'|)\, d\underline{r} \qquad (5)$$

The matrix material in two ways influences the proportionality constant B1. Firstly the intensity and distribution of the fission inducing thermal neutron flux and secondly the fission neutron leakage both are influenced by the matrix material.

A theoretical evaluation of eq.(3) and (4) is rather difficult and further complicated due to the 3 dim. geometry. Therefore evaluation was done experimentally. The system was calibrated using different matrix materials and sample distributions. The matrix materials used are listed in Table 1.

During the measurement the drum rotates (see Fig.2). The neutron target and 4 thermal neutron flux monitors are located in the cavity. The cavity dimensions are 80 x 100 cm by height 140 cm. The thickness of the composite moderator is given in Fig.1. Both the moderator and the cavity size are not optimized for 220 l drums. The rather large cavity was chosen because of ease of drum handling.

Optimization studies were done for the layout of the composite moderator surrounding the cavity and for the epithermal neutron detector design /3/. The Monte Carlo code MCNP /4/ was used.

The layout of the composite moderator has to be done with respect to

high thermal neutron intensities in the cavity
long lifetime of thermalized source neutrons
short lifetime of epithermal source neutrons.

Results of the optimization studies are listed in Table 2. A thick graphite layer is the best choice due to the increase of thermal neutron intensity and lifetime in the cavity. This has to be combined with a cavity as small as possible.

As is also seen from Table 2 a thick graphite layer increases the epithermal neutron lifetime and thus is somehow conflicting with the requirement for a short lifetime of epithermal neutrons. This lifetime and the lifetime of neutrons thermalized in the epithermal detector are determining the delay time after the neutron pulse.

Summarizing the results of optimization studies:

Optimization only results in an overall gain of about a factor of 2 in comparison with the system used and therefore does not change the conclusions discussed.

A long-counter outside the setup is used for control of the neutron source intensity. The neutron source monitoring is estimated to be reproducible between ± 5%. The neutron generator has a duoplasmatron ion source /5/. Pulserate and pulslength are adjustable between 10-200 Hz and 5-40 µs. A mean source intensity of 1,5 10^8 n/s is attainable using a pulse cycle of 80 Hz and a pulse length of 20 µs. For measurement of epithermal induced fission neutrons 12 He-3 detectors are used. The overall sensitivity of these detectors is 3% for epithermal neutrons emitted in the cavity.

The electronics is shown schematically in Fig.3. An external pulse generator triggers the neutron source and via a delay generator the CAMAC multi channel scaling modules for measuring the time dependent countrate of the 12 He-3 detectors and the BF3 neutron flux monitors in the cavity. The delay generator also triggers two 32 fold integral counters for determination of total countrates. Control of the CAMAC modules and storage and analysis of the data is done with a CAMAC compatible Le Croy 3500 computer.

Fig.4 shows measured time dependences of the source neutrons in the cavity for different matrix materials in 220 l drums. Two decay modes are identified. The fast ($1/\alpha_1 = 75$ µs) is due to epithermal, the slow due to thermalized source neutrons. The matrix material in the cavity only weakly influences the decay time of the source neutrons, but strongly influences the neutron intensity. Fig.5 shows the time dependent countrate of the epithermal detectors (CR_{dir}) without any fissile material present in the cavity. The epithermal source neutrons are completely thermalized about 1,4 ms after neutron injection. The measurement is started 1 ms after the neutron burst.

Time dependent epithermal countrates $CR_{ind}(t)$ are shown in Fig.6 for a rather large Pu sample at different positions in drum no.4. Two different decay modes can be identified. The decay mode $1/\alpha_2 = 320$ µs is due to the lifetime of source neutrons thermalized in the drum, the decay mode with $1/\alpha_2 = 1605$ µs is due to the lifetime of source neutrons thermalized in the reflector walls surrounding the cavity. The small contribution of the decay mode $1/\alpha_2 = 320$ µs to the fission induced countrate CR_{ind} demonstrates that the source neutrons mainly are thermalized in the walls of the cavity.

2.2 Neutron well counter

The measurement system is shown schematically in Fig.7 /6/. It consists essentially of a 40 cm thick polyethylene (PE) annulus with top and bottom PE plates. In the annulus 2 rings of 36 counters are embedded. The inner ring is comprised of He-3, the outer ring of BF_3 detectors. Top and bottom are containing 7 counters each in only one layer. These counters are belonging to the inner counter layer. The system is installed underground and is additionally shielded by concrete in order to minimize the neutron background. The drums hydraulically are moved into the measuring position, the movable top plate is closed and the measurement is started.

Total neutron and coincidence counting is done. However, the counting of totals will be discussed only in connection with neutron radiography. Coincidence counting is done using the Böhnel shift register /7/. The principle is shown in Fig.8. The width of the N channels of the shift register are adjusted according to

$$N\delta t = \Delta t = 1/\alpha \qquad (6)$$

with $1/\alpha$ thermal neutron life time in the monitor.

The number of pulses in the shift register is detected using an up-down counter. For each ingoing pulse the number of pulses in the register is summed up in an external counter. Thus the countrate CR_{cc} assuming m pulses in $N\delta t$ is given according to

$$CR_{cc} = \binom{m}{2} = \frac{1}{2}\, m\, (m-1) \qquad (7)$$

The proper functioning of the shift register has been controlled using Pu samples of different composition and different masses. The mass dependent real coincidence countrate is shown in Fig.9. It is independent from the (αn) neutron background. The different Pu samples (C,D and E) are having different (α,n) neutron emission. Their isotopic composition is given in Table 3.

Coincidence counting detects neutron pairs from spontaneous fission of the even Pu isotopes 238, 240 and 242. The equivalent mass of ^{240}Pu ($m^{240}Pu_{eq}$) is given according to

$$m^{240}Pu_{eq} = m^{240}Pu + 2{,}66\, m^{238}Pu + 1{,}64\, m^{242}Pu \qquad (8)$$

The coincidence countrate CR_{cc} is given according to

$$CR_{cc} = {}^{240}q_{sp}\; m\; {}^{240}Pu_{eq} \left(\frac{\overline{\nu(\nu-1)}}{2\bar{\nu}} \right)^{240} (1-e^{-\alpha\Delta t})\; \varepsilon^2_{cc,o\,drum} \int \frac{q^2_{sp}(\underline{r})}{q^2_{sp}}\; T(|\underline{r}-\underline{r}'|)\, d\underline{r}$$

with

$\bar{\nu}$ number of neutrons per spontaneous fission

${}^{240}q_{sp}$ spontaneous fission neutron emission rate per unit mass of ^{240}Pu:

${}^{240}q_{sp} = 898$ n/sg

$$\left(\frac{\overline{\nu(\nu-1)}}{2\bar{\nu}} \right)^{240} = 0{,}869$$

$\varepsilon_{cc,o}$ detection sensitivity for spontaneous fission for neutrons with $T(|r-r'|) = 1$

$$\varepsilon^2_{cc,eff} = \varepsilon_{cc,o} \int \frac{q^2_{sp}(\underline{r})}{q_{sp}}\; T^2(|\underline{r}-\underline{r}'|)\, d\underline{r} \qquad (10)$$

effective detection sensitivity

$\frac{1}{2}\,\overline{\nu(\nu-1)}\,\varepsilon^2_{cc,eff}$ probability that for ν fission neutrons per spontaneous fission 2 are detected

$T(|\underline{r}-\underline{r}'|)$ leakage probability of fission neutrons

$1-e^{-\alpha\Delta t} = 0{,}5366$ with $1/\alpha = 125\ \mu s$ /6/

$$CR_{cc} = B_2\, m^{240}Pu_{eq} \qquad (11)$$

According to eq. (10) the effective detection sensitivity $\varepsilon_{cc,eff}$ and hence the constant B_2 is influenced by the matrix composition. The dependence was determined experimentally. The matrix matrials used are listed in Table 1. The leakage probability $T(|\underline{r}-\underline{r}'|)$ too has been determined experimentally using the same matrix materials. $T(|\underline{r}-\underline{r}'|)$ is plotted in Fig.10 for 220 l drums. $T(|\underline{r}-\underline{r}'|)$ is given as

$$T(|\underline{r}-\underline{r}'|) = A \exp\left[-\Sigma_R |r-r'|\right] \qquad (12)$$

The countrate values for the empty drum only in a limited range of distances shows an exponential dependence. The countrate values in this case are influenced by neutrons back scattered from the reflector walls of the well counter.

The relaxation length $1/\Sigma_R$ depends on the matrix material as is seen in Fig.11 for a hydrogeneous matrix and for concrete.

The drums are placed axially symmetrical inside the cavity. For the 220 l and the 100 l drums this means that the drums are not symmetrical with respect to the counters as is seen from Fig. 12. Due to this arrangement which couldn't be changed because of restrictions in the downward movement of the hydraulic piston the axial detection sensitivity will be asymmetrical showing higher sensitivity in the lower part of the drums.

Each detector is equipped with it's own electronics. The electronic arrangement schematically is shown in Fig.13. Standarized pulses from these are fed to a microprocessor equipped with a 100 channel counting register and after summing up are fed to 3 different shift registers for coincidence analysis of the inner, outer and total detectors for the two counter layers.

The system with its 86 counters is fully computer controlled /8/. Disturbances can be identified and disturbed measuring lines are switched off automatically, taking into account the change in detection sensitivity. Disturbances in most cases are occurring as high frequency events, being due to sputtering at the high voltage connectors of the BF_3 counters, caused by moisture. He-3 counters due to

their lower high voltage are operating more satisfactorily. High frequency events are mainly influencing the coincidence meausrement because those events are recognized as coincidences having high v values.

The proper functioning of the counter electronics is verified by computer controlled testpulses switched to the preamplifier inputs. Moreover tests of the proper functioning of the counters are possible by computer controlled setting of the lower discriminator levels of each measuring line.

These measures have proved to be valuable for the routine operation of the well counter. They allow detection and documentation of long term sensitivity changes of the individual counters.

The long term operation of the well counter is shown in Fig.14. The test, the calibration and the measurement phase lasted for 11 months. In this time intervall the inner counter layer worked quite satisfactorily without disturbances and failure. The background countrates total and coincidence are plotted in Fig.14. Disturbances more often are occurring in the outer counter layer. But finally after controlling the atmosphere surrounding the high voltage connectors the operation of the outer detector counter layer became stable too. The plot demonstrates that a routine operation of a well counter is possible.

The background countrates are: totals (280 $\pm$ 15) c/10 min, coincidences (4 $\pm$ 1) c/10 min. This results in a miniumum detectable quantitiy of 1 mg $^{240}Pu_{eq}$ in 220 l drums. For low active waste the system is capable of establishing the limit of 100 nCi/g as long as the ratio $^{240}Pu_{eq}/Pu_{tot}$ is above 13% /8/.

3. Calibration program

Both systems were calibrated using 220 l drums with different matrix materials, one 100 l drum and one 25 l drum with a PE matrix. For calibration, all drums from Table 1 are equipped with irradiation channels at 4 different radial positions as is shown in Fig.15. 4 different Pu samples were used. Their isotopic and chemical composition are given in Table 3. Calibration was done using quasi-homogeneous Pu sample distributions with totally 12 small samples distributed uniformly over the volume of the drum and positioned in the irradiation channels.

Numerous measurements with single samples in different matrix materials at different positions were done additionally to evaluate the influence of the matrix material and the sample distribution.

The results of the calibration measurements are listed in Table 4-9 for the coincidence and in Tables 10-13 for the pulsed neutron method. The sample positions are labelled NMx with N drum no, M Pu sample (C,D or E or Pellet P) and x sample position. The sample positions are given in Table 14. The homogeneous sample distributions are labelled NC1 and ND1 with N: drum no.

The results for the pulsed neutron method (Tables 10-13) given as background and global net countrates are normalized to an overall neutron source rate of 2,2 10^{11} n. For measuring time intervalls of 180 s this corresponds to a neutron source strength of 1,2 10^{9} n/s. The actual neutron source intensity was between 5 10^{7} and 5 10^{8} n/s.

The results for the coincidence measurements are plotted in Fig. 16-19 for the single sample measurements. The countrates are lower for sample positions in the upper part of the drums. This is due to the asymmetrical position of the drums with respect to the surrounding counters and due to the larger distance of the top reflector plate (see Fig.12). In Fig.20a and b finally a comparison of axial countrates (totals) is given with and without counters in the top and bottom reflector. These counters somewhat improve the flatness of the axial sensitivity profile.

Sample position dependent signal countrates for the pulsed neutron method are shown in Fig.21-23. The decreased sensitivity in the lower part of the drums is due to the rotation table made from stainless steel (neutron absorber) and due to the not symmetrical position of the neutron target relative to the drums as is indicated in Fig.23.

4. Pulsed neutron system

4.1 Parameters influencing the assay

4 parameters are influencing the Pu assay. These are Pu isotopic composition, fissile material distribution, sample mass and matrix material.

The influence of the isotopic composition is rather small if the Plutonium is coming from spent LWR fuel with burnup above 15 GWd/tHM as is seen from Fig.24.

From Fig.25 it is seen that CR_{ind} depends on the position of the Pu sample. Increase in hydrogen and / or neutron absorber content reduces the penetrability of the fission inducing thermalized neutrons. Thus the inner regions of the drums are increasingly shielded as is shown for concrete, water and water flooded rashig rings. The same effect was observed for dry rashig rings. That means, neutron absorbers in the matrix are also causing severe shielding effects.

From the calibration measurements with homogeneous Pu sample distribution the dependence of the signal countrate on matrix density was determined. This is shown in Fig.26. The matrix is PE foam. The data shown in the Fig. thus are reflecting the influence of hydrogen. No calibration was done for more typical waste materials such as PVC. These contain less hydrogen but neutron absorbers (chlorine acts as neutron absorber).

The results of the calibration for the homogeneously distributed samples are given in Table 15a. In Table 15b the signal countrate ratio obtained from the homogeneously distributed C- and D-samples is given. The ratio corresponds within the error limits to the $^{239}Pu_{eq}$ mass ratio of the samples. For drum no.3 the measured value is low. This could be due to inadequate source monitoring.

For a homogeneous distribution of Pu in 220 l drums, the reduction of the signal countrate has been determined. It is correlated in Fig.27 with the intensity normalized monitor countrate in the cavity. For a homogeneous Pu distribution, the influence of the matrix can be determined and eliminated according to Fig.27. For the 220 l drum no 11 (concrete) for example the signal countrate is reduced by a factor of 8 compared to the empty drum. The monitor countrate is due to monitor M1, M1 according to Fig.2 is located behind the drum. The source normalized monitor countrate is influenced by the global parameters of the drum, thus representing drum averaged thermal neutron flux values. Local changes of these parameters due to an inhomogeneous matrix distribution are not taken into account with this method.

A comparison of Fig.25 and 27 reveals that sample distribution and matrix material both are of great influence on the assay. From Fig.25 it follows that for hydrogeneous matrix materials (as long as $\rho_{H2O} < 0{,}3$ g/cm^3) without neutron absorbers the influence of the sample distribution is rather small. This changes

drastically if materials acting as neutron absorbers are present. Drum no.11 contains a smaller amount of water than for example drum no.1 but obviously contains neutron absorbers, what not only increases the countrate reduction factor but also increases the influence of sample distribution and thus finally increases drastically the measurement error.

Thermalized neutrons are inducing fission. Their intensity is influenced by neutron absorbers in the matrix. Fissile materials are neutron absorbers. Thus thermal neutrons can't penetrate into the sample. The effect of self-shielding is shown in Fig.28 for Pu samples of different density and different masses. Self-shielding leads to a systematic underestimation of the amount of fissile material if the sample mass is above 100 mgPu.

A correction for matrix effects according to Fig.27 doesn't take into account local effects due to sample self-shielding and local neutron absorbers and also doesn't take into account inhomogeneous sample distribution. Thus this matrix correction procedure only represents a first correction.

4.2 Results for sealed drums

The results for the sealed drums without any correction for sample distribution, matrix material and Pu sample self shielding are given in Table 16, together with the background countrate, net signal countrate and amount of $^{239}Pu_{eq}$. For the evaluation it has been assumed that the sample distribution is homogeneous and that the matrix of all 220 l drums is equivalent to that of drum no.1. The matrix of all 100 l drums is assumed to be equivalent so that of drum no.3.

For evaluation a linear relation between the signal countrate and the mass of fissile material is assumed according to eq. (4). For higher fissile masses this may be changed due to multiplication. However multiplication effects are believed to be unimportant in the few gram mass range.

As can be seen from Fig.27 the matrix composition influences the assay. In this Fig.27 also indicated are the measured source normalized monitor countrates for the actual waste drums 5S, 6S, 9R, 12R and 13R. From these it is concluded that the matrix of the sealed drums 5S and 6S is similar to that of modular drum no.1 in agreement with the data furnished by the producer of the drums no.5 and no.6. The drums are containing PE foam with densities 0,23 (no.5) and 0,263 g/cm3 (no.6). The modular drum no.1 has the density 0,29 g/cm^3 . The drums 12R and 13R yield rather low monitor countrates. According to Fig.27 this results in a

rather large countrate reduction factor for these two drums. This is not due to hydrogeneous materials present in the unknown matrix as is revealed for instance by comparison with water. Obviously it is due to neutron absorbers being present in the matrix.

The countrate reduction factors for the sealed 220 l drums have been determined. They are listed in Table 17a. For 100 l drums no experimental countrate reduction factors are available but source normalized monitor countrates were measured. From these it is concluded that the matrix of drums no. 7S and 8S is similar to that of drum no.3, whereas drums 10R and 14R are containing neutron absorbers clearly manifested by lower source normalized monitor countrates.

To obtain a rough estimation for the countrate reduction factors of the sealed 100 l drums 10R and 14R the data as given in Fig.27 for 220 l drums have been used. The countrate reduction values for 100 l drums are given in Table 17b together with estimated errors.

The final evaluation is done by correcting for the influence of matrix material according to Table 17. However this doesn't take into account effects due to local neutron absorbers. The final results again valid for a homogeneous sample distribution are given in Table 18 together with the error sources and where possible the error estimation.

Indications for sample distribution have been obtained from neutron autoradiography (see next chapter). The results though not unequivocal are indicating that homogeneous sample distribution to a first approximation can be assumed for data evaluation.

Again it has to be stressed that the influence of the error sources sample self shielding and local neutron absorbers cann't be estimated. From Fig.27 it is concluded that neutron absorbers are present in drums no.9R,12R and 13R. The errors in Table 18 are estimated under the assumption that the neutron absorbers are homogeneously distributed.

5. Well counter

5.1 Parameters influencing the assay

Three parameters are influencing the Pu assay. These are Pu isotopic composition, fissile material distribution and matrix material.

The influence of the isotopic composition if the Plutonium is coming from spent LWR fuel with burnup above 10 GWd/tHM is seen from Fig.29. The determination of the total Plutonium from the measured $^{240}Pu_{eq}$ requires further information as is seen from this Figure. Either the origin of the drum should be known or γ-spectroscopy has to be applied to determine the ratio $^{240}Pu_{eq}/Pu_{tot}$.

The numerous measurements with single samples in different matrix materials at different positions were used to evaluate the influence of the matrix and the sample distribution. From Fig.30 it is seen to what extent the coincidence countrate of the inner counter layer CR_{CC} is depending on the position of the Pu sample. The neutron leakage from the drum mainly is influenced by the hydrogen content of the matrix and decreases with increasing hydrogen content. In Fig.30 the additionally used matrix materials empty, concrete with high water content and water are included also. In Fig.30 there is also given the influence of the sample distribution for the 100 l drum no.3.Assuming a homogeneous distribution the error due to an inhomogeneous distribution amounts up to about 20%. Reducing the PE density means also a reduction of the influence of the sample distribution.

In Fig.31 the dependence of the coincidence countrate of the inner and outer counter layer is given as function of the matrix density for hydrogeneous materials (PE-foam) for homogeneous Pu sample distributions.

The results for the inner counter layer are listed in Table 19a. Calibration was also done for 3 modular drums using other Pu samples with 147,4 mg $240Pu_{eq}$. In Table 19b the coincidence countrate ratio as obtained from the two different but homogeneously distributed samples is given. This ratio differs from the $240Pu_{eq}$ mass ratio of the samples. For drums no.1 and no.3 the measured values are higher than the actual mass ratio also if the uncertainties (mainly due to the statistical error) are taken into account. The reason for the systematic

overstimation is unknown but because of the small amount of Pu present in the drums the overestimation is not due to multiplication effects.

The inner counter layer is undermoderated. As a consequence, the coincidence countrate only for densities above 0,1 g/cm3 shows an exponential decrease, whereas for the outer counter layer the countrate is highest for the empty drum. The dependence of the coincidence countrate in the density range $0,1 < \rho < 0,3$ g/cm3 is identical for both counter layers.

It is not yet clear whether there is a small maximum in the density range $\rho < 0,1$g g/cm3. But anyhow the influence of the matrix density remains small in this density region and in practical cases can be neglected.

In Fig.31 are included the sealed drums 5S-8S containing PE foam. As became known after evaluation, the Pu samples are distributed quasihomogeneously. For plotting the data, the declared Pu values were used. The results of drums 5S-8S support the conclusion of an exponential dependence of the coincidence countrate from the matrix density.

5.2 Sensitivity

From the results of the calibration measurements detection sensitivities $\varepsilon_{cc,eff}$ (eq(10)) were obtained. They are given in Table 20 for the two counter layers inner and outer. For Pu samples in the centre of the drum $\varepsilon_{cc,eff}$ is 13,1% for an empty drum and decreases to 5% for drum no.11. The reduced sensitivity of the outer counter layer is due to a moderating PE layer of thickness of 9 cm in front of these detectors.

5.3 Correction procedures

The well counter is equipped with 2 measures which in principle allow to correct for the influence of matrix and sample distribution. These are 1) detection of totals for each individual counter and 2) two counter layers with different spectral sensitivity. The first measure gives rise to neutron autoradiography of the drums to be assayed and thus in principle allows to control the sample distribution. The countrate ratio inner to outer in principle is a function of the neutron energy and thus is influenced by the matrix composition (mainly the matrix hydrogen content). However the spectral sensitivity of the countrate ratio

turned out to be rather weak and thus is not usable in practical cases, as can be seen from Fig.31. The coincidence countrate ratio inner to outer (although not of practical importance due to excessively long measuring times) only shows a clear dependance on the matrix as long as $\rho_{H_2O} < 0{,}15$ g/cm^3. However in this range it is so weak that accuracies better $\pm$ 5% in the measured countrate ratio are necessary what requires measuring times of at least 4000 s.

From the single sample measurements with sample position close to the surface of the drum a correlation between the coincidence countrate reduction factor and the totals countrate has been found which allows to correct for the global influence of the matrix again in case of homogeneous sample distribution. This add a gramm technique is shown in Fig.32. The values are preliminary due to the small number of matrix materials investigated so far. Fig.32 demonstrates that the well known add a gramm technique /10/ in principle could be able to correct for matrix effects. Unfortunately this simple correction procedure was not used because at the time of the measurements the coincidence countrate ratio measurement was believed to allow for the matrix correction. However the data base for the add a gram technique still is rather poor. More data are needed especially for real waste materials. Therefore the accuracy achievable with this method presently is not known.

The neutron autoradiography to some extend gives information on the sample distribuiton in the drum. However this technique not in any case yields unique results. Sample positions in the outer part of the drum are clearly screened against a homogeneous distribution but no screening is possible between homogeneous distribution and samples at or near the centre of the drum.

5.4 Results

The results for the sealed drums without any correction for matrix material and sample distribution are given in Table 21. For the evaluation it has been assumed that the sample distribution is homogeneous and the matrix of the 220 l drums is equivalent to that of modular drum no.1. The matrix of all 100 l drums is assumed to be equivalent to that of drum no.3. From the coincidence countrate ratio there are some hints that the matrix of drum 9R more resembles that of drum no.2.

From the neutron radiography of the sealed 220 l drums it only was possible to draw the following rather unspecific conclusions:

1) homogeneous sample distribution or sample in the inner drum region in drums 5S, 12R

2) inhomogeneous sample distribution for drums 6S, 9R, 13R .

From radiography of the 100 l drums the following conclusions are drawn:

inhomogeneous sample distribution for the drums 7S, 8S, 10R and 14R

Due to lack of further knowledge it is assumed for the 220 l drums with inhomogeneous sample distribution that the fissile material is homogeneous and not concentrated in the inner drum region.

For the 100 l drums with apparently inhomogeneous sample distribution it is concluded from the neutron autoradiography that the fissile material is concentrated in the drum region R≈10 cm. This sample region approximately is equivalent to a homogeneous sample distribution.

Due to the rather large uncertainties in the coincidence countrate ratio (up to ±30%) and the weak dependence of that ratio on the matrix composition (see Fig.31) the matrix identification for the drums 12R, and 13R is rather questionable. Therefore a mean value of drums no.1 and no.2 has been used. Only in case of drum 9R the coincidence countrate ratio gave some hints that the matrix is equivalent to that of drum no.2.

Final results of the coincidence measurements for sealed drums are given in Table 22. The errors due to matrix and sample distribution are rather large. This is due to the fact that neither the matrix composition nor the sample distribution of drums 12R, and 13R could be determined uniquely.

For the 100 l drums the matrix composition still is of importance. Assuming a homogeneous sample distribution the coincidence countrate is increased by 66% if the equivalent water content is decreased from $\rho_{PE} = 0{,}29$ cm^3 to $\rho_{PE} = 0{,}14$ g/cm^3, compared to a factor of two in the case of the 220 l drums.

6. Comparison of methods and results

The matrix composition influences the assay results for both methods. A correction procedure for the influence of the matrix in principle is available however was not applied for the coincidence measurements. The matrix

identification and correction formally worked well with the pulsed neutron system. However due to the different parameters influencing the assay in case of coincidence and pulsed measurements the matrix identification obtained from the pulsed measurements is not applicable to the coincidence method. A comparison of matrix identification as obtained for the two systems is given in Table 23. As is seen from Table 23 the findings of the pulsed measurements for drums no 5S, 6S, 7S and 8S have been used for the evaluation of the coincidence results. This is supported by the fact that for these drums the principal matrix material is known and neutron absorbers are not present. In case of the drums 9R-14R and A-C nothing is known about the matrix material. Here the matrix identification of the pulsed measurements cann't be applied to the evaluation of the coincidence measurement. The neutron absorbers obviously present in these drums are influencing the pulsed neutron assay but are only of minor importance for the coincidence measurement.

A matrix identification using the coincidence countrate ratio inner to outer counter layer doesn't clarify the situation. Therefore the assumptions given in Table 23 have been used for the evaluation of the coincidence measurements.

The results obtained with the two NDA systems are compared in Table 24. Also given in this Table are the true Pu masses contained in the drums. The coincidence method in most cases overestimates the amount of Plutonium for the 220 l drums. This is due to conservative assumptions on the matrix correction factors.

Therefore in a second step the matrix density values for the sealed drums were used for a reevaluation. However it should be stressed that this is not appropriate in real measurement compaigns because the density as determined by weighing could be falsified by heavy pieces (metals) in the drums. The reevaluation is done here only in order to demonstrate the influence of the matrix density and it's chemical composition and to show that without additional means for matrix identification the coincidence method is inaccurate or requires administrative means to guarantee a well defined waste matrix composition also in case of low matrix density.

If for evaluation the matrix density values as given in Table 25 and the dependence of the coincidence countrate on the matrix density according Fig.31 would have been used, Pu masses according to column 3 of Table 25 would have been obtained.

Using the density dependence of the coincidence countrate as shown in Fig.31 immediately brings the Pu mass values for the drums 5S-8S in the range of + 5% to the actual values. However for the drums 9R-14R an overestimation of up to 30% remains.

Now this is due to the lower hydrogen content of the matrix material contained in these drums as compared to the PE foam as used for the evaluation. The hydrogen content of these "real" waste materials is about a factor of 1.5 smaller than for the PE foam of equal matrix density. Correcting for this lower hydrogen content finally yields good agreement in the range of + 15% with the actual Pu values.

For the pulsed neutron method the situation is even more unfavourable. There are 4 cases where the measurement yields considerably higher Pu values despite the fact that the sample self shielding always results in an underestimation of the Pu mass. From the transmission values for instance the drums 12R and 13R yield about the same matrix correction values (see Table 17a). The Pu value of drum 12R however significantly is overestimated.

The too high results for drums 9R, 10R and 12R for the active method are indicating that the correlation between the countrate reduction factor and the neutron transmission has to be improved. This should be done using typical waste matrix materials, typical not only with respect to the hydrogen content and the matrix density but also typical with respect to the neutron absorption properties. The high result of drum 10R is influenced by the presence of enriched uranium. An active method cannot distinguish Uranium from Plutonium. The U-235 mass being equivalent to 0,68 $^{239}Pu_{eq}$ according to eq. (2).

A reevaluation of the active measurements was done for drums 5S-8S using the given matrix density values, assuming a homogeneous sample distribution and using the given data on the Pu sample sizes which simulated the Pu mass distribution.

The sample sizes used were 6S:800 mg Pu; 7S: 350 mg Pu; 8S:350 mg Pu. From these values it is immediately clear that self shielding occurs. Using Fig.28 the self shielding factors were determined to be

5S: 1.0 7S:1,5

6S: 1,9 8S:1,5

The samples for 8S are diluted with natural uranium. For a first but rough estimation the uranium was neglected.

In a next step the influence of the matrix density was corrected according to Fig.26 using the density dependent signal countrates. The final results are listed in Table 26. As can be seen the agreement with the actual Pu values is rather good. The still existing small underestimations could be due to insufficient self shielding corrections and to the influence of sample distribution.

7. Waste matrix identification

The results of the coincidence measurement are influenced by the matrix compostion and the density. The most sensitivie parameter being the hydrogen content. Without means for correction of this influence the accuracy of the coincidence measurement is rather low. The time correlator analysis (TCA) technique as developped by Ispra /11/ is able to correct for the matrix influence. This technique measures tripletts to dupletts yields the effective detection sensitivity and thus in principle permitts the matrix correction.

However the measurement of tripletts requires minimum Pu masses in 220 l drums of about 100 mg assuming homogeneous distribution in a low density matrix.

An alternative would be using the neutron transport properties of the matrix which are mainly influenced by the hydrogen content and to a far lesser extent by the matrix composition and the density. As is seen from Fig.11 the thermal neutron relaxation length for matrix water densities above 0.1 g/cm^3 is a function of the hydrogen content of the matrix. By applying an external neutron source the totals countrate (singles) of the individual counters is measured. For azimuthal angels above 60° the totals countrate-ratio $CR_{tot}(o) / CR_{tot}(\varphi)$ is a function of the matrix thus correction of the influence of the matrix becomes possible as is shown in Fig.32. Using the relaxation values $1/\Sigma_R$ as given in Fig.11 $CR_{tot}(o) / CR_{tot}(\varphi)$ is easily calculated according to

$$CR_{tot}(o) / CR_{tot}(\varphi) = \exp\left[+ D(\varphi) / \Sigma_R\right] \qquad (13)$$

with $D(\varphi)$ being the distance the neutrons travel in the drum. The simple eq.(13) only is valid as long as neutorn backscattering from the reflector walls only gives minor contributions to the local thermal neutron flux. Calculated values

according to eq.(13) are plotted together with the experimental ones in Fig.32. However for the values shown the neutron source was placed inside the drum near the surface and not outside is in practical cases. Therefore the data of Fig.32 are preliminary and the abszissa values change if the neutron source is positioned outside the drums. However in the density range $0,1 < \rho < 0,3$ g/cm^3 the "add a gram" technique should work and should yield matrix corrected coincidence values as long as $\varphi > 120°$.

8. Conclusions

The coincidence method mainly has to deal with 2 parameters influencing the results and the accuracy of the assay: matrix composition and Pu distribution.

The results of the measurement campaign are demonstrating that the hitherto assumed dependence of the coincidence countrate from the matrix density especially for low densities is inadequate. Better data are suggested but still need experimental verification.

The measurements revealed that

- careful calibration of the well counter is essential

- the calibration has to be done using typical waste materials

- corrections to the calibration are necessary if matrix composition and density differ from the calibrated waste composition

- an independent identification of the waste matrix is important. The add a gram technique is an attractive means for establishing this.

If all these points are taken into account, the assay accuracy assuming a homogeneous Pu distribution is in the range of $\pm$ 15%.

However the assumption of a homogeneous Pu distribution is not always fulfilled. If an inhomogeneous Pu distribution has to be admitted - the reality in practial cases - the assay of 220 l drums only is reasonable if the waste material has low density ($\rho_{H_2O} < 0,3$g/cm^3). In cases of high matrix water content as for conditioning with concrete the individual measurement can lead to large errors despite means for matrix identification because in these cases the unknown Pu

distribution dominates the error. Only the Pu mass value obtained for a large number of drums remains reasonable.

The pulsed neutron method automatically yields a possibility for matrix correction. However this correction procedure is not usable for the coincidence method due to the difference in the energy of the assaying neutrons. The pulsed neutron method despite the attractive feature of matrix correction suffers from three error sources: sample self shielding, local neutron absorbers and sample distribution.

Due to the additional parameters influencing the active measurement the accuracy is inferior to that of the coincidence method.

From the test exercise the following conclusions can be drawn:

- a good calibration is necessary taking into account matrix, source position and sample self shielding

- a correction for the matrix composition and density is necessary when different from the matrix used for the calibration

- a correction for the source distribution is necessary when different from the calibration item,

- sample self shielding has to be taken into account for sample sizes above 100 mg Pu_{tot}. It leads to a systematic underestimation. However the effect remains unknown and cann't be evaluated. Sample self shielding is occurring for the 3 waste drums 6S-8S. The effect decreases the signal countrate for 6S by a factor of 1,9 and for 7S and 8S by a factor of 1,5,

- the effect of local neutron absorbers is rather complicate and requires more experimental data. Inhomogeneous neutron poisons also lead to a systematic underestimation of the Pu mass. Again it's influence cann't be evaluated.

References

/1/ H. Eberle, H. Ottmar
Internal Report 1984.

/2/ H. Würz
Die pulste Neutronenmessung - eine neue Methode zur Bestimmung von geringen Plutoniummengen im Abfall.
Jahrestagung Kerntechnik, München, 1985, p.317-320

/3/ B. Milicic, H. Würz, T. Zoltowski
The differential die away time method: an attractive method for the assay of α-waste from LWR fuel reprocessing? Proceedings Annual Meeting of the INMM, June 22-25, 1986, New Orleans p.421-426 27th

/4/ MCNP, A general Monte Carlo Code for Neutron and Proton Transport Rep. LA 7396-M, Rev. (1981)

/5/ W. Eyrich, A. Schmidt
Two Compact high intensity pulsed neutron sources, IAEA Conf. on Pulsed Neutron Research Karlsruhe, May 1965, paper SM-62/4

/6/ W. Eyrich et al.
A Neutron Well Counter for Plutonium Assay in 200 l Waste Drums.
Internat. Meeting on Monitoring of Pu Contaminated Waste , Rep. EUR 6629 EN , 1979, p. 159-174.

/7/ K. Böhnel
Die Plutoniumbestimmung in Kernbrennstoffen mit der Neutronenkoinzidenzmethode, KfK 2203, 1975

/8/ W. Klotz, H. Würz
Eine Neutronenfaßmeßanlage zur Plutoniumbestimmung in α-haltigen Abfällen, Jahrestagung Kerntechnik, München, 1985, p.321-324.

/9/ W. Eyrich et al.
Zerstörungsfreie Plutoniumbestimmung in Abfallgebinden der Eurochemic, Mol, Rep. KfK 3369, 1982.

/10/ H.O. Menlove, R.B. Walton
A 4π-Coincidence Unit for One Gallon Cans and Smaller Samples, LA-4457 MS p.26, 1970.

/11/ L. Bondar, F. Girardi
A waste instrument for classifying of Pu contaminated wastes based on passive neutron assay. Proc. International Seminar on Radioactive Waste Products 10-13 June 1985, Jülich, p.133.

Table 1: Matrix materials for calibration of the pulsed system and of the well counter.

drum no	vol (1)	matrix	equivalent water content (g/cm^3) (3)	dimension of the drum ϕ(cm)	H(cm)
7	220	empty	0	58	83,8
2	220	PE foam	0,14	58	83,8
1	220	PE foam	0,29	58	83,8
11	220	concrete	0,17(1)	58	83,8
5	220	concrete	0,5(2)	58	83,8
6	220	water	1,0	58	83,8
3	100	PE foam	0,29	43,2	65,3
8*	220	rashig rings dry	0	58	83,8
9*	220	rashig rings flooded	0,7	58	83,8
4	25	PE foam	0,28	24,3	49,5

* no.8 and no.9 are only used for the pulsed system

(1) water added to cement. Water content of additives unknown.

(2) calibration measurements about 2,5 years after concrete production. Water losses due to evaporation estimated to be about 5%.

(3) The equivalent water content of the PE foam has been obtained by multiplying the PE density by the factor 1,1.

Table 2: Results of Monte Carlo Optimization Studies; Cavity Size 75x75x100 cm

(a,b)	relative thermal neutron intensity in the cavity	$1/\alpha_1$ (μs)
(0,30)	0,3	51±10
(10,30)	0,5	61±8
(20,30)	0,8	75±8
(40,30)	1,0	80±8

(a,b): a layer thickness of graphite (cm); inner layer
b PE layer (cm); outer layer

$1/\alpha_1$ epithermal neutron lifetime

Table 3: Pu samples used for the calibration measurements

sample	C	D	E	Pellet (P)
material	PuO_2	$(Pu+U)O_2$	$(Pu+Am)O_2$	PuO_2
Pu vector				
Pu 238	1,39	0,18	0,22	0,09
240	23,54	23,15	49,58	12,9
242 (%)	4,59	0,85	6,48	0,25
239	59,53	72,0	33,44	85,33
241	10,95	3,82	10,29	1,43
$^{241}Am/Pu$ mass ratio	$7\ 10^{-4}$	$3,4\ 10^{-4}$	$2,1\ 10^{-2}$	$2,1\ \ 10^{-3}$
PuO_2 density (g/cm^3)		2,6		9,7
$^{239}Pu_{eq}$	0,725	0,763	0,45	0,873
$^{240}Pu_{eq}$	0,347	0,25	0,608	0,135
n-emission n/g Pu s	311,6	224,5	546	121,2
Pu mass (g)		variable		15,1

Table 4.1: Passive and coincidence neutron measurement Drum no.1: PE density ρ=0,262 g/cm³, V=220 l

drum No. 1; PE; density ρ=0,262 g/cm³

CEC code	t_m (sec)	date	N_m	totals inner ring		coincidences inner ring		totals outer ring		coincidences outer ring		$^{240}Pu_{eq}$ (mg)
				back-ground	net	back-ground	net	back-ground	net	back-ground	net	
1C1	300	6.2.84	10	167±14	20140±180	10±4	301±10	160±14	6608±190	7±7	35±10	383
1C2	1800	11.5.84	30	816±12	9072±120	15±8	99±4	741±36	2427±50	43±15	1±10	31,8
1C3	1800	14.5.84	20	820±28	13450±121	10±8	150±6	804±36	3666±61	10±2	26±9	53,3
1C4	1800	15.5.84	20	818±27	36260±224	15±8	400±8	804±36	9856±100	10±3	47±11	131,8
1C5	1800	4.4.84	5	809±29	74035±268	16±8	805±30	855±28	20193±215	30±15	86±20	269,5
1C6	360	6.2.84	15	201±16	22290±210	12±4	243±7	192±13	6146±130	9±8	20±10	383
1C7	300	17.1.84	10	155±15	10930±112	6±3	120±5	159±21	3418±63	5±8	16±8	261,6
1C8	300	17.1.84	10	155±15	11220±110	6±3	119±5	159±21	3511±95	5±8	3±7	264,3
1C9	240	3.2.84	12	128±18	20230±142	6±2	244±12	128±11	5876±118	6±8	22±8	540,8
1C10	600	31.1.84	15	339±24	19560±155	19±7	211±6	324±20	4278±91	11±8	12±6	269,5
1C11	600	30.1.84	20	338±25	24800±155	19±7	370±10	324±20	7789±115	11±8	38±10	269,5
1C12	600	15.3.84	15	250±17	20205±150	5±2	248±8	324±20	7196±107	18±10	35±17	269,5
1C13	240	23.3.84	10	128±18	14510±245	5±2	353±9	129±16	5700±112	4±5	61±8	269,5
1C14	600	21.3.84	10	250±14	31090±178	4±2	690±9	324±20	12654±157	11±8	114±10	269,5
1D1	600	24.1.84	15	405±25	11120±111	18±12	232±8	325±18	3262±95	13±10	27±11	147,4
1D2	1800	16.5.84	10	810±32	2792±89	8±3	46±6	912±30	744±54	18±8	12±14	13,3
1E1	1800	16.5.84	10	810±32	10100±99	8±3	154±10	912±30	2645±148	18±8	16±13	47,1
1E2	600	3.2.84	20	323±19	7130±96	15±7	100±4	320±16	1923±47	14±10	11±8	102,2
1E3	600	24.1.84	15	351±27	16090±131	19±10	244±5	310±19	4466±45	17±10	22±11	234,2
1E4	300	2.2.84	10	162±12	16580±127	8±5	245±9	160±12	4677±84	6±5	23±10	479,2
1E5	600	26.1.84	18	333±21	24560±157	19±5	755±8	310±19	8712±114	17±10	94±18	234,3
1E6	600	25.1.84	15	351±28	21690±163	19±10	537±10	310±19	6796±100	17±10	53±12	234,3
1E7	600	2.284	15	323±19	20670±147	15±7	613±10	310±19	8212±105	11±7	94±18	234,3

Table 4.2: Additional measurements: drum no.1

geometry pos.of sample		t_m (sec)	date	N_m	totals inner ring bg	totals inner ring net	coincidences inner ring bg	coincidences inner ring net	totals outer ring bg	totals outer ring net	coincidences outer ring bg	coincidences outer ring net	^{240}Pu eq (mg)
z=	-H/4	900	19.3.84	6	380±19	37260±194	6±2	450±16	430±18	10120±105	30±13	38±11	269,5
τ=0	H/4	600	19.3.84	10	255±17	21450±186	4±2	206±5	287±14	5275±73	20±10	26±10	269,5
	-H/2	600	15.3.84	12	250±19	26650±183	5±2	485±9	287±14	9089±76	20±10	55±14	269,5
	-H/4	1200	20.3.84	5	520±27	56505±238	8±3	862±30	574±20	17025±75	41±15	93±11	269,5
τ=	0	600	15.3.84	6	250±19	28000±167	5±2	391±15	287±14	8090±85	20±10	52±15	269,5
144mm	H/4	900	19.3.84	5	385±18	36470±271	6±3	454±18	430±17	9820±125	30±12	40±11	269,5
	H/2	600	16.3.84	6	260±21	20230±172	5±2	252±12	287±14	4290±56	20±10	18±12	269,5
	-H/2	600	15.3.84	6	250±19	29790±144	5±2	619±12	287±14	10360±138	20±10	72±11	269,5
	-H/4	900	20.3.84	20	385±18	50576±203	6±3	1054±10	430±18	15920±159	30±13	149±15	269,5
τ=	0	480	16.3.84	40	208±19	26740±110	4±2	516±8	230±12	8100±74	16±8	34±11	269,5
204mm	H/4	600	21.3.84	6	255±20	28733±259	5±2	379±20	287±14	8573±162	20±10	49±13	269,5
	H/2	600	16.3.84	6	260±21	19805±137	5±2	248±17	287±14	5033±65	20±10	8±8	269,5

All measurements with Pu sample C46

Table 4.2: Additional measurements drum no.1

Code	t_m (sec)	date	N_m	totals inner ring background	totals inner ring net	coincidences inner ring background	coincidences inner ring net	totals outer ring bg	totals outer ring net	coincidences outer ring bg	coincidences outer ring net	$^{240}Pu_{(mg)}^{eq}$
1D2*	1800	21.5.	10	810±32	11120±104	8±3	163±12	924±19	2933±90	21±8	20±10	53,8
1D2**	1800	22.5.	15	810±32	17570±140	8±3	265±10	924±19	4624±62	21±8	29±10	85,4
1D2***	1800	23.5.	10	810±32	36460±190	8±3	525±12	918±21	9828±162	17±8	60±9	181,4
1E3*	1800	18.5.	15	810±32	69400±260	8±3	1026±12	918±28	18480±172	22±8	90±10	336,5
1E3**	900	29.3	6	402±16	90690±296	5±3	1316±40	429±18	24262±157	14±7	119±11	889,1

measurements 1D2* 1D2** 1D2*** in the same geometry as 1D2 but with different Pu samples

1D2*; D32

1D**; D44

1D2***; D44+D46

measurements 1E3*, 1E3** in the same geometry as 1E3 but with different Pu samples

1E3*; E23 + E37

1E3**; E43 + E44

Table 5.1: Passive and coincidence neutron measurement. Drum no.2: PE density ρ=0,126 g/cm^3, V=220 l

CEC code	t_m (sec)	date	N_m	totals: inner ring bg	totals: inner ring net	coincidences: inner ring bg	coincidences: inner ring net	totals outer ring bg	totals outer ring net	coincidences: outer ring bg	coincidences: outer ring net	^{240}Pu eq (mg)
2C1	1200	3.4.84	5	540±22	104380±198	10±3	2470±61	855±26	35970±75	30±11	303±32	383
2C2	1800	25.4.84	15	855±28	14175±146	14±4	337±8	930±31	4591±97	33±7	30±9	31,8
2C3	1800	28.5.84	10	855±28	20940±215	13±4	499±17	813±51	6982±128	30±6	59±8	53,5
2C4	600	9.3.84	12	250±17	18640±144	5±2	425±10	256±23	6165±108	12±6	57±7	131,8
2C5	300	5.3.84	12	128±12	19080±152	2±2	462±16	138±12	6447±75	6±5	54±9	269,5
2C6	300	7.3.84	12	129±12	12555±161	3±2	212±6	132±12	3390±49	5±4	15±9	269,5
2C7	300	6.3.84	12	129±12	17210±116	3±2	412±12	132±18	6529±109	5±4	49±9	269,5
2C8	600	7.3.84	12	268±18	21865±184	5±2	290±11	264±24	7341±24	11±6	44±9	269,5
2C9	300	5.3.84	15	128±12	20590±88	2±2	557±10	138±12	7847±82	6±5	82±8	269,5
2C10	300	6.3.84	12	129±12	17568±137	2±2	464±16	138±12	7187±55	6±5	64±9	269,5
2D1	600	29.2.84	12	268±16	14634±94	5±2	432±11	276±16	5065±97	12±8	55±11	147,4
2D2	1800	29.5.84	11	840±25	4205±77	12±4	134±16	813±26	1413±59	30±	23±15	13,3
2E1	1800	29.5.84	15	840±25	15710±123	12±4	489±12	813±51	5168±82	30±6	61±8	47,1
2E2	600	23.1.84	10	405±25	25615±128	28±6	798±10	343±22	8520±108	15±11	98±12	234,3
2E3	600	29.2.84	11	268±16	27140±164	5±2	963±12	276±16	10105±112	12±8	141±8	234,3

Table 5.2: Additional measurements; drum no.2, V=220 l

sample	pos.of sample	t_m (sec)	date	N_m	totals:inner ring bg	totals:inner ring net	coincidences:inner ring bg	coincidences:inner ring net	totals:outer ring bg	totals:outer ring net	coincidences:outer ring bg	coincidences:outer ring net	$^{240}Pu_{eq}$ (mg)
C46	r=144mm-H/2	480	8.3.84	12	194±34	27219±162	4±2	672±14	205±32	10215±150	9±8	98± 6	269,5
	0	300	5.3.84	12	133±28	19560±163	2±2	484±12	132±15	6990±102	5±6	68± 9	269,5
	H/2	480	8.3.84	12	194±33	20773±117	4±2	359±8	205±32	5670±74	9±8	30± 6	269,5
	-H/2	480	8.3.84	12	194±33	28320±181	4±2	745±13	205±32	10725±138	9±8	118± 8	269,5
	r=204mm 0	300	5.3.84	12	133±28	20420±149	2±2	537±15	132±15	7434±89	5±6	77± 6	269,5
	H/2	480	8.3.84	24	194±33	19517±152	4±2	308±7	205±32	5930±71	9±8	31± 4	269,5
C33+34	r=0, z=0	1200	30.3.84	15	560±25	75630±305	10±3	1774±22	572±15	24894±133	18±6	193± 9	264,3
C33+34 46	r=0, z=0	900	2.4.84	6	420±22	114860±185	8±3	2779±75	427±18	37790±175	15±8	302± 31	533,8
C33+344 46+E43+ E44	r=0, z=0	600	2.4.84	6	280±18	172195±473	5±2	4740±65	285±15	56327±213	10±9	533±42	1422,9
D44+46	r=0, z=0	1200	2.4.84	6	560±25	39075±170	10±3	1207±14	570±21	12629±221	21±13	147±21	181,4
E37	r=0 -H/2	600	1.3.84	12	275±16	22487±135	5±2	676±10	276±16	8304±89	12±8	92±13	234,3
	H/2	600	2.3.84	12	275±16	17130±110	5±2	355±6	303±17	4537±68	15±7		234,3
C45	r=0, z=0	1800	3.4.84	20	840±30	116713±295	15±5	2756±21	855±26	38682±160	31±6	30±7	269,5

Table 5.2: Additional measurements drum no.2

sample	pos. of sample	t_m (sec)	date	N_m	totals: inner ring bg	totals: inner ring net	coincidences: inner ring bg	coincidences: inner ring net	totals: outer ring bg	totals: outer ring net	coincidences: outer ring bg	coincidences: outer ring net	^{240}Pu eq (mg)
E37	r=204mm -H/2	600	1.3.84	12	275±16	23405±187	5±2	770±21	276±16	8660±73	21±9	99±9	234,3
	0	600	8.3.84	12	275±16	26835±181	5±2	937±22	256±38	9544±116	12±8	117±11	234,3
	H/2	600	2.3.84	12	275±16	16170±146	5±2	336±14	303±17	4781±71	15±8	29±9	234,3
E23+44	r=0 z=0	900	30.3.84	6	420±22	94880±433	8±3	2937±85	429±14	30580±178	14±12	325±19	581,5
E43+44		900	30.3.84	6	420±22	143710±462	8±3	4342±100	429±14	46590±212	14±12	500±21	889,1

Table 6.1: Passive and coincidence neutron measurement, drum no.3: PE density ρ=0,266 g/cm³, V=220 l

CEC code	t_m (sec)	date	N_m	totals inner ring bg	totals inner ring net	coincidences inner ring bg	coincidences inner ring net	totals outer ring bg	totals outer ring net	coincidences outer ring bg	coincidences outer ring net	$^{240}Pu_{eq}$ (mg)
3C1	1200	11.4.84	5	632±20	100980±245	18±5	1986±45	540±31	32750±175	11±7	261±22	383
3C2	1800	10.4.84	15	840±30	12670±116	14±6	197±11	816±38	3662±56	17±9	29±9	31,8
3C3	1800	5.4.84	20	813±29	18960±170	15±6	316±8	855±29	5461±75	31±9	14±6	53,5
3C4	1200	7.5.84	6	534±23	33925±190	9±3	564±20	543±28	9760±120	14±17	59±13	131,8
3C5	1800	5.4.84	20	813±29	104010±390	14±6	1734±19	855±29	30071±200	31±16	184±8	269,5
3C6	1800	6.4.84	5	810±29	103420±370	14±6	2282±85	855±29	37068±250	31±16	281±12	269,5
3C7	1800	6.4.84	5	810±29	116610±270	14±6	2850±45	855±29	44045±90	31±16	410±22	269,5
3D1	1800	11.4.84	5	948±32	42645±120	18±6	1082±38	816±38	13690±125	17±9	132±25	147,4
3D2	1800	11.4.84	15	948±32	3630±58	18±6	74±5	816±38	1077±48	17±9	14±7	13,3
3D3	1800	30.4.84	20	912±34	5851±100	19±5	118±6	1000±51	1573±48	65±10	30±15	20,5
3D4	1200	2.5.84	5	915±41	15645±215	17±5	318±17	951±28	4377±35	65±15	19±11	53,8
3D5	1200	7.5.84	6	534±22	16350±180	9±4	358±12	542±27	4648±60	14±14	43±10	85,4
3D6	1800	2.5.84	5	915±41	17605±125	17±5	540±9	951±28	6369±85	65±19	56±19	53,8
3D7	1800	2.5.84	20	915±41	16355±185	17±5	510±10	951±28	6482±59	65±8	73±11	53,8
3E1	1800	3.5.84	20	900±38	14360±262	16±5	295±9	951±28	3885±70	65±8	-	47,1
3E2	900	4.5.84	10	442±25	33953±160	8±4	712±20	406±28	9670±86	12±14	71±10	234,3
3E3	1200	7.5.84	6	534±22	51485±175	9±4	1609±28	542±27	18765±200	14±17	228±11	234,3

Table 6.2: Additional measurements, drum no.3 sample C46 and Cf source with source strength q=4,65 10^4 n/s

sample pos r (cm)	z	t_m (sec)	date	N_m	totals inner ring bg	totals inner ring net	coincidences inner ring bg	coincidences inner ring net	totals outer ring bg	totals outer ring net	coincidences outer ring bg	coincidences outer ring net	^{249}Pu eq (mg)
10,8	-H/2	1800	6.4.84	20	810±29	104370±767	14±6	2402±30	813±35	38700±455	17± 5	337± 9	269,5
	0	1800	9.4.84	5	795±28	108970±270	13±4	2090±40	813±35	33620±120	17± 12	248± 30	269,5
	H/2	1800	10.4.84	5	840±30	75790±370	14±6	1090±30	813±35	21600±185	17± 12	135± 20	269,5
15,3	-H/2	1800	10.4.84	5	840±30	109720±170	14±6	2720± 80	813±35	42180±260	17± 12	380± 18	269,5
	0	1800	9.4.84	15	795±28	116645±290	13±4	2670± 25	813±35	37935±245	17± 5	321± 12	269,5
	H/2	1800	10.4.84	5	840±30	78180±440	14±6	1180± 35	813±35	23810±185	17± 12	140± 16	269,5
0	-H/2	60	8.5.84	10	27±5	224950±915	1±1	15980± 300	27±5	79115±205	1±1	2262± 65	Cf-source
	0	90	8.5.84	10	41±6	335960±552	1±1	18540± 410	41±6	93950±110	1±1	2080± 75	Cf-source
	H/2	60	8.5.84	10	27±5	178940±424	1±1	8240± 190	27±5	43640±160	1±1	615± 20	Cf-source
20cm	-H/2	30	8.5.84	10	14±4	119940±540	1±1	8930± 72	14±4	47330±115	1±1	1580± 55	Cf-source
	0	30	8.5.84	10	14±4	127880±240	1±1	9440± 185	14±4	45360±115	1±1	1500± 58	Cf-source
	H/2	30	8.5.84	10	14±4	97460±240	1±1	5620± 95	14±4	33655±190	1±1	810± 51	Cf-source

Table 7: Passive and coincidence neutron measurement
Drum no. 4: PE density ρ=0,256 g/cm³; V=25 l

CEC	t_m (sec)	date	N_m	totals inner ring bg	totals inner ring net	coincidences inner ring bg	coincidences inner ring net	totals outer ring bg	totals outer ring net	coincidenes outer ring bg	coincidenes outer ring net	$^{240}Pu_{eq}$ (mg)
4C1	1800	10.5.84	20	849±32	175290±420	20±10	4729± 42	813±40	66820±185	21± 5	715± 14	383
4C2	1800	8.5.84	7	816±28	15625±75	16±7	443± 28	813±40	5525±65	21± 11	55±8	31,8
4C3	1800	9.5.84	20	834±30	23330±180	17±8	618± 13	813±40	8235±100	21± 5	115± 10	53,5
4C4	1800	9.5.84	8	834±30	62510±205	17±8	1680± 65	813±40	22150±200	21± 11	265± 28	131,8
4C5	1800	9.5.84	20	816±28	128110±315	16±7	3495± 32	813±40	45800±170	21± 5	520± 17	269,5

additional measurements with Cf-source, sourcestrength 4,65 10^4 n/s

source pos. r(cm)	z	t_m (sec)	date	N_m	totals inner ring bg	totals inner ring net	coincidences inner ring bg	coincidences inner ring net	totals outer ring bg	totals outer ring net	coincidences outer ring bg	coincidences outer ring net
0	-H/2	30	11.5.84	10	14±4	129710± 220	1±1	11350±315	13±5	51370±260	1±1	1940± 55
	0	30	11.5.84	10	14±4	140100± 180	1±1	12090±450	13±5	47960±350	1±1	1665±53
	H/2	30	11.5.84	10	14±4	117930± 205	1±1	11490±415	13±5	39430±210	1±1	1145±58
10,8	-H/2	30	11.5.84	10	14±4	129180± 145	1±1	10580±415	13±5	55300±155	1±1	2255± 125
	0	30	11.5.84	10	14±4	137050± 230	1±1	12080±340	13±5	53350±165	1±1	2140±90
	H/2	30	11.5.84	10	14±4	116950± 195	1±1	8840±300	13±5	45010±170	1±1	1470±55

Table 8.1: Passive and coincidence measurement

Drum no.11: concrete density ρ=2,29 g/cm^3, V=220 l

CEC	t_m (sec)	date	N_m	totals: inner ring		coincidences: inner ring		totals: outer ring		coincidences: out ring		$^{240}Pu_{eq}$ (mg)
				bg	net	bg	net	bg	net	bg	net	
11C1	1800	12.4.84	5	900±31	107504±216	18±4	1039± 34	816±28	24170± 152	17±9	76±43	540,8
11C2	1800	16.4.84	5	948±34	117000±303	22±7	1555± 85	816±28	31040± 180	17±9	108±21	540,8
11C3	1800	16.4.84	5	948±34	101745±358	22±7	1097± 92	816±28	14185± 225	17±9	29±22	540,8
11C4	1800	12.4.84	5	900±31	150137±265	18±4	2221± 61	816±28	39890± 66	17±9	157±17	540,8
11C5	1800	12.4.84	15	900±31	195190±582	18±4	4423± 35	816±28	61080± 170	17±6	382±18	540,8
11C6	1200	13.4.84	6	608±28	150940±420	14±3	4499± 55	544±21	62720±440	12±7	677±45	540,8
11C7	1200	13.4.84	6	608±28	119530±340	14±3	2960± 42	544±21	52900±250	12±7	494±46	540,8
11C8	1200	13.4.84	5	608±28	96330±320	14±3	1825± 35	544±21	32890±90	12±7	204±27	540,8
11D1	1800	18.4.84	5	942±32	26180±170	22±7	287± 15	835±30	5695±76	31±16	14±19	181,4
11D2	1800	18.4.84	5	942±32	48900±100	22±7	1424± 13	835±30	15015±143	31±16	123±27	181,4
11D3	1800	18.4.84	20	942±32	57090±260	22±7	2152± 16	835±30	23270±180	31±9	400±21	181,4
11E1	1800	17.4.84	5	948±34	127280±255	22±7	1498± 76	816±28	27570±180	31±16	56±26	889,1
11E2	1800	17.4.84	5	948±34	240440±170	22±7	6928± 95	835±30	73140±200	31±16	625±58	889,1
11E3	1800	17.4.84	20	632±28	187170±480	14±3	7168± 41	555±20	76040±290	21±9	1058±17	889,1

Table 8.2: Additional measurements drum no.11

sample	sample pos		t_m (sec)	date	N_m	totals:inner ring bg	totals:inner ring net	coincidences:inner ring bg	coincidences:inner ring net	totals:outer ring bg	totals:outer ring net	coincidences:outer ring bg	coincidences:outer ring net	$^{240}Pu_{eq}$ (mg)
C45+C46	r=144mm z	-H/2	1800	24.4.84	20	928±27	131396±344	21±9	2121± 18	835±30	42196±251	35± 7	206± 8	540,8
		-H/4	1800	26.4.84	5	928±27	144120±710	21±9	2074± 38	950±37	37074±127	45±18	146± 21	540,8
		H/4	1800	26.4.84	20	928±27	126490±420	21±9	1551± 25	950±37	31065±117	45± 7	109± 10	540,8
		H/2	1800	25.4.84	5	928±27	108180±225	21±9	1325± 34	835±30	21295±265	35±16	114± 25	540,8
	r=204mm	-H/2	1800	25.4.84	20	928±27	155690±380	21±9	3182± 26	835±30	57680±297	35± 6	422±16	540,8
		H/2	1800	25.4.84	5	928±27	124050±750	21±9	1741± 75	835±30	33120±165	35±16	156±21	540,8
	r=275mm	-H/4	1200	26.4.84	5	610±22	147890±410	14±7	4427±45	630±26	61575±234	30±17	639±21	540,8
		H/4	1200	26.4.84	5	610±22	137970±342	14±7	3776±90	630±26	56130±137	30±17	553±19	540,8
C33+C34	r=0, z=0		1800	19.4.84	20	928±27	52875±233	21±9	472± 14	928±27	11705±134	21± 5	222±18	264,3
C33+C34 +C46	r=0, z=0		1800	24.4.84	5	928±27	107470±549	21±9	977± 50	835±30	23965±105	35±16	47±15	533,8
C33+34 +46+E43 +E44	r=0, z=0		1200	19.4.84	5	610±22	158520±270	14±7	1682±79	618±24	34960±175	18±11	185± 38	1422,9
homogeneous			1800	24.4.84	5	928±27	108520±211	21±9	2028±66	835±30	33353±197	35±16	191±15	383

Table 9: Additional passive and coincidence measurements; V=220 l

9a: empty drum P-sample

sample pos.	t_m (S)	date	totals: inner ring bg	inner ring net	coincidences: inner ring bg	inner ring net	totals: outer ring bg	outer ring net	coincidences: outer ring bg	outer ring net	$^{240}Pu_{eq}$ (mg)
0	300	13.9.84	155±28	117400±480	5±6	4765±62	155±28	61000±320	4±6	1180±31	2038
8,5	300	13.9.84	155±28	118640±430	5±6	4820±82	155±28	61420±270	4±6	1164±47	2038
17,0	300	13.9.84	155±28	123600±310	5±6	5280±150	155±28	61950±220	4±6	1140±41	2038
25,5	300	13.9.84	155±28	128900±240	5±6	5750±155	155±28	61400±125	4±6	1190±85	2038

9b: water filled drum; P-sample

sample pos.	t_m (S)	date	totals: inner ring bg	inner ring net	coincidences: inner ring bg	inner ring net	totals: outer ring bg	outer ring net	coincidences: outer ring bg	outer ring net	$^{240}Pu_{eq}$ (mg)
0	900	14.9.84	500±60	12950±60	13±12	12±7	500±60	3600±70	13±12	-	2038
8,5	900	14.9.84	500±60	23400±150	13±12	31±14	500±60	6270±85	13±12	2±14	2038
17	900	14.9.84	500±60	78340±340	13±12	390±70	500±60	20110±140	13±12	32±11	2038
25,5	900	14.9.84	500±60	266750±500	13±12	6780±100	500±60	85940±190	13±12	650±75	2038

Table 9c: P sample, drums no. 1,2 and 11

sample, pos.	drum	t_m (s)	totals: inner ring bg	totals: inner ring net	coincidences: inner ring bg	coincidences: inner ring net	totals: outer ring bg	totals: outer ring net	coincidence outer ring bg	coincidence outer ring net	$^{240}Pu_{eq}$ (mg)
	1	180	85±20	47100±260	1±3	720±62	95±8	13260±125	5±8	85±20	2038
(0,0)	2	300	140±28	123230±320	3±4	3785±145	140±28	41500±240	3±4	485±35	2038
	11	900	450±35	170000±580	12±8	2090±100	450±35	38720±275	28±18	100±35	2038

Table 10.1: Pulsed neutron measurement. Drum no.1; V = 220 l

Countrate normalized to a neutron source rate of 2,2 10^{11} n

CEC-code	t_m (sec)	N_m	background	global net	$^{239}Pu_{eq}$ (mg)
1C1	180	10	16650±310	159150±2120	790,1
1C2	180	8	13400±350	12170±890	65,6
1C3	180	5	13400±350	16710±940	110,4
1C4	180	5	13400±350	29320±880	272,0
1C5	180	10	16350±390	45170±1020	555,9
1C6	180	8	16650±310	107450±1600	790,1
1C7	180	6	16650±310	69520±1200	539,5
1C8	180	5	16650±310	52700±1100	545,1
1C9	180	6	15500±350	84150±1400	1115,6
1C10	180	10	20340±1250	68150±1480	555,9
1C11	180	10	16350±390	28030±890	555,9
1C12	180	5	15600±370	104200±1950	555,9
1C13	180		16410±390	85860±1750	555,9
1C14	180	5	16410±390	59400±1350	555,9
1D1	180	6	13620±610	96500±1200	445,3
1D2	180	8	15750±780	5150±790	40,1
1E1	180	10	19600±980	6950±880	33,5
1E2	180	5	19600±980	9800±910	72,7
1E3	180	5	19600±980	20200±920	166,8
1E4	180	5	19600±980	32900±940	341,3
1E5	180	5	15800±970	38220±1070	166,8
1E6	180	5	15800±970	25150±1040	166,8
1E7	180	5	15800±970	27350±1080	166,8

Table 10.2: Additional measurements, drum no.1

samples	sample pos	t_m (sec)	N_m	bg	global net	$^{239}Pu_{eq}$ (mg)
C34+45+46	(r=0,z=0)	180	5	13400±620	97800±1860	1387,2
E43+44	(r=0,z=0)	180	5	14250±780	54600±1420	633
C33+34+45+46	(r=0,z=0)	180	5	13900±350	110280±1820	1660,7
D32+44+46+E43+44	(r=0,z=0)	180	5	13900±350	130760±1740	1344,0
C33+34+45+46+E43+44	(r=0,z=0)	180	5	13900±350	163540±2200	2293,7
C33+34+45+46+ D32+44+46+ E43+44	(r=0,z=0)	180	5	18410±810	226050±2400	3004,6
D12	(r=0,z=0)	180	8	15750±780	3750±920	30,6
D21	(r=0,z=0)	180	8	15750±780	9250±870	62
D32	(r=0,z=0)	180	8	15750±780	22410±990	162,7
D44	(r=0,z=0)	180	8	15750±780	32350±1020	258,1
D44+46	(r=0,z=0)	180	8	15750±780	58170±1180	548,2

Table 11.1: Pulsed neutron measurements. Drum no.2, V = 220 l

Countrate normalized to a neutron source rate of $2,2\ 1o^{11}n$

CEC-code	t_m (sec)	N_m	background	global net	$^{239}Pu_{eq}$ (mg)
2C1	180	5	15900 ± 890	345540 ± 2750	790,1
2C2	180	5	14250 ± 820	36100 ± 1180	65,6
2C3	180	5	14250 ± 820	44600 ± 1490	110,4
2C4	180	5	14250 ± 820	93100 ± 1130	272,0
2C5	180	5	13110 ± 760	148500 ± 1620	555,9
2C6	180	5	14250 ± 820	128350 ± 1480	555,9
2C7	180	5	14250 ± 820	75900 ± 1950	555,9
2C8	180	5	14250 ± 820	149530 ± 2380	555,9
2C9	180	5	14250 ± 820	143100 ± 3900	555,9
2C10	180	5	14250 ± 820	105700 ± 1600	555,9
2D1	180	5	15900 ± 890	201730 ± 2150	445,3

Table 11.2: Additional measurements. Drum no.2

samples	sample pos.	t_m sec	N_m	background	global net	$^{239}Pu_{eq}$ (mg)
C45	r=0; z=-H/2	180	6	14580 ± 760	75900 ± 1650	559,7
C45	r=0; z= H/2	180	6	14580 ± 760	128350 ± 1350	559,7
C45	r=0 -H/4	180	6	14580 ± 760	119500 ± 1950	559,7
C45	r=0 H/4	180	5	14240 ± 760	138430 ± 1860	559,7
C45	r=27,5; z=-H/4	180	6	14580 ± 760	133360 ± 2280	559,7
	r=27,5; H/4	180	6	14580 ± 760	148020 ± 2790	559,7
C45+46	(0,0)	180	5	13110 ± 480	251100 ± 4250	1115,6
C33+34+ 45+46	(0,0)	180	5	13110 ± 480	364700 ± 7950	1660,7
C45+46+ E43+44	(0,0)	180	5	13110 ± 480	406100 ± 2700	1748,6
C33+34+45 +46+E43+ 44	(0,0)	180	5	13110 ± 480	520000 ±12800	2293,7

Table 12.1: Pulsed neutron measurement. Countrate normalized to a neutron source rate of 2,2 10^{11} n. Drum no.3, V = 100 l

CEC code	t_m (sec)	N_m	background	global net	$^{239}Pu_{eq}$ (mg)
3C1	300	10	15850 ± 670	264050 ± 4800	790,1
3C2	300	5	15850 ± 670	23400 ± 1980	65,6
3C3	600	3	15850 ± 670	28400 ± 1450	110,4
3C5	300	6	15850 ± 670	78650 ± 2950	555,9
3C7	300	6	15850 ± 670	142000 ± 2400	555,9
3D1	600	5	16390 ± 690	151500 ± 3450	445,3
3D3	300	5	16390 ± 690	21450 ± 1900	62
3D4	600	5	16390 ± 690	38250 ± 1280	162,7

Table 12.2: Additional measurements, drum no.3

samples	samples pos	t_m (sec)	N_m	background	global net	$^{239}Pu_{eq}$ (mg)
C45	r=0; z=-H/2	300	6	15850 ± 670	67450 ± 2900	559,7
	-H/4	300	6	15850 ± 670	76700 ± 3100	559,7
	H/4	300	6	15850 ± 670	93240 ± 2700	559,7
	H/2	300	6	15850 ± 670	162400 ± 7600	559,7
C45	r=200;z=-H/2	300	6	15290 ± 690	100820 ± 2480	559,7
	-H/4	600	5	15290 ± 690	132300 ± 1480	559,7
	H/4	600	3	15290 ± 690	140210 ± 1160	559,7
	H/2	300	6	15290 ± 690	185500 ± 3950	559,7

Table 13.1: Pulsed neutron measurements. Drum no.11; concrete; V=220 l
Countrate normalized to a neutron source rate of $2,2\ 10^{11}$ n.

CEC code	t_m (sec)	N_m	background	global net	$^{239}Pu_{eq}$ mg
11C1	180	10	14300±480	6950±1820	1115,5
11C2	180	5	16040±580	24250±1730	1115,5
11C3	180	5	16590±530	80250±950	1115,5
11C4	180	10	16900±590	21000±980	1115,5
11C5	180	10	16590±630	56110±1200	1115,5
11C6	180	10	16590±530	132600±1280	1115,5
11C7	180	5	16900±590	97290±1090	1115,5
11C8	180	5	16900±590	169650±1440	1115,5
11E1	180	10	20050±780	4780±1400	633,0
11E2	180	10	13480±390	33480±920	633,0
11E3	180	10	13480±390	93050±980	633,0
11D1	180	10	13480±390	6700±2090	548,2
11D2	180	10	13480±390	34000±980	548,2
11D3	180	10	13480±390	105040±1710	548,2

Table 13.2: Additional measurements. Drum no.11

samples	sample position	t_m (sec)	N_m	background	global net	$^{239}Pu_{eq}$ (mg)
C	homogeneous	180	5	17650±890	78100±1400	790,1
D	homogeneous	180	8	18410±790	44600±1150	445,3
E43	r=20,4;z=0	180	5	13960±490	15780±980	291,7
	r=27,5;z=0	180	5	13960±490	44610±760	291,7
E44	r=20,4;z=0	180	5	14620±760	17530±1060	341,3
C45+C46	r=0;z=-H/4	180	5	14620±760	4600	1115,5
	-H/4	180	5	14620±760	4400	1115,5
C45+C46	r=27,5;z=-H/4	180	5	14680±760	116210±1850	1115,5
	H/4	180	5	14680±760	138270±2920	1115,5
C45+D44+D46+ E43+E44	r=0;z=0	180	5	14680±760	14550±1240	1741
	r=20,4;Z=0	180	5	14680±760	98700±2380	1741
	r=27,5;z=0	180	5	14680±760	295950±2240	1741

Table 14: Sample positions for the calibration measurements

CEC code	pos. (r,z)	CEC code	pos. (r,z)	CEC code	pos. (r,z)	CEC code	pos. (r,z)
1C2	(0;0)	2C2	(0;0)	3D2	(0;0)	11C7	(27,5;H/2)
1C3	"	2C3	"	3D3	"	11C8	(27,5;H/2)
1C4	"	2C4	"	3D4	"	11D1	(0;0)
1C5	"	2C5	"	3D5	"	11D2	(20,4;0)
1C6	"	2C6	(0;H/2)	3D6	(20;0)	11D3	(27,5;0)
1C7	"	2C7	(0;-H/2)	3D7	(20;-H/2)	11E1	(0;0)
1C8	"	2C8	(27,5;H/2)	3E1	(0;0)	11E1	(0;0)
1C10	(0;H/2)	2C9	(27,5;0)	3E2	"	11E2	(20,4;0)
1C11	(0;-H/2)	2C10	(27,5;-H/2)	3E3	(20;0)	11E3	(27,5;0)
1C12	(27,5;H/2)	2D2	(0;0)	4C2	(0;0)		
1C13	(27,5;0)	2E1	"	4C3	"		
1C14	(27,5;-H/2)	2E2	"	4C4	"		
1D2	(0;0)	2E3	(27,5;0)	4C5	"		
1E1	"	3C2	(0;0)	11C1	(0;0)		
1E2	"	3C3	(0;0)	11C2	(0;-H/2)		
1E3	"	3C4	"	11C3	(0;H/2)		
1E4	"	3C5	(0;0)	11C4	(14,4;0)		
1E5	(27,5;0)	3C6	(0;-H/2)	11C5	(20,4;0)		
1E6	(20,4;0)	3C7	(20;0)	11C6	(27,5;0)		
1E7	(27,5;-H/2)						

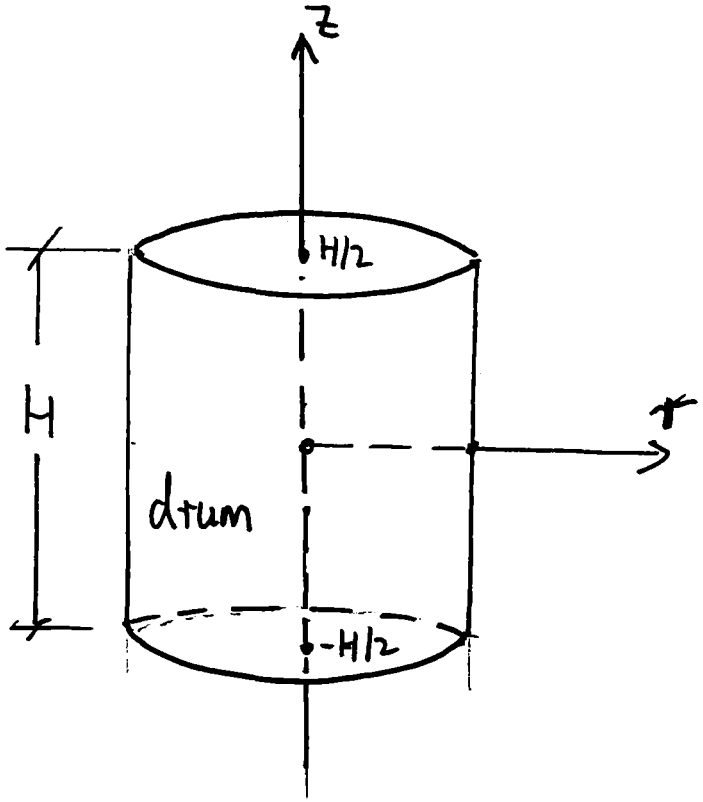

Table 15a: Results of calibration of the pulsed neutron system. The signal countrates CR_{ind} are normalized to an overall neutron source rate of 2,2 10^{11} n. Also included in Table 13a are the background countrates, measurement times, number of measurements and statistical errors. Homogeneous Pu sample distribution, C-sample

drum vol. (l)	matrix	t_m (s)	N_m	background	global net (1)	$^{239}Pu_{eq}$ (mg)
100	drum no.7	300	10	15850±670	264050±4800	790
220	no.3	180	10	16650±310	159150±2120	790
220	no.2	180	5	15900±900	345540±2750	790
220	no.4	180	10	17650±890	6950±1820	790

(1) the error only includes the statistical uncertainty

Table 15b: Single countrate raito K for homogeneously distributed C- and D-samples and comparison with the actual value. C-sample: 790 mg $^{239}Pu_{eq}$; D-sample 445,3 mg $^{239}Pu_{eq}$

$K = CR_{ind}(C\text{-hom})/\ CR_{ind}(D\text{-hom})$

drum	K	$^{239}Pu_{eq}(C)/^{239}Pu_{eq}(D)$
no.2	1,71±0,14	1,77
no.1	1,65±0,13	
no.11	1,75±0,14	
no. 3	1,74±0,14	

The error in K includes uncertainties due to statistics, long term instability and source monitoring.

Table 16: Results of the pulsed neutron measurement; sealed drums

drum code	drum vol (l)	t_m (sec)	N_m	background	global net	$^{239}Pu_{eq}$ (1) mg	g Pu_{tot}
5S	220	300	10	14450±480	183480±1090	910±30	1,24
6S	220	300	15	14450±480	276320±2750	1371±45	1,86
7S	100	300	5	13450±620	284100±1170	850±24	1,87
8S	100	300	10	13450±620	306400±2780	917±27	1,19
9R	220	300	10	13750±690	438320±3400	2174±15	3,03
10R	100	300	10	14160±520	893400±5250	2674±72	3,3
12R	220	300	5	14295±480	339200±1950	1682±35	2,23
13R	220	300	10	14300±480	81750±2960	406±20	0,57
14R	100	300	6	14160±790	314600±3900	941±22	1,11
A	220	300	10	14860±670	229850±4300	1,14	1,4
B	220	300	5	14160±540	126400±2700	0,63	0,8
C	100	300	5	14860±670	243700±2750	0,73	0,91

(1) Evaluation without any correction for sample distribution, matrix material and self shielding. It has been assumed that the matrix of all 220 l drums is equivalent to that of modular drum no. 1. The matrix of all 100 l drums is equivalent to that of modular drum no. 3.
The sample distribution is assumed to be homogeneous. The errors given only are due to counting statistics. In a second step evaluation is done by using the features of the system as described in the text.

Table 17a: Countrate reduction factor for the 220 l drums as determined from the source normalized monitor countrates relative to drum no.1. The values given are valid for homogeneous matrix material.

drum no.	countrate reduction factor
5 S	1,0
6 S	1,0
9 R	3,0
12 R	6,3
13 R	6,8
A	6,5
B	6,5

Table 17b: Countrate reduction factor for the 100 l drums as determined from the source normalized monitor countrates relative to drum no.3 using the matrix correction curve for 220 l drums (Fig.9).

drum no.	countrate reduction factor
7 S	1,0
8 S	1,0
10 R	$3,0 \pm 1,0$
14 R	$4,0 \pm 1,2$
C	$4,0 \pm 1,2$

Table 18 Final results of pulsed neutron measurements for sealed drums . Errors are given in %.

code	mass Pu_{tot} (g)	sources of error and amplitues (1) statistics (1σ)	isotope composition (2)	matrix	sample (4) self shielding and local neutron absorbers	Sample distribution (5)
5S	1,2	8	3	10(3)		15
6S	1,8	8	3	10(3)	effect unknown	15
7S	1,9	8	3	10(6)	systematic	10
8S	1,2	8	3	10(6)	underestimation	10
9R	9,2	8	5	30(3)		20
10R	9,9	8	3	30(6)	effect unknown	15
12R	14,0	8	5	20(3)	systematic	20
13R	4,1	8	5	20(3)	underestimation	20
14R	4,4	8	5	30(6)		15
A	9,6	8	5	20(3)	effect unknown	20
B	5,3	8	5	20(3)	systematic	20
C	3,5	8	5	20(6)	underestimation	20

(1) the error includes uncertainty due to calibration long term instability and source monitoring

(2) the isotopic composition has been determined by γ-spectroscopy

(3) matrix correction from thermal neutron transmission, taking into account only global parameters

(4) sample self shielding and local neutron absorbers lead to systematic underestimation; effect is unknown

(5) hints for sample distribution from neutron radiography

(6) matrix correction from thermal neutron transmission. Countrate reduction factors obtained using data for 220 l drums.

Table 19a: Results of the calibration of the coincidence measurements. Homogeneous Pu sample distribution; C-samples, 12 small samples, total mass of $^{240}Pu_{eq}$ = 383 mg

drum no	measuring time t_m(s)	number of measurements N	totals inner ring bg	totals inner ring net	coincidences inner ring bg	coincidences inner ring net
2	1200	5	540±22	104380±200	10±3	2470±60
1	300	10	170±15	20140±180	10±4	301±10
11	1800	5	928±27	108520±210	21±9	2028±66
3	1200	5	632±20	100980±245	18±5	1986±45
4	1800	20	849±32	175290±420	20±10	4729±42

bg: background

Table 19b: Coincidence countrate ratio K for homogeneous distributed C- and D-samples and comparison with the actual value.
C-sample: 383 mg $^{240}Pu_{eq}$; D-sample: 147, 4 mg $^{240}Pu_{eq}$
$K=CR^{i}_{cc}$ (C-hom)/CR^{i}_{cc} (D-hom)

drum no.	K	$^{240}Pu_{eq}$(C) / $^{240}Pu_{eq}$(D)
2	2,86±0,15	
1	2,59±0,13	2,598
3	2,75±0,14	

Table 20: Detection sensitivity for different matrix materials. Homogeneous Pu sample distribution and sample in drum centre

Vol of drum (l)	matrix	sensitivity $\varepsilon_{cc,eff}$ homogeneous inner (%)	homogeneous outer (%)	centered inner (%)	centered outer (%)
220 l	empty*	12,9	5,5	13,1	6,3
220 l	PE foam no.2	11,2	3,7	11,5	3,9
220 l	PE foam no.1	8	2,5	6,2	2,0
220 l	concrete	8,3	2,5	5,0	1,3
100 l	PE foam no.7	9,8	3,6	9,1	3,0
25 l	PE foam no.10	12,6	4,2	13	5,0

(*) Actually no homogeneous sample distribution was used but a single sample. Homogeneous sample distribution was obtained by superposiiton.

Table 21: Results of coincidence measurements: sealed drums

CEC code	t_m (sec)	date	N_m	totals inner ring		coincidences inner ring		totals outer ring		coincidences outer ring		$^{240}Pu_{eff}$ (1)	gPu_{tot}
				bg	3,18 net	bg	3,1 net	bg	net	bg	net	(mg)	
5S	1800	27.4.84	20	912±35	115740±436	24±12	2168±35	1000±48	36300±190	120±35	227±60	460±22	1,3±0,1
6S	900	30.4.84	10	458±28	184900±470	9±13	3345±65	475±18	59470±250	33±6	376±32	1420±60	4,0±0,2
7S	360	30.4.84	10	184±12	146640±536	4±2	3931±90	190±12	48654±126	13±6	492±31	2520±80	4,1±0,2
8S	1200	30.4.84	6	610±31	113160±342	12±3	2687±75	634±19	33310±192	44±8	273±22	520±20	2,1±0,1
9R	300	27.4.84	10	152±11	460175±267	4±3	3811±210	167±20	170740±514	20±7	543±155	4860±280	13,0±1,0
10R	600	27.4.84	10	304±15	166820±380	8±5	4682±72	333±27	68860±221	40±11	705±40	1800±45	8,8±0,2
12R	240	3.5.84	15	122±21	224290±378	3±2	3394±105	127±10	96885±318	9±6	387±118	5410±210	17,7±0,7
13R	240	3.5.84	15	122±21	185850±356	3±2	2975±85	127±10	76360±262	9±6	307±98	4740±185	13,2±0,6
14R	900	3.5.84	10	458±28	254060±533	9±3	3818±80	475±18	112450±270	33±13	497±76	980±25	5,3±0,2
A	20		15		25260±165		220±20		12810±140		29±6	4210±420	17,4 ± 1,7
B	20		15		18160±180		185±15		9360±320		34±7	3543±300	14,7 ± 1,2
C	40		15		20530±250		247±15		9930±180		38±5	1417± 80	5,6 ± 0,35

(1) Evaluation without any corrections for sample distribution and matrix material. It has been assumed that the matrix of all 220 l drums is equivalent to that of modular drum No.1 and that the matrix of all 100 l drums is equivalent to that of modular drum No.3.
The sample distribution is assumed to be homogeneous.
The errors given only are due to counting statistics. In a second step evaluation is done, by using the features of the well counter as described in the text.

Table 22: Final results of coincidence measurements for sealed drums

CEC code	t_m (sec)	$^{240}Pu_{eq}$ (1) mg	mass Pu_{tot} g	Sources of error and amplitudes (%) statistics (1)	isotope composition (2)	matrix and sample distribut.	
5S	1800	460±22	1,3	3	3	20	(3)
6S	900	1665±60	4,6	3	3	30	(3)
7S	360	2520±80	4,1	3	3	20	(4)
8S	1200	520±20	2,1	4	3	20	(4)
9R	300	2920±240	7,8	8	5	30	(5)
10R	600	1800±40	8,8	2	5	25	(4)
12R	240	4360±150	14,2	5	5	30	(5)
13R	900	3780±120	10,5	4	5	30	(5)
14R	900	980±25	5,3	3	5	25	(4)
A	20		13	10	5	30	(5)
B	20		10,9	8	5	30	(5)
C	40		5,6	6	5	25	(4)

(1) the errors only are due to statistics (1σ), including uncertainty due to calibration

(2) the isotopic composition has been determined by γ-spectroscopy

(3) sample distribution from neutron autoradiography, matrix from transmission measurement of pulsed method

(4) matrix equivalent to drum no.3, samples in drum region R≈10 cm, sample distribution approximately equivalent to homogeneous distribution

(5) matrix guess from coincidence countrate ratio, sample distribution from neutron radiography. Matrix for drum 9R equivalent to drum no.2; for drums 12R and 13R and A and B matrix equivalent to a mean from drum no.1 and no.2.

Table 23: Matrix identification for the two systems

drum no.	pulsed	coincidence
5S	equivalent to no. 1	matrix identification from pulsed measurement
6S		
7S	equivalent to no.3	
8S		
9R	obscured due to additional neutron absorbers, however matrix corrections factor known from calibration measurement	coincidence countrate ratio equivalent no.2
10R		equivalent to drum no.3
12R		no clear decision possible
13R		therefore matrix as mean of no.2 and no.1
14R		equivalent to drum no.3
A		matrix as mean of no.2 and no.1
B (*)		
C		equivalent to drum no.3

(*)
From the monitor countrate it is concluded that the drums A,B and C are containing very similar matrix materials to drums 12R, 13R and 14R, therefore the same matrix correction factors have been used.

Table 24: Comparison of results

drum	Vol. (l)	g Pu_{tot}		
		coincidence	pulsed	true
5S	220	1,3 ±0,26	1,2±0,24	0,95
6S	220	4,6 ±1,5	1,8±0,36	3,49
7S	100	4,1 ±0,8	1,9±0,3	4,13
8S	100	2,1 ±0,4	1,2±0,2	2,4
9R	220	7,8 ±2,4	9,2±3,4	4,8
10R	100	8,8 ±2,2	9,9±3,4	5,2
12R	220	14,2 ±4,2	14,0±4,1	10,4
13R	220	10,5 ±3,0	4,1±1,2	7,6
14R	100	5,3 ±1,3	4,4±1,5	3,83
A	220	13,0 ±4	9,6±2,0	15,0
B	220	10,9 ±3,2	5,3±1,5	10,6
C	100	5,6 ±1,1	3,4±1,0	5,1

Table 25: Results of evaluation of the coincidence measurements for the scaled drums using known matrix density values.

drum	Vol. (l)	matrix g/cm³	density correction g Pu_{tot}	hydrogen correction	actual Pu_{mass}
5S	220	0,206	0,85	0,85	0,95
6S	220	0,236	3,17	3,17	3,49
7S	100	0,254	4,0	4,0	4,13
8S	100	0,297	2.23	2.23	2.4
9R	220	0,117	6,15	5,0	4,8
10R	100	0,193	7,0	5,6	5,2
12R	220	0,217	12,4	8,7	10,4
13R	220	0,243	11,2	7,0	7,6
14R	100	0,222	4,65	3,8	3,83

Table 26: Comparison of Pu values after matrix and self shielding corrections for the pulsed measurement

drum	actual $^{239}Pu_{eq}$	measured
5S	0,7	0,6
6S	2,5	2,1
7S	1,7	1,2
8S	1,8	1,5

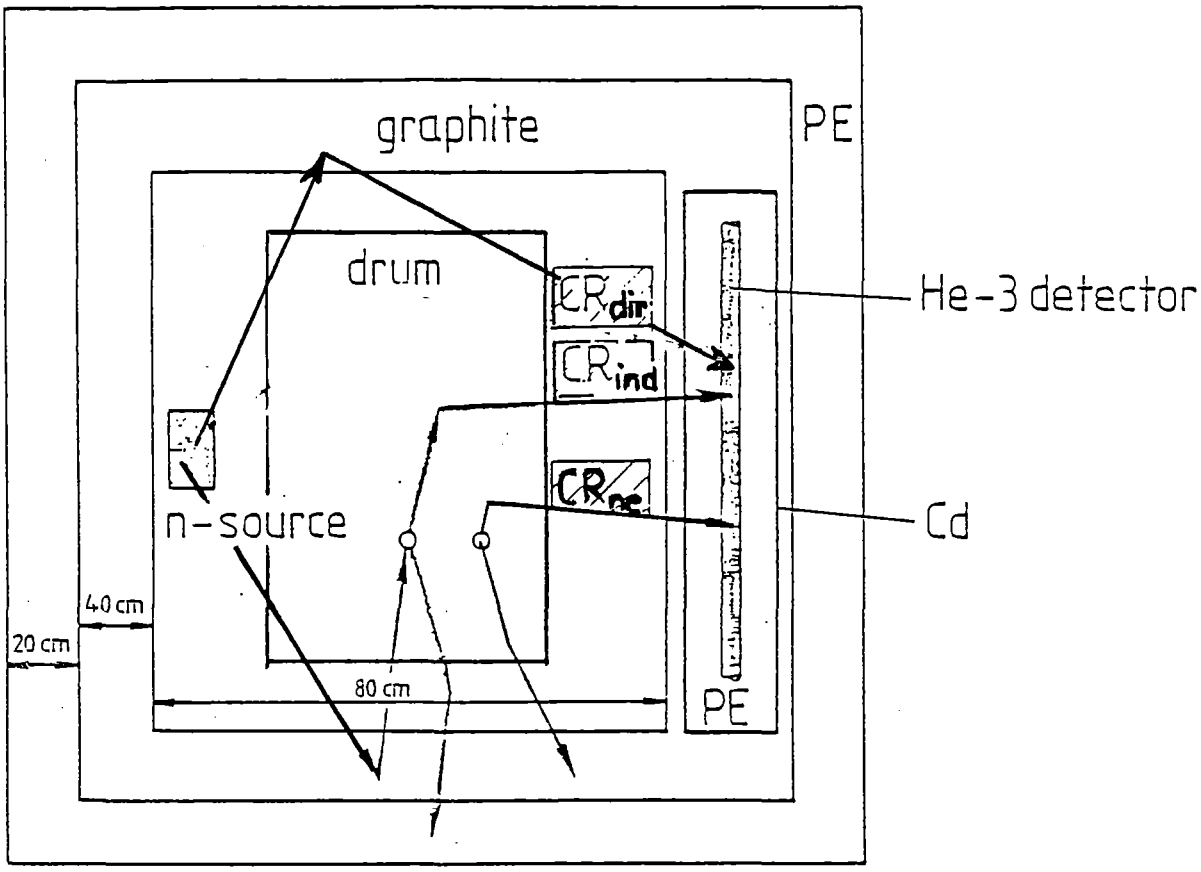

$$CR_{tot} = CR_{dir} + CR_{ind} + CR_{ne}$$

Fig.1

Principle: pulsed neutron source method, cavity size 80 x 100 x 140 cm

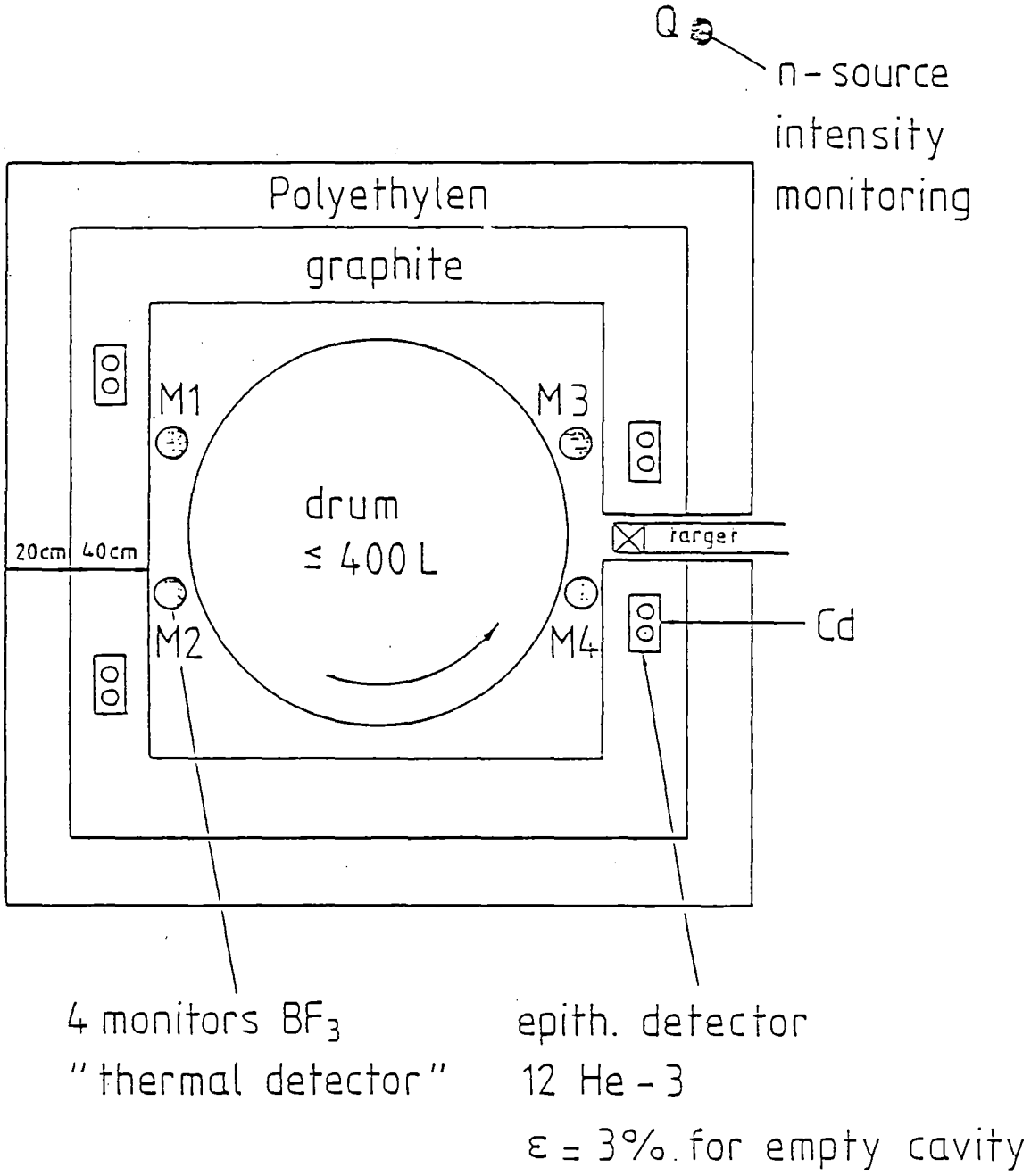

Fig.2

Schematical arrangement for pulsed source measurement

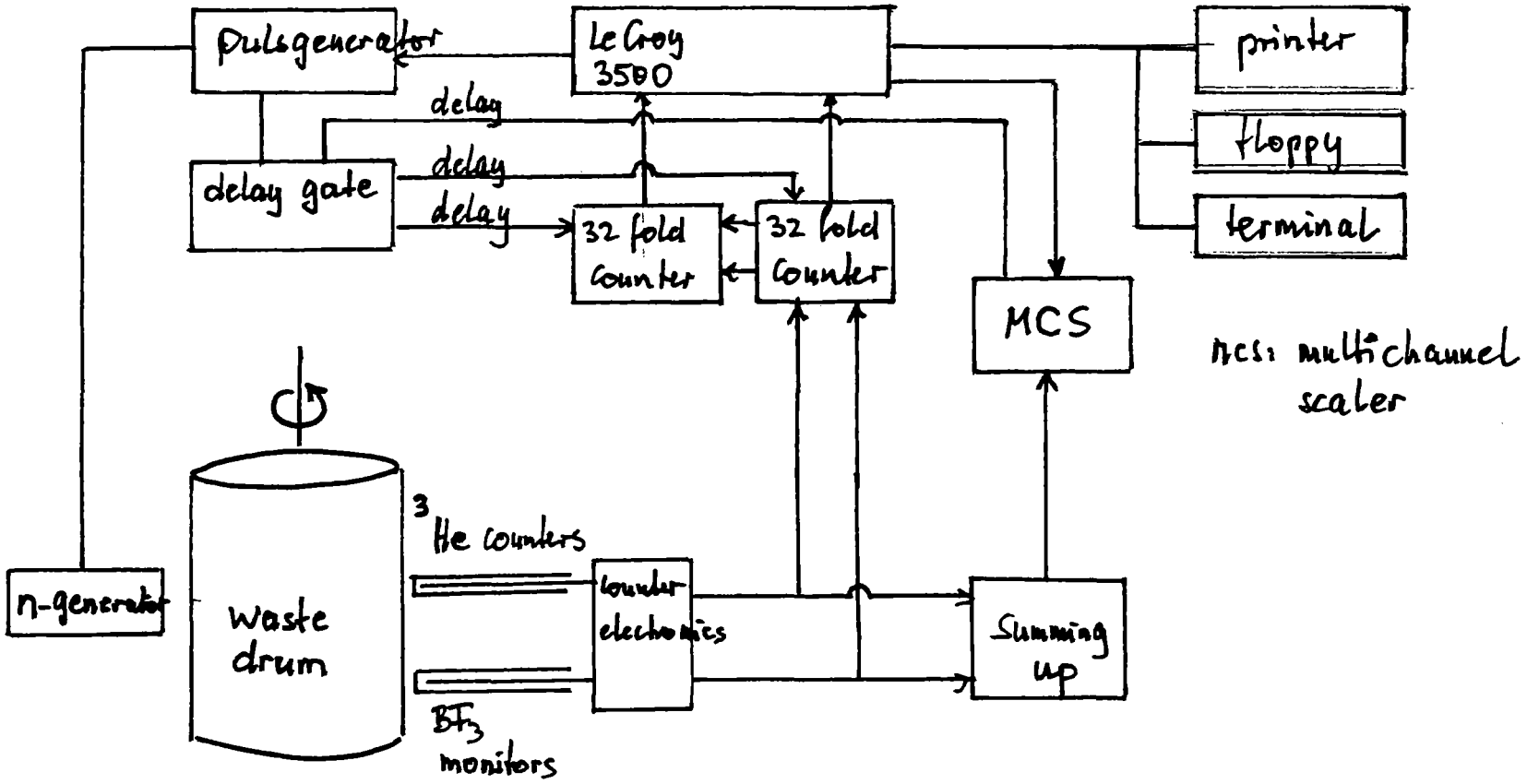

Fig.3:

Schematical arrangement for pulsed measurement system.

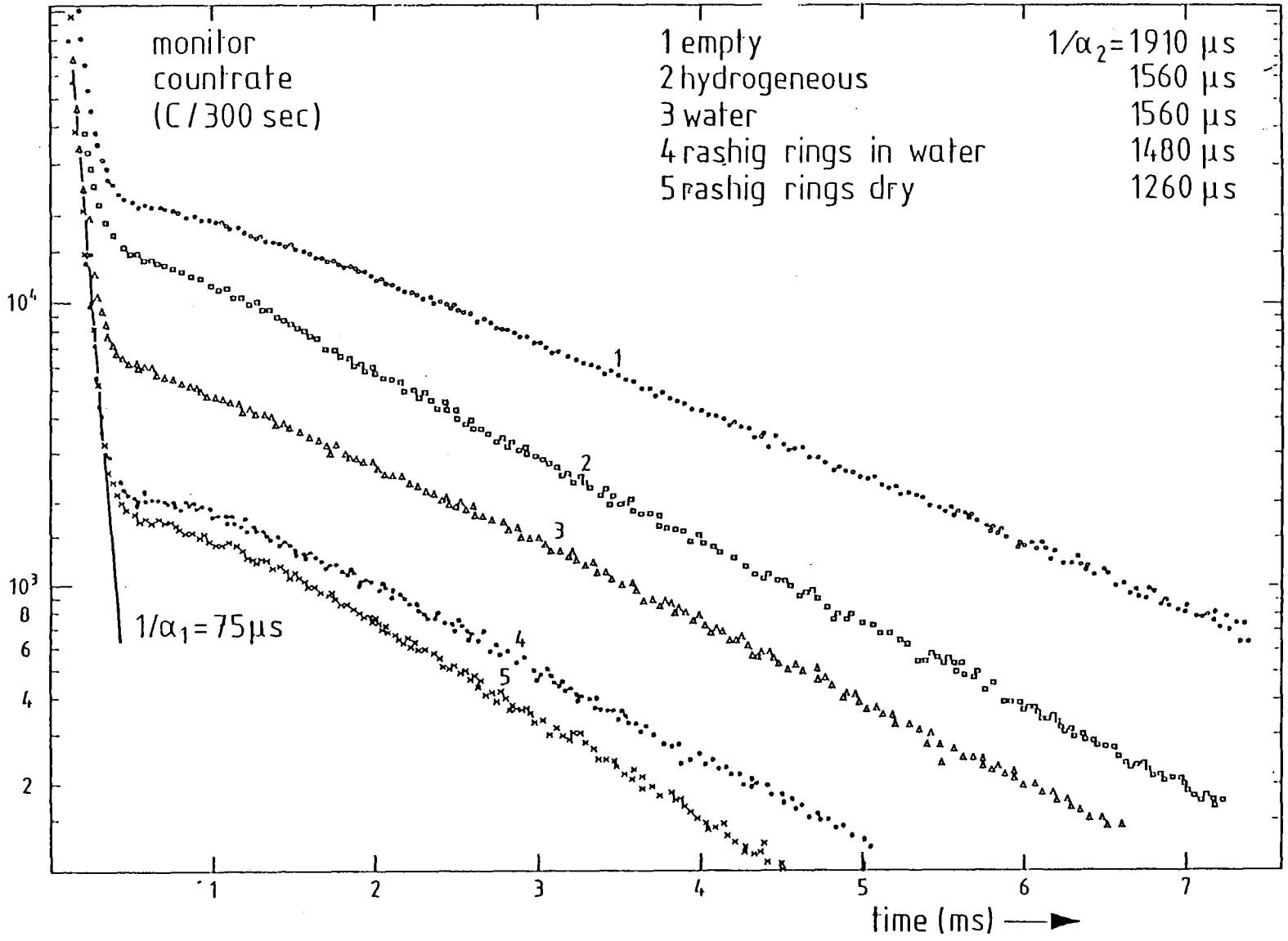

Fig.4

Time dependent monitor countrates. $1/\alpha_2$: thermal neutron life time

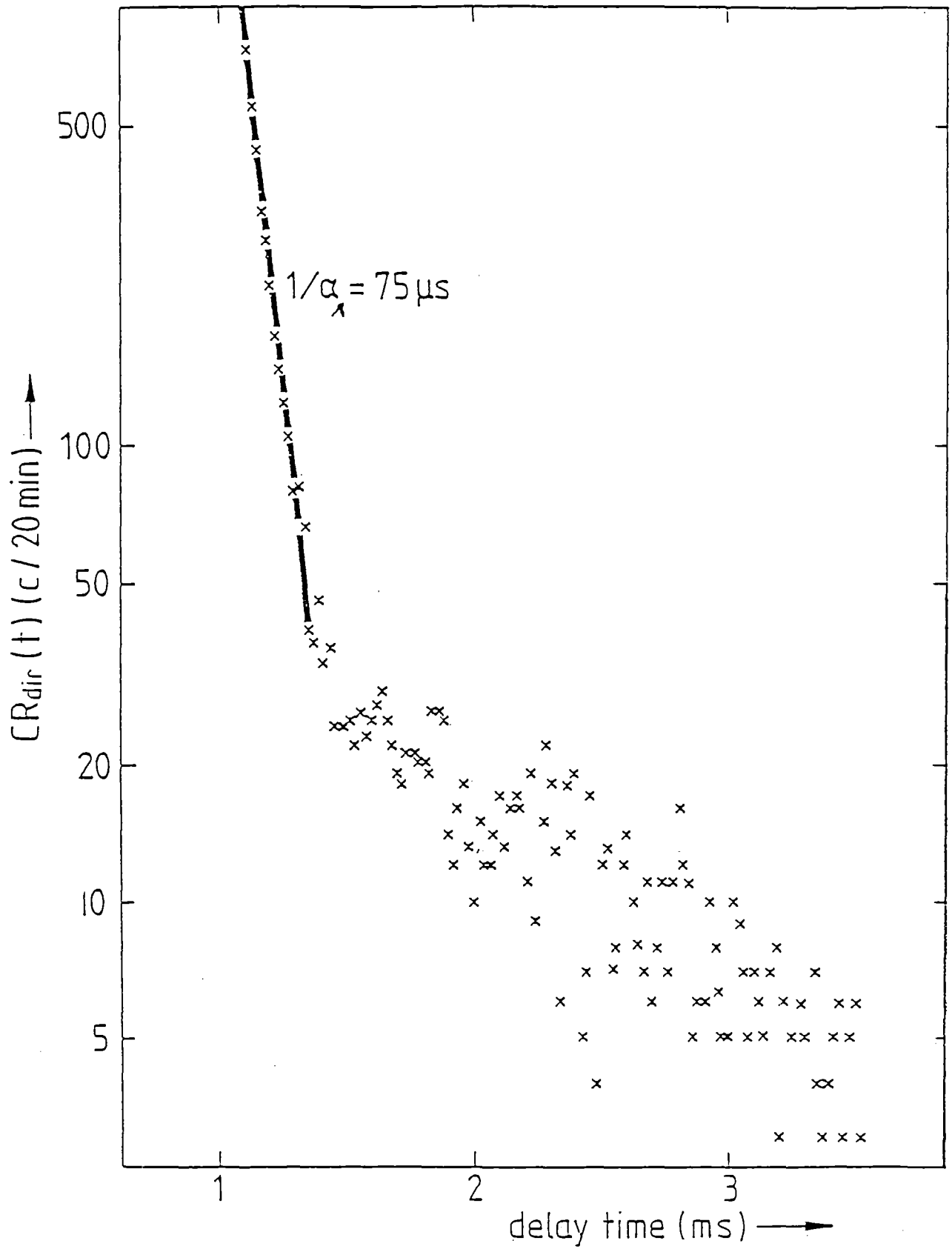

Fig.5

Time dependent background, neutron source 6 10^8 n/sec

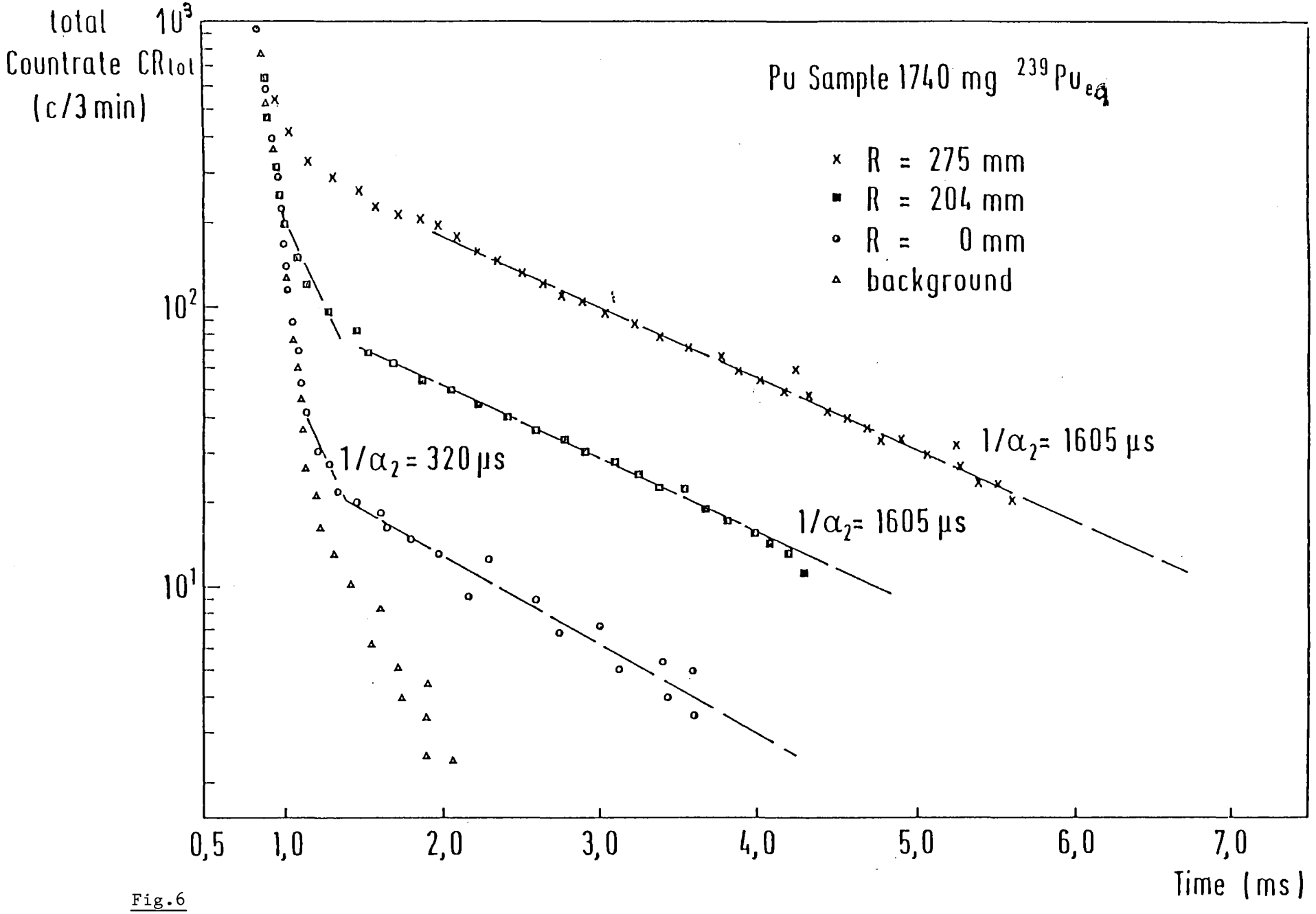

Fig.6

Time dependent total countrates for Pu sample in concrete drum, net corrected for sample self shielding.

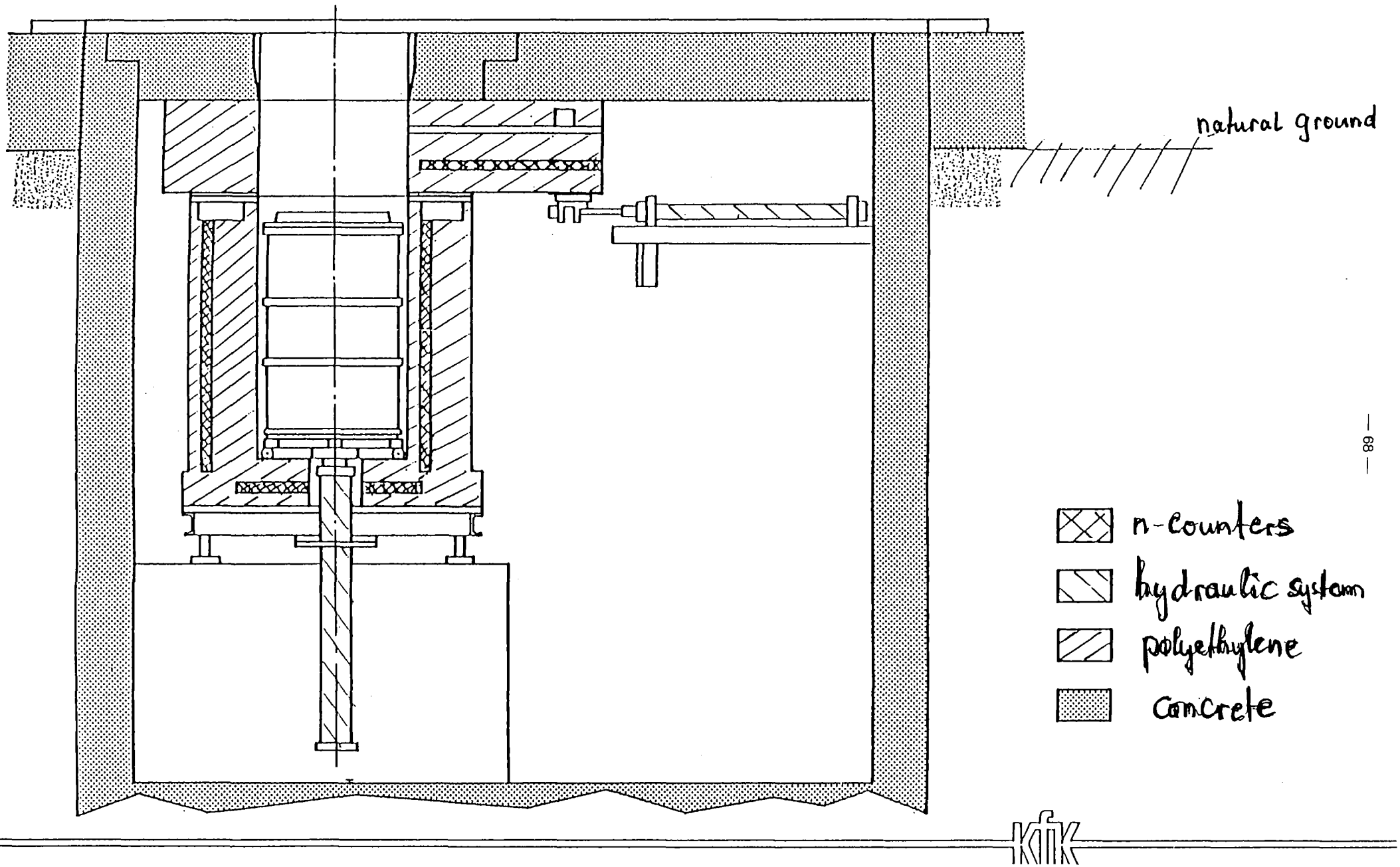

Fig.7

Neutron well counter.

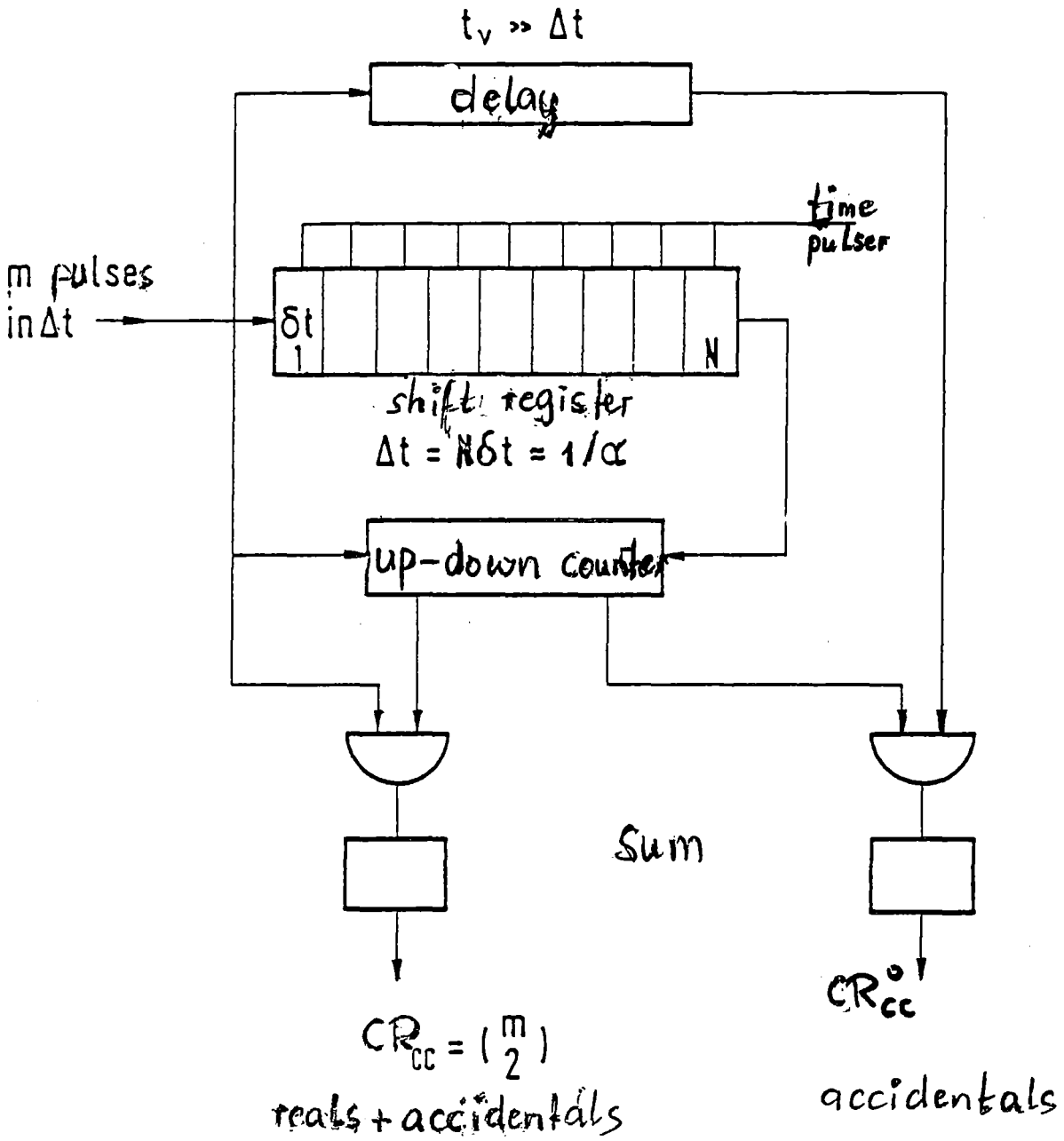

Fig.8

Principle of coincidence measurement.

Discrimination between neutrons from (α,n) and spontaneous fission.

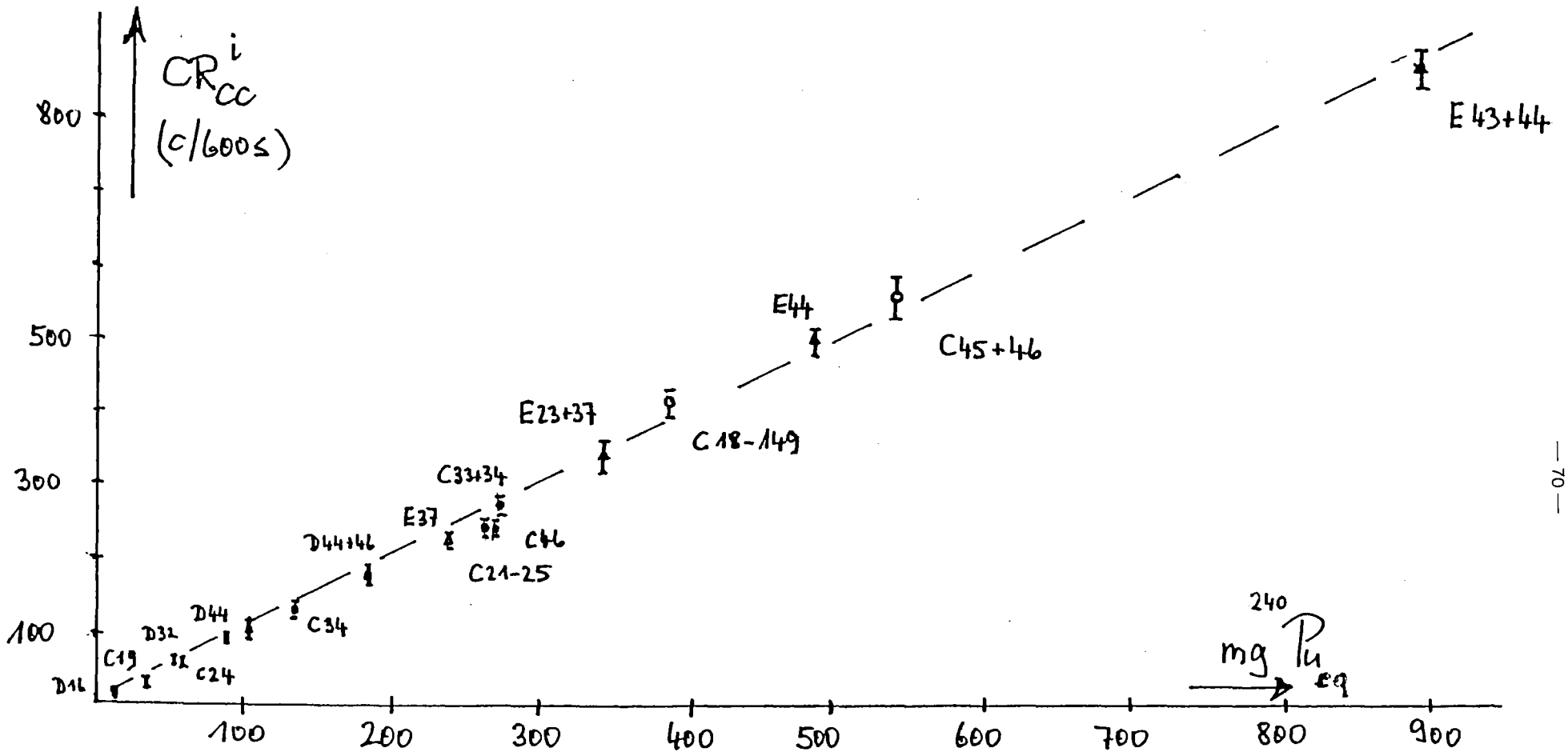

Fig.9

Coincidence countrate for different samples; inner detector layer.

Drum no.1

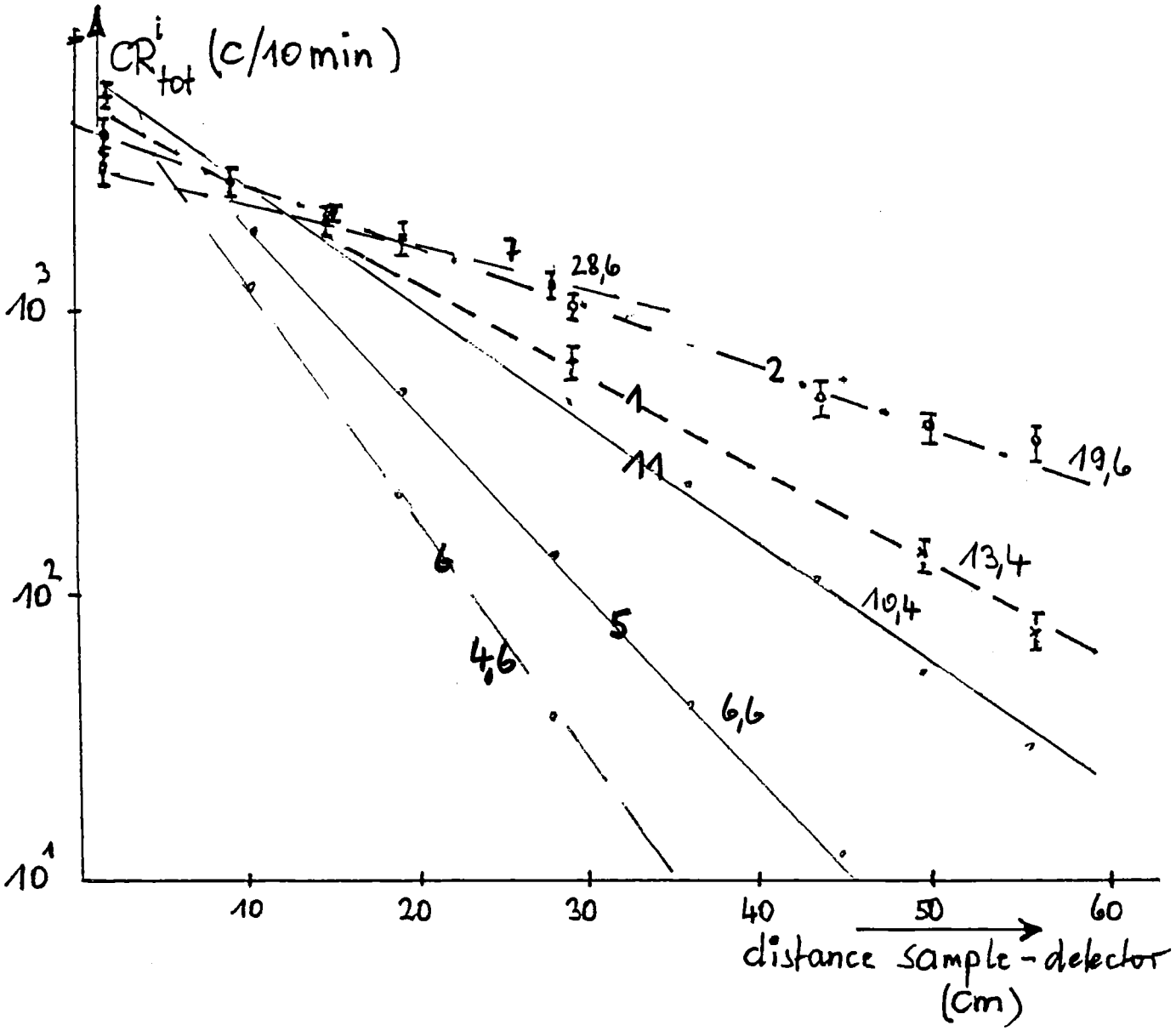

Fig.10

Space dependent total countrate for different matrix materials, normalized to the same source intensity. Numbers at the curves correspond to the matrix according to Table 1. The $1/\Sigma_R$ values are indicated also.

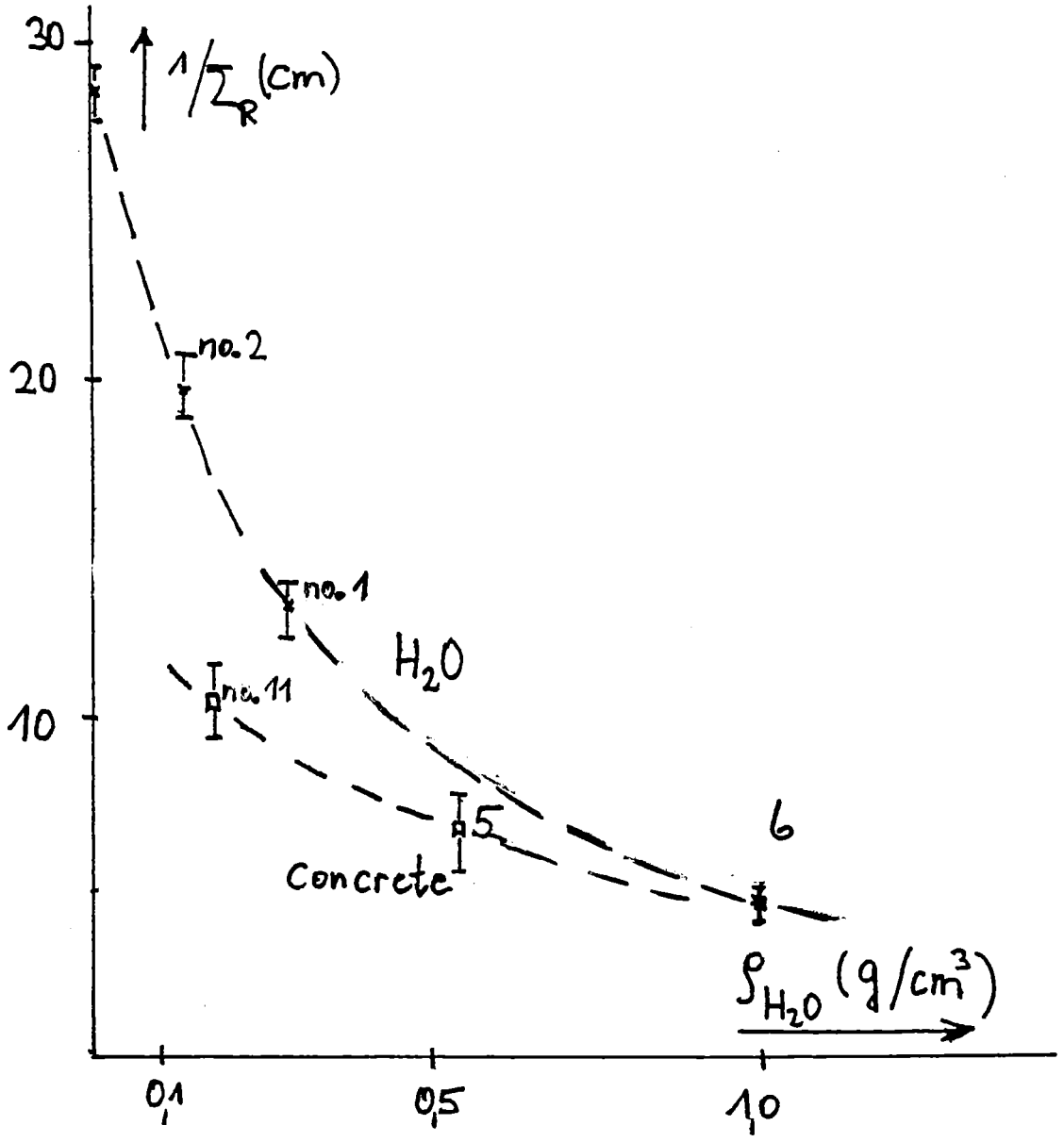

Fig.11

Relaxation length $1/\Sigma_R$ as function of matrix water content. Numbers correspond to the matrix materials according to Table 1. Concrete values are extrapolated to lower and higher water content.

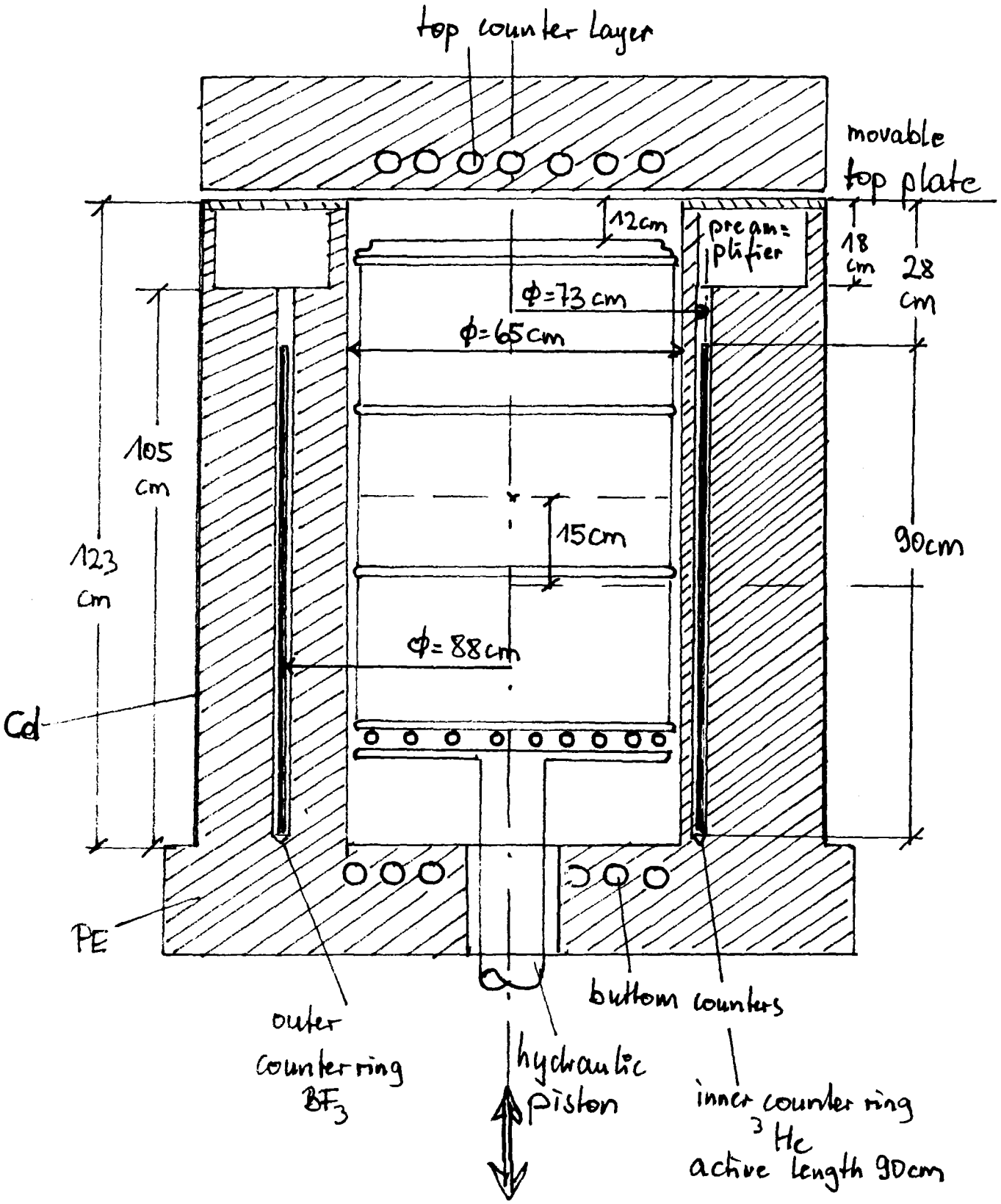

Fig.12

Well counter schematical arrangement

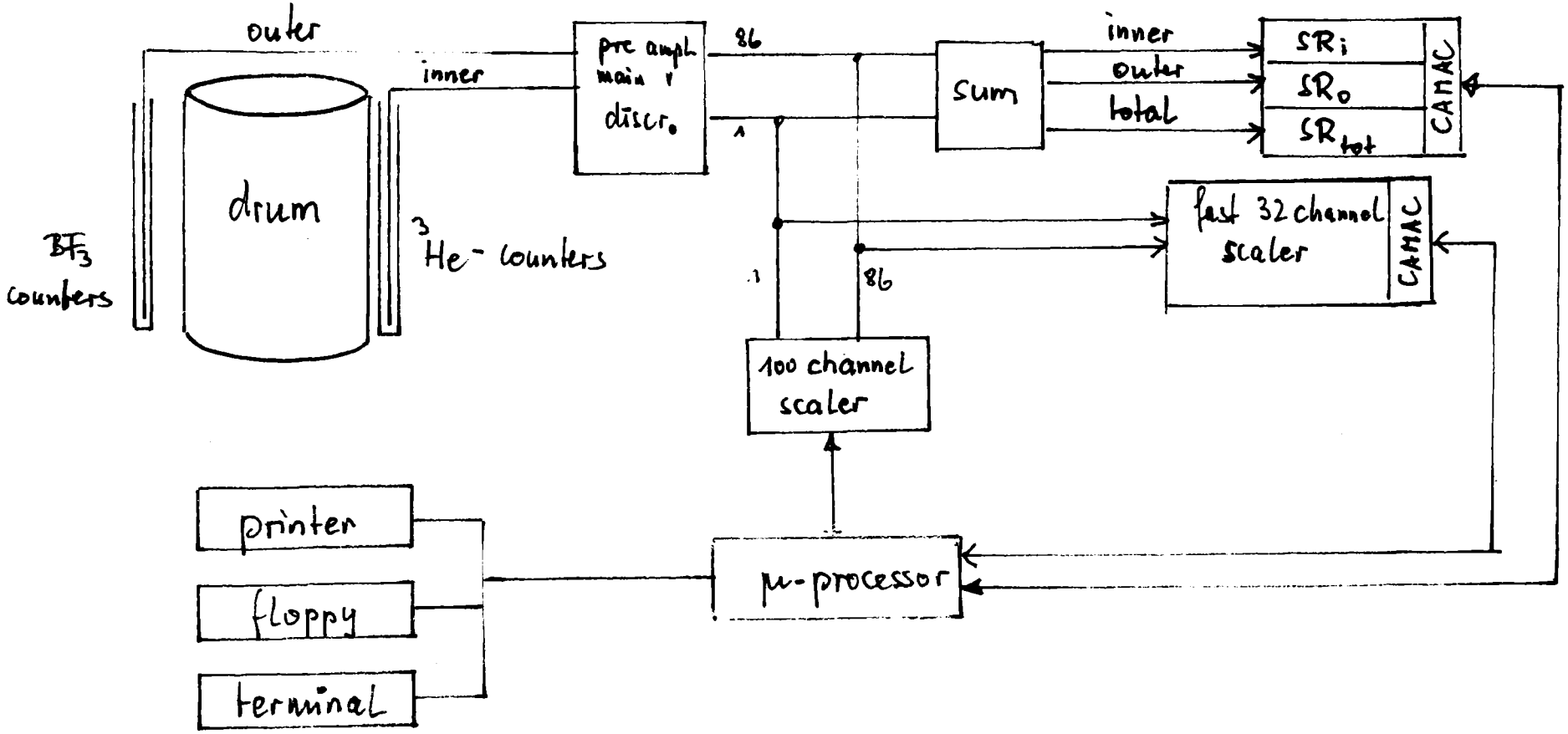

Fig.13

Block diagram of the electronics for the well counter

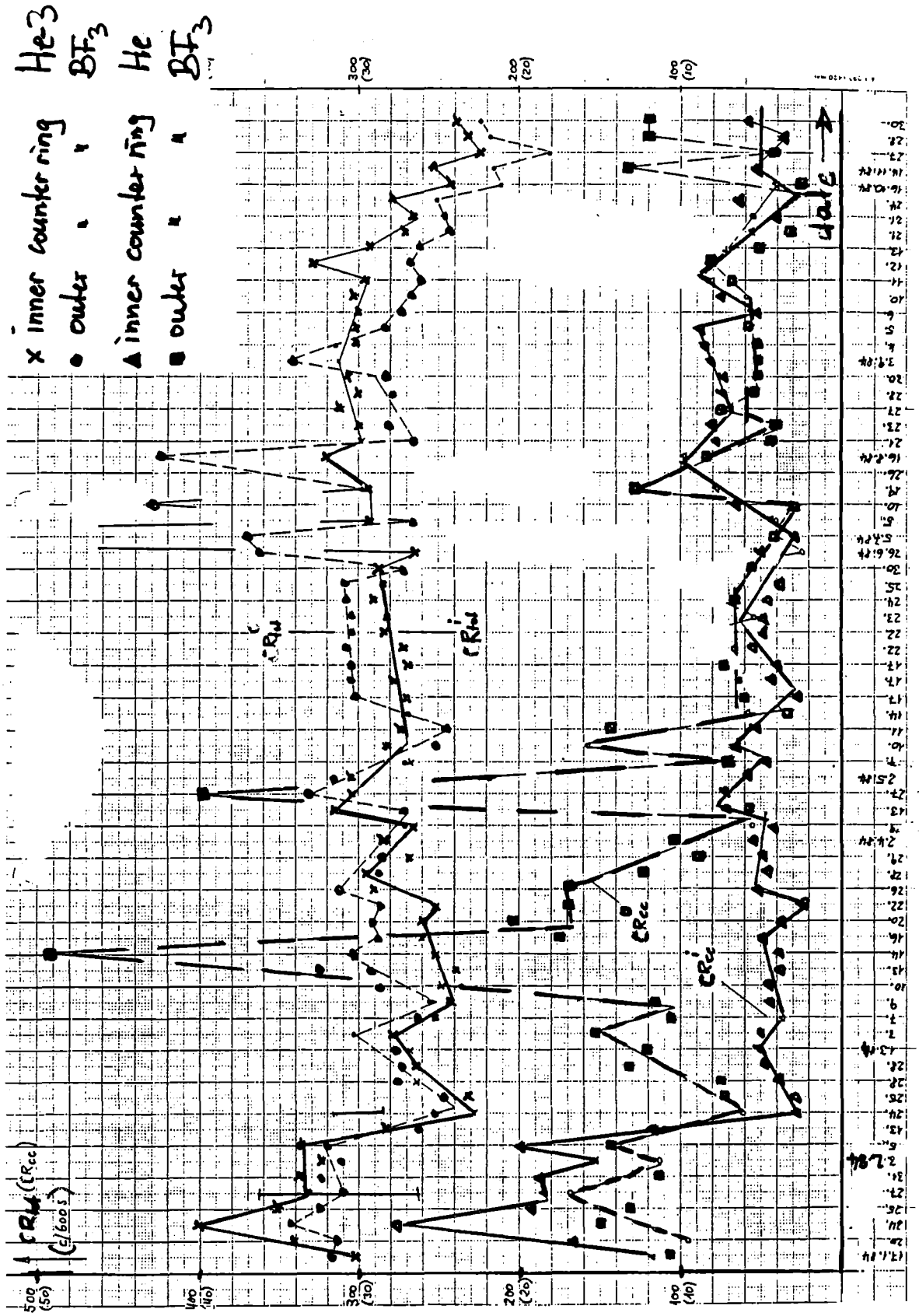

Fig.14

Longtime behavior of the well counter

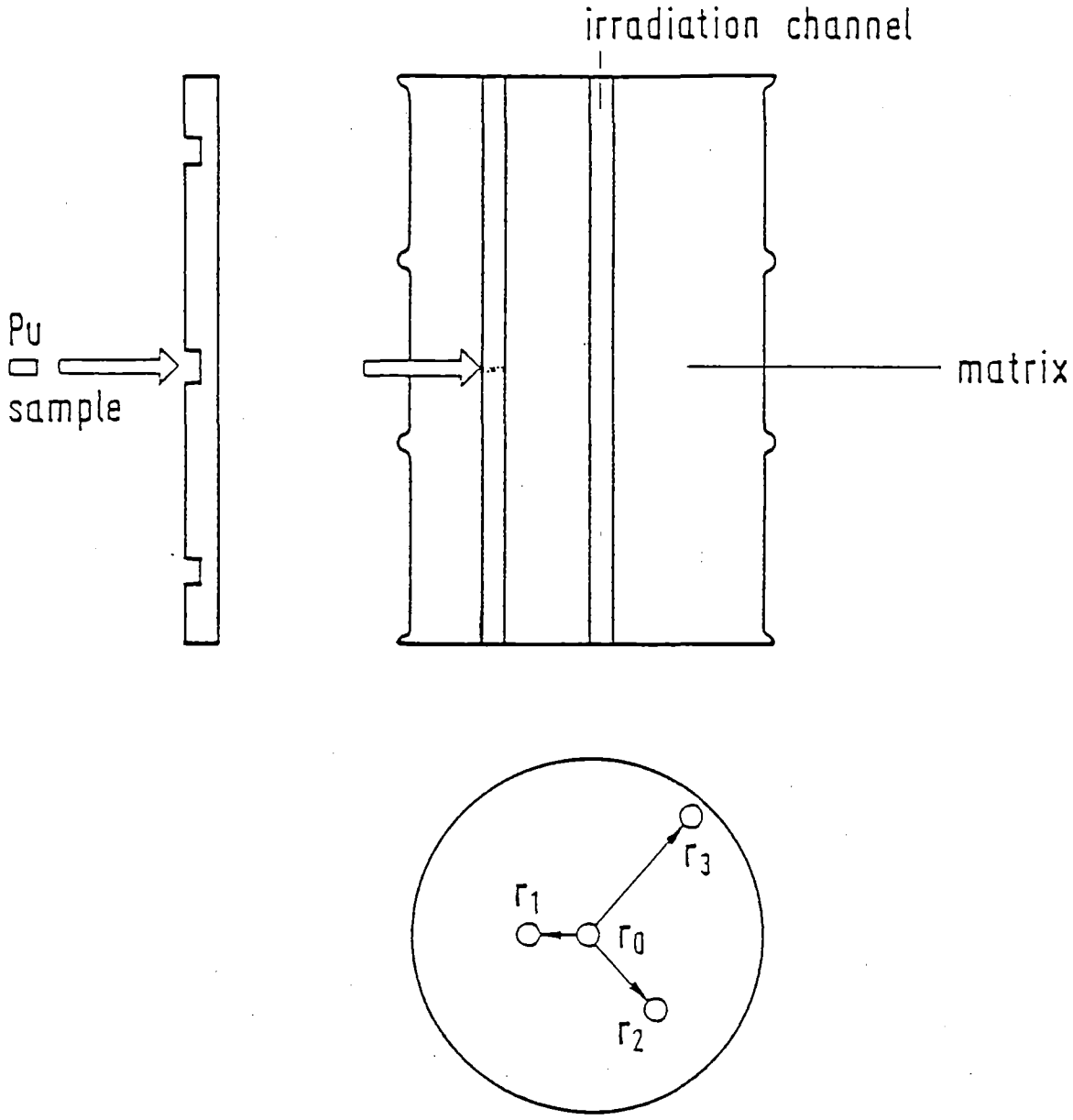

r_1 = 144 mm
r_2 = 204 mm
r_3 = 275 mm

matrix
empty
PE foam
concrete
rashig rings
water

Fig.15

Calibration program

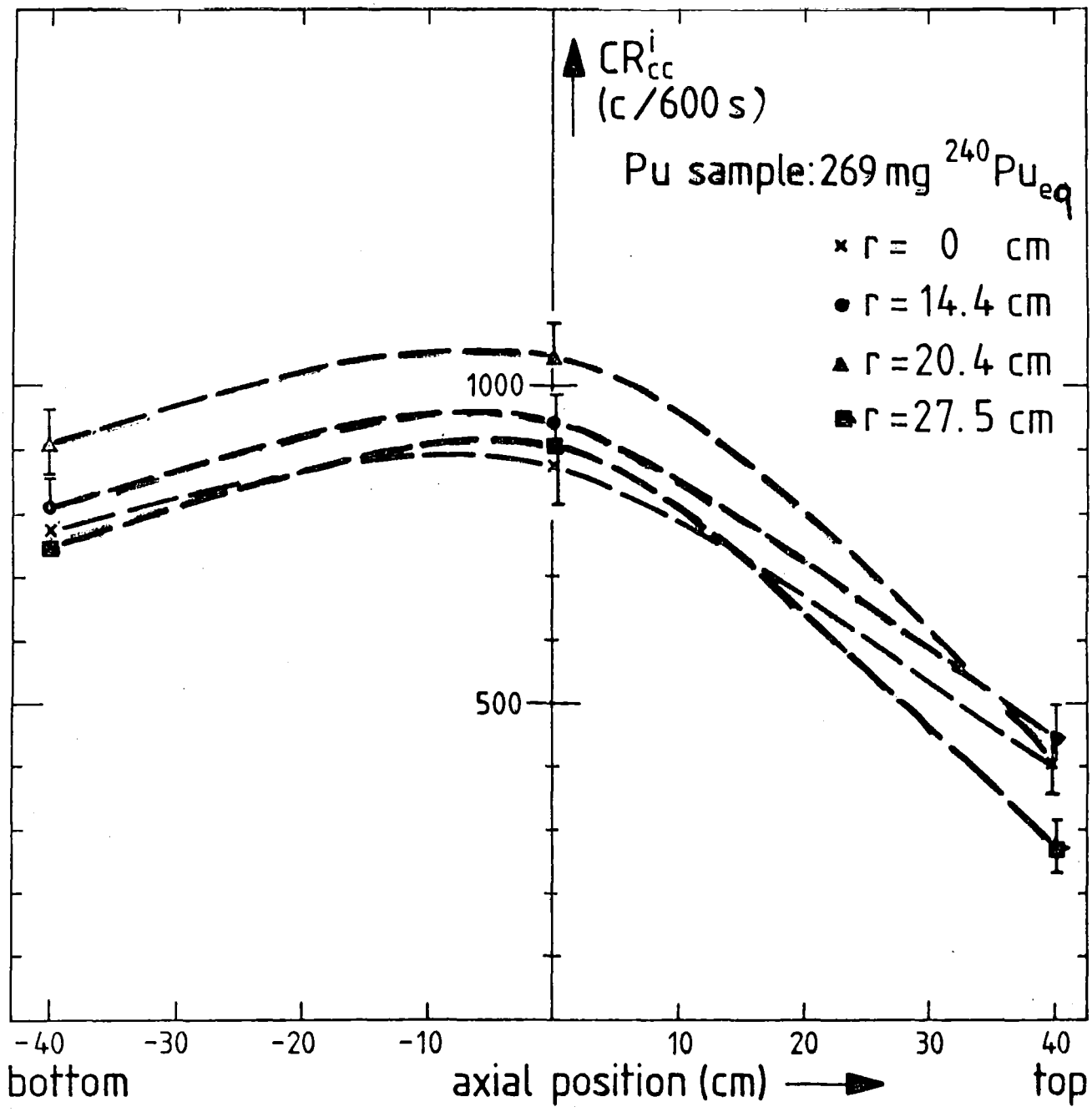

Fig.16

Position dependent coincidence countrates. Drum no.2, inner counter layer, Pu sample at half height.

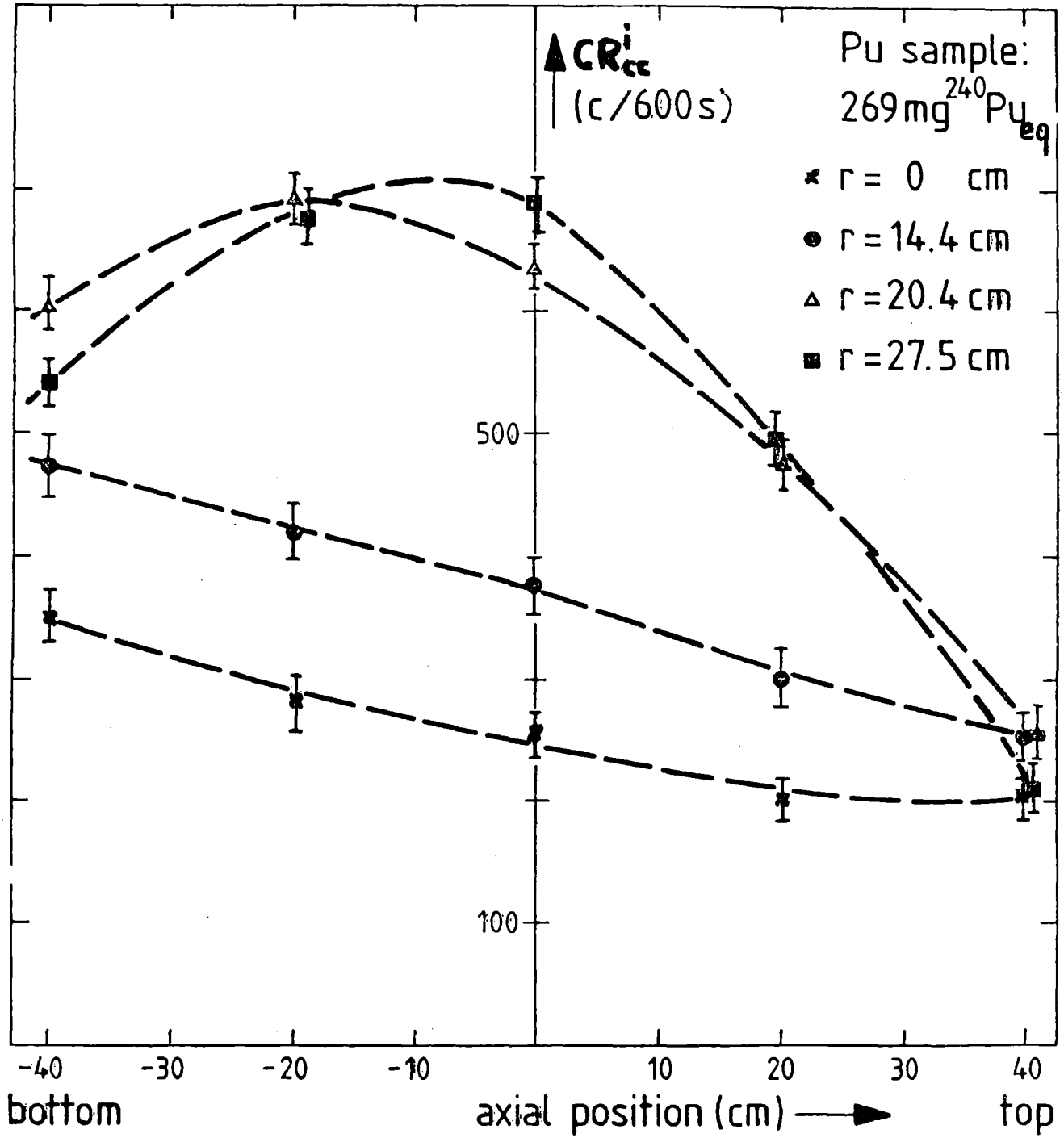

Fig.17

Position dependent coincidence countrates. Drum no.1, inner counter layer, Pu sample at half height.

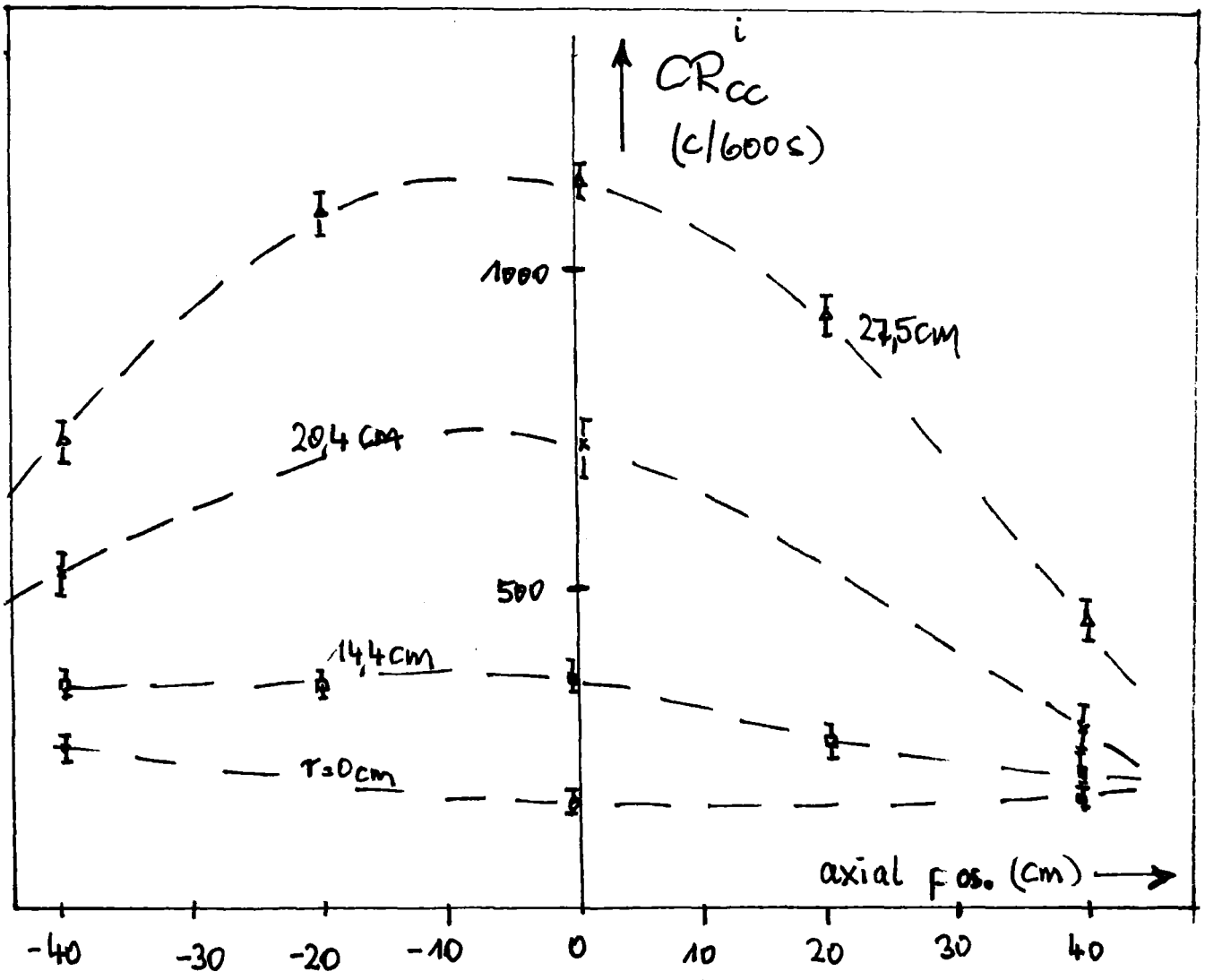

Fig.18

Position dependent coincidence countrate. Drum no.11, inner counter ring, Pu sample 269,5 mg $^{240}Pu_{eq}$.

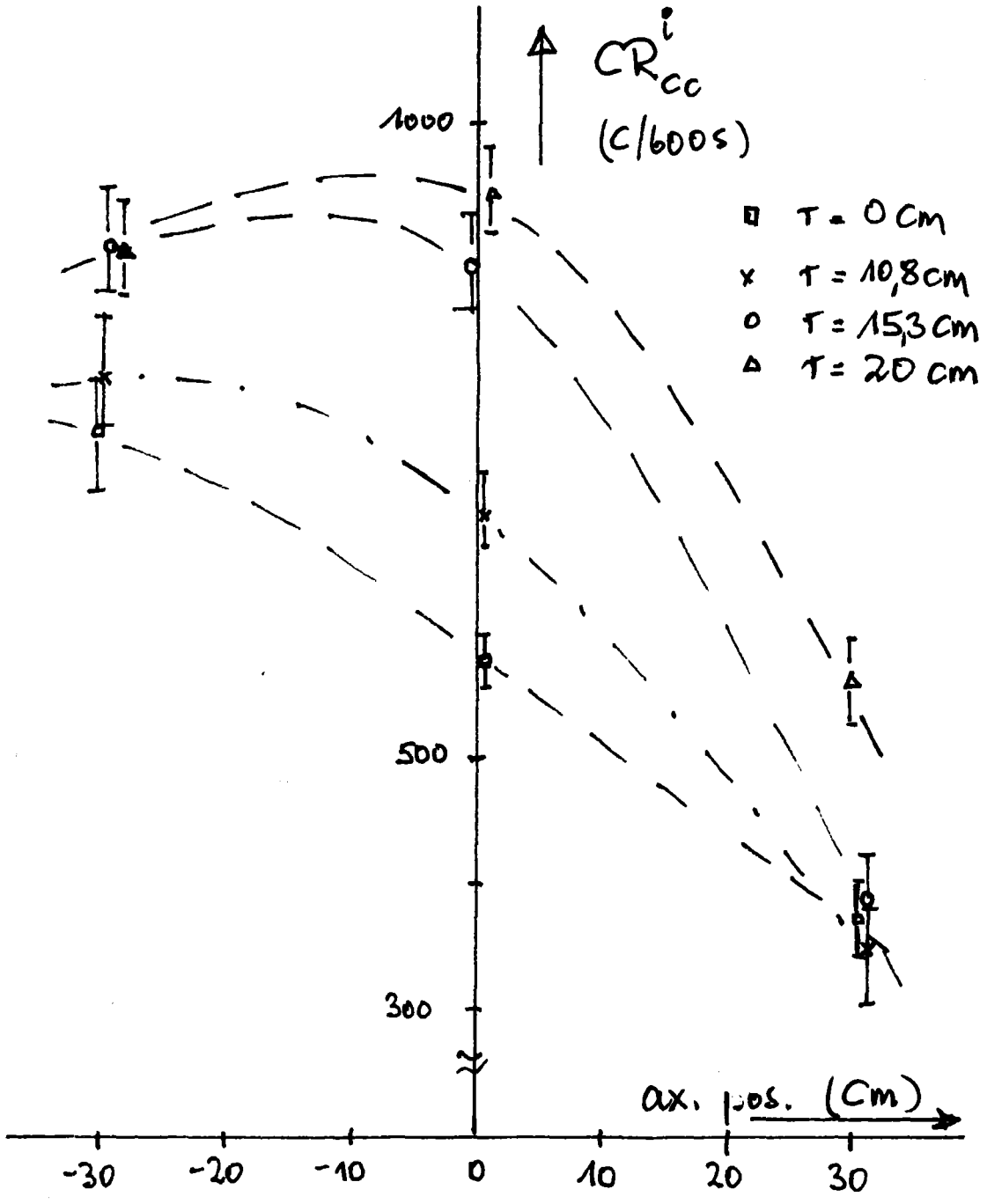

Fig.19

Position dependent coincidence countrate. Drum no.3 (V=100 l), inner counter ring with top and buttom counters; Pu sample 269,5 mg $^{240}Pu_{eq}$.

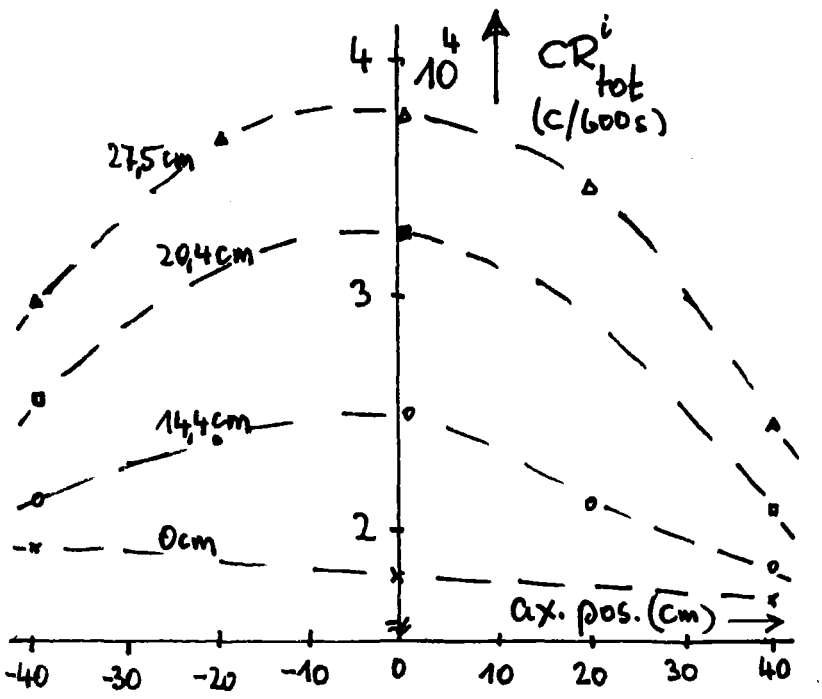

Fig.20a

Axial countrate profiles of totals, counters in the top and buttom reflector.

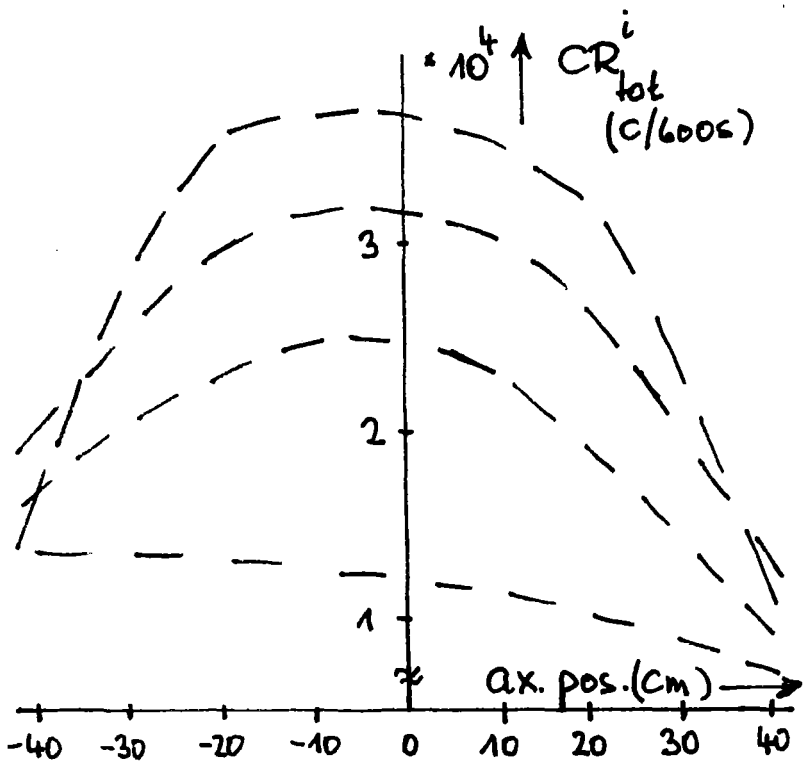

Fig.20b

The same drum and matrix but without top and buttom counters.

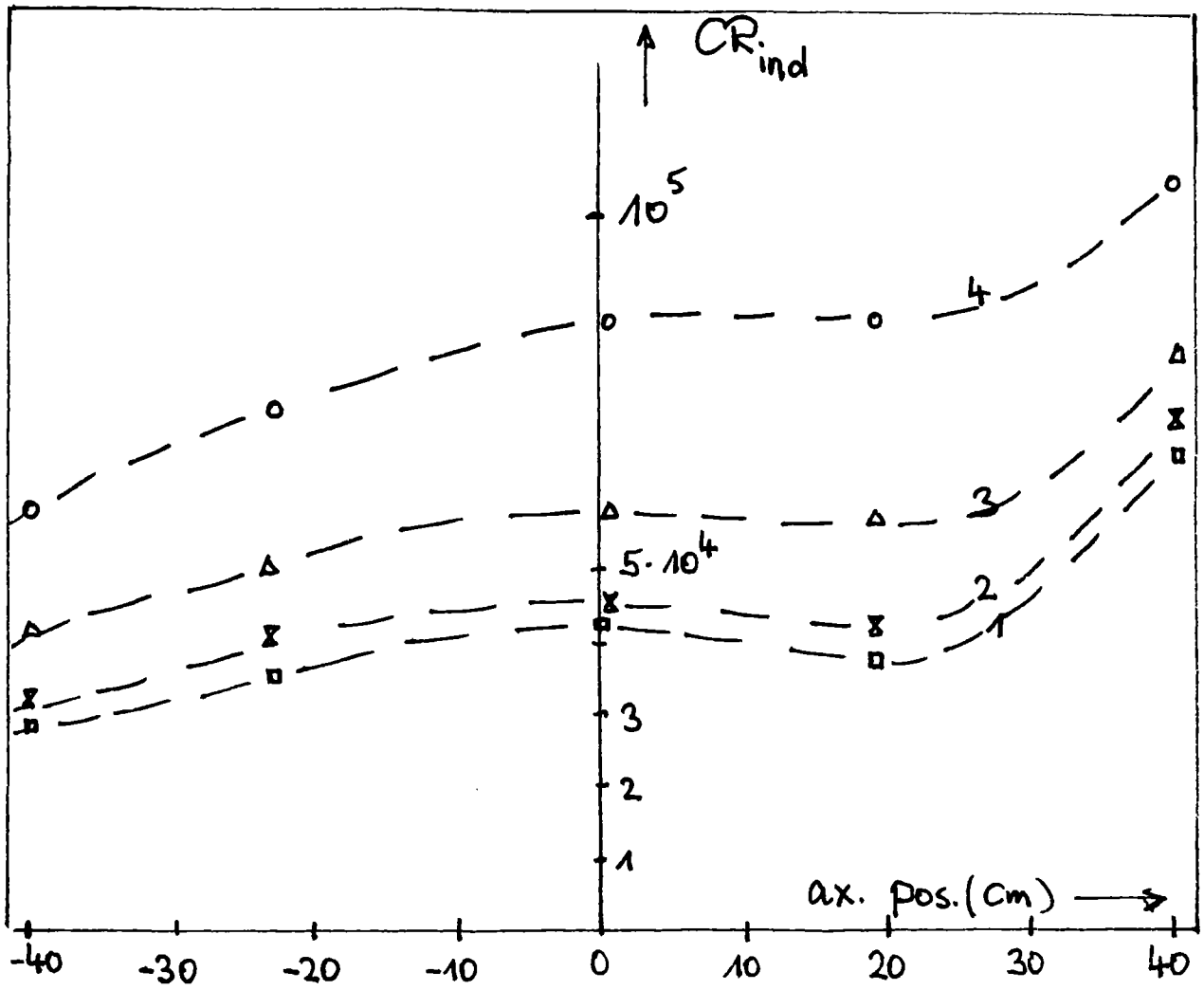

Fig.21

Position dependent induced countrate.
Drum no.1; Pu sample 555,9 mg $^{239}Pu_{eq}$ countrate normalized to a neutron source rate of 2,2 10^{11} n/s, not corrected for sample self shielding-

1: 0 cm
2: 14,4 cm
3: 20,4 cm
4: 27,5 cm

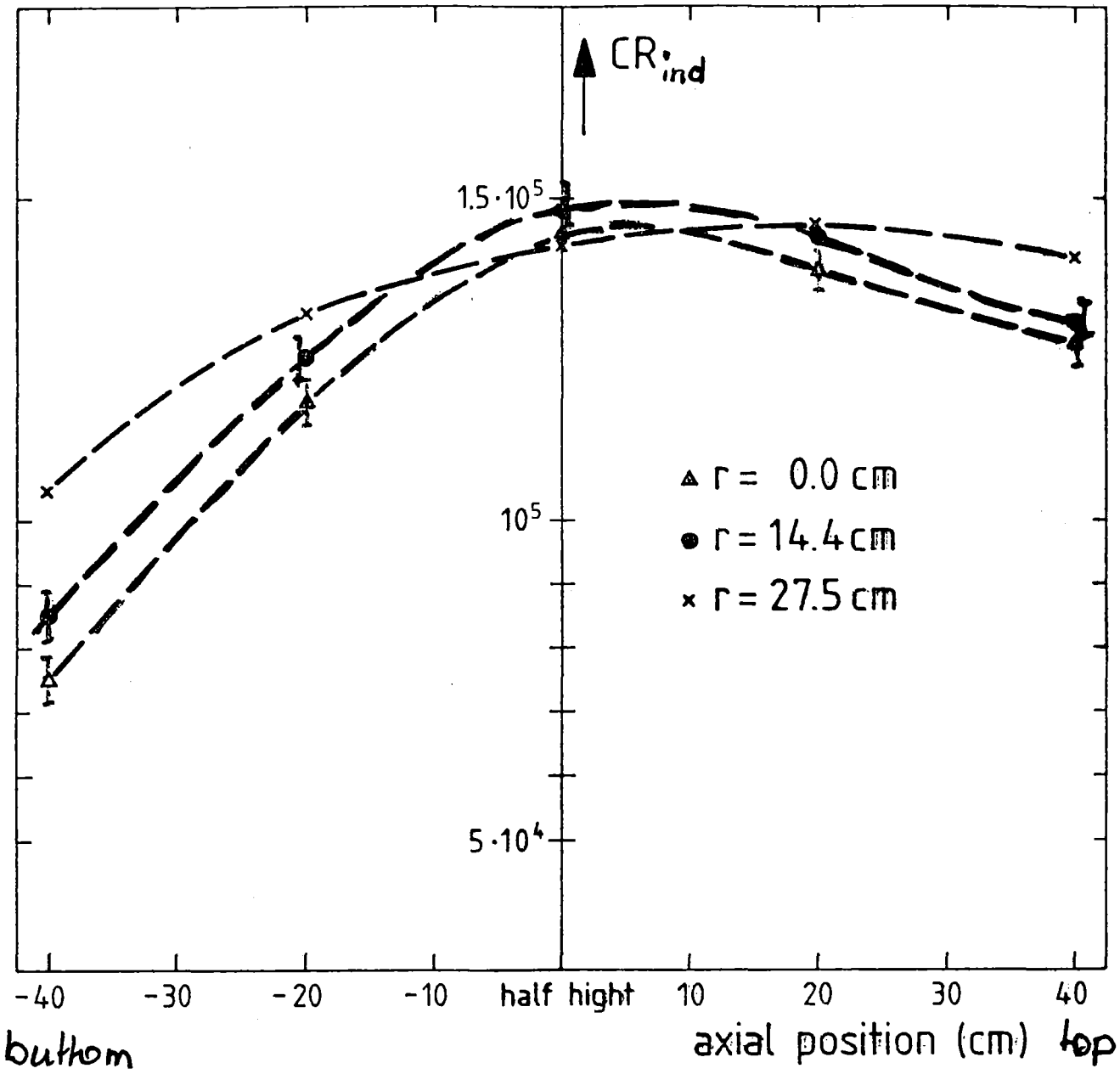

Fig.22

Position dependent countrate. Drum no.2, Pu sample 550 mg $^{239}Pu_{eq}$ at half height. Not corrected for self shielding.

Countrate normalized to a neutron source rate of 2,2 10^{11} n/s.

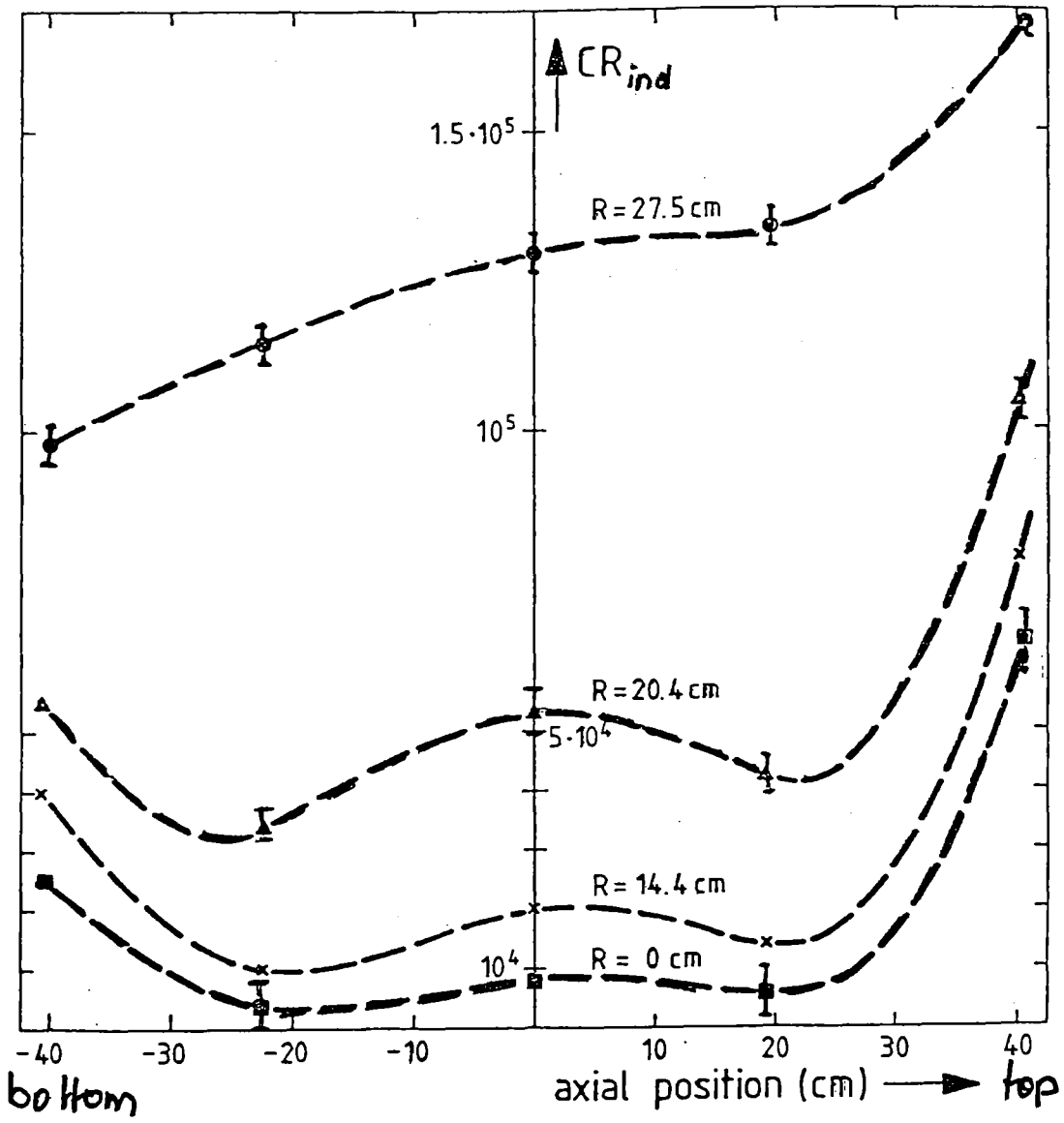

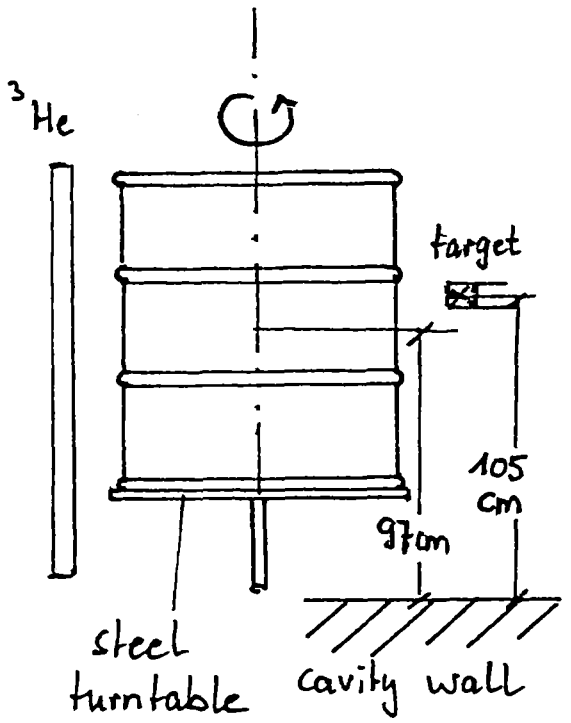

Fig.23

Position dependent countrate. Drum no.11 Pu sample: 1161 mg $^{239}Pu_{eq}$ at half height. Not corrected for self shielding.

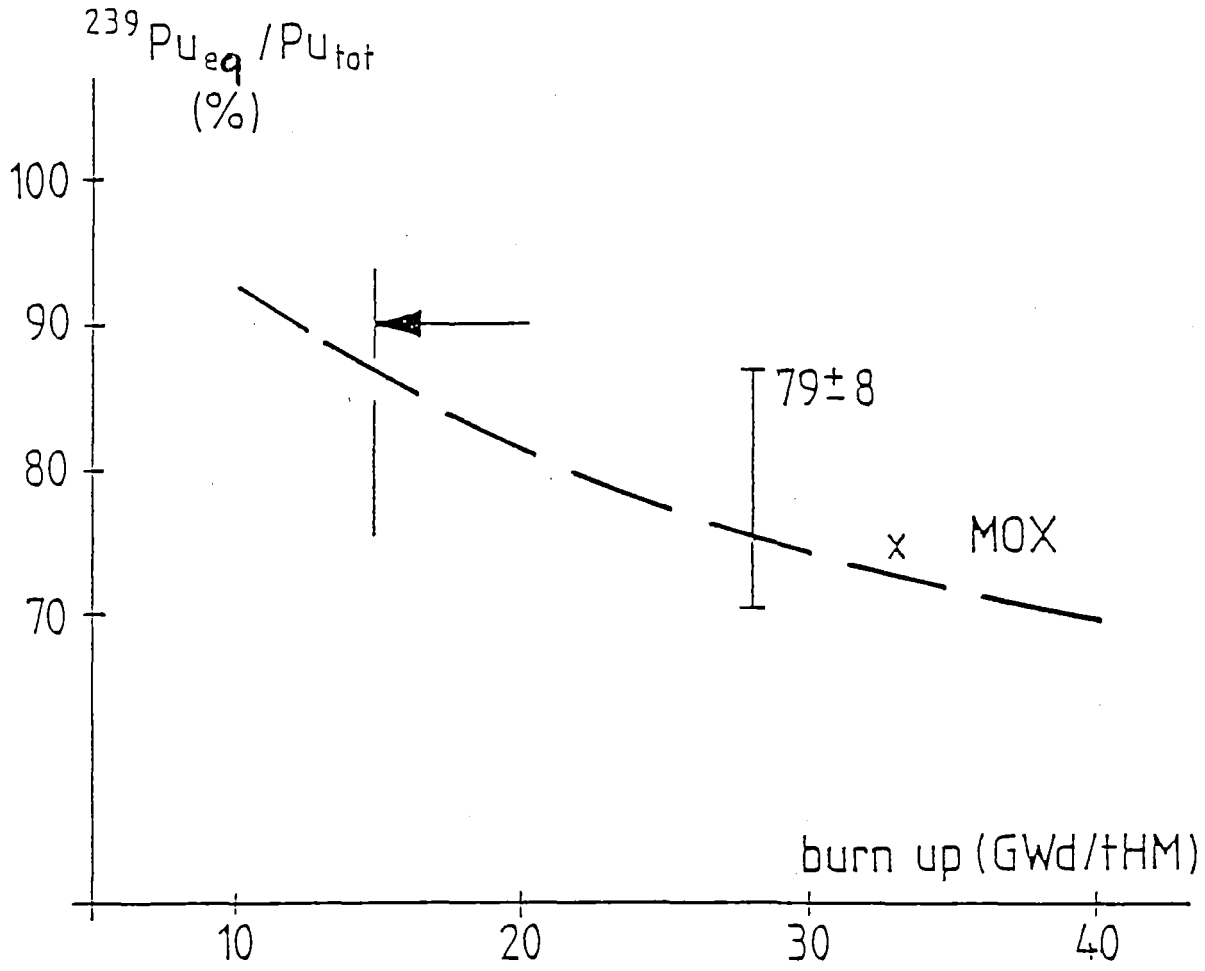

Fig.24

Burn up dependence of $^{239}Pu_{eq}$ for LWR Uranium fuel, initial enrichment: 3,1% U-235

$$^{239}m_{Pu_{eq}} = {}^{239}m_{Pu} + \frac{(v\sigma_f)^{241}}{(v\sigma_f)^{239}} \; {}^{241}m_{Pu} + \frac{(v\sigma_f)^{235}}{(v\sigma_f)^{239}} \; {}^{235}m_U$$

$$= {}^{239}m_{Pu} + 1{,}38 \; {}^{241}m_{Pu} + 0{,}658 \; {}^{235}m_U$$

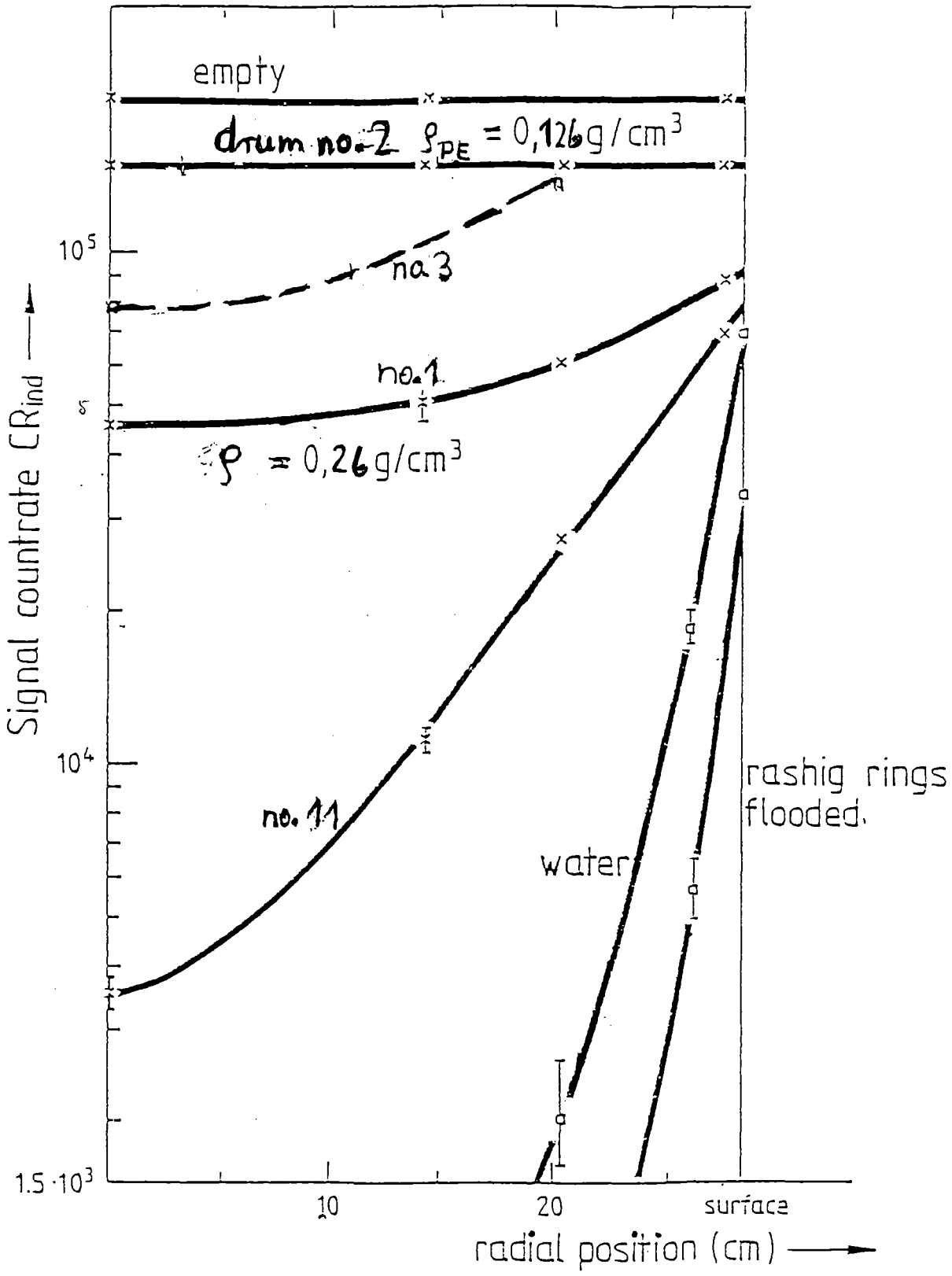

Fig.25

Influence of sample distribution.
Pu sample 550 mg $^{239}Pu_{eq}$ in drums at half height, not corrected for sample selfshielding.

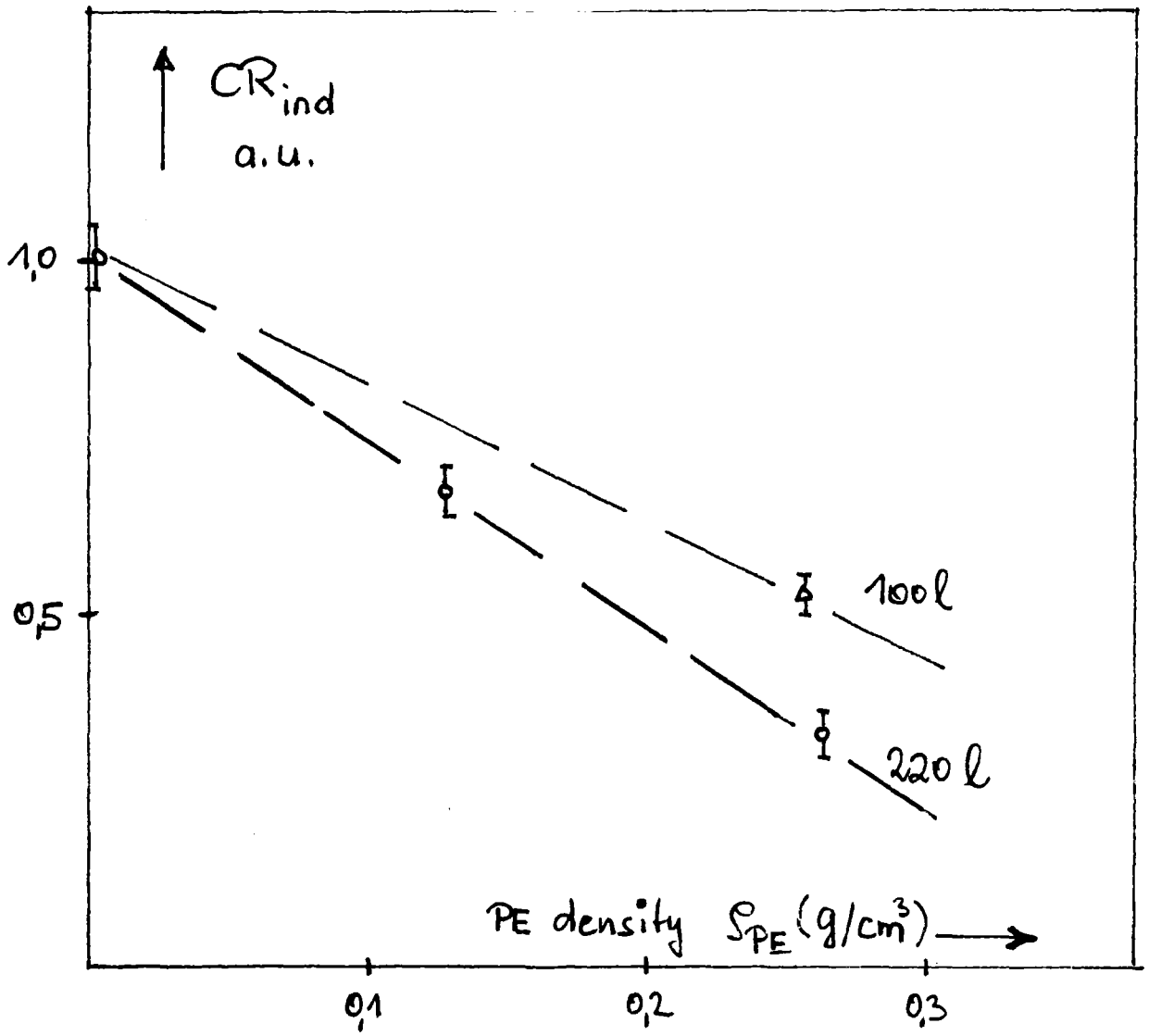

Fig.26

Dependence of the signal countrate on the matrix density. Homogeneous Pu sample distribution, matrix PE foam.

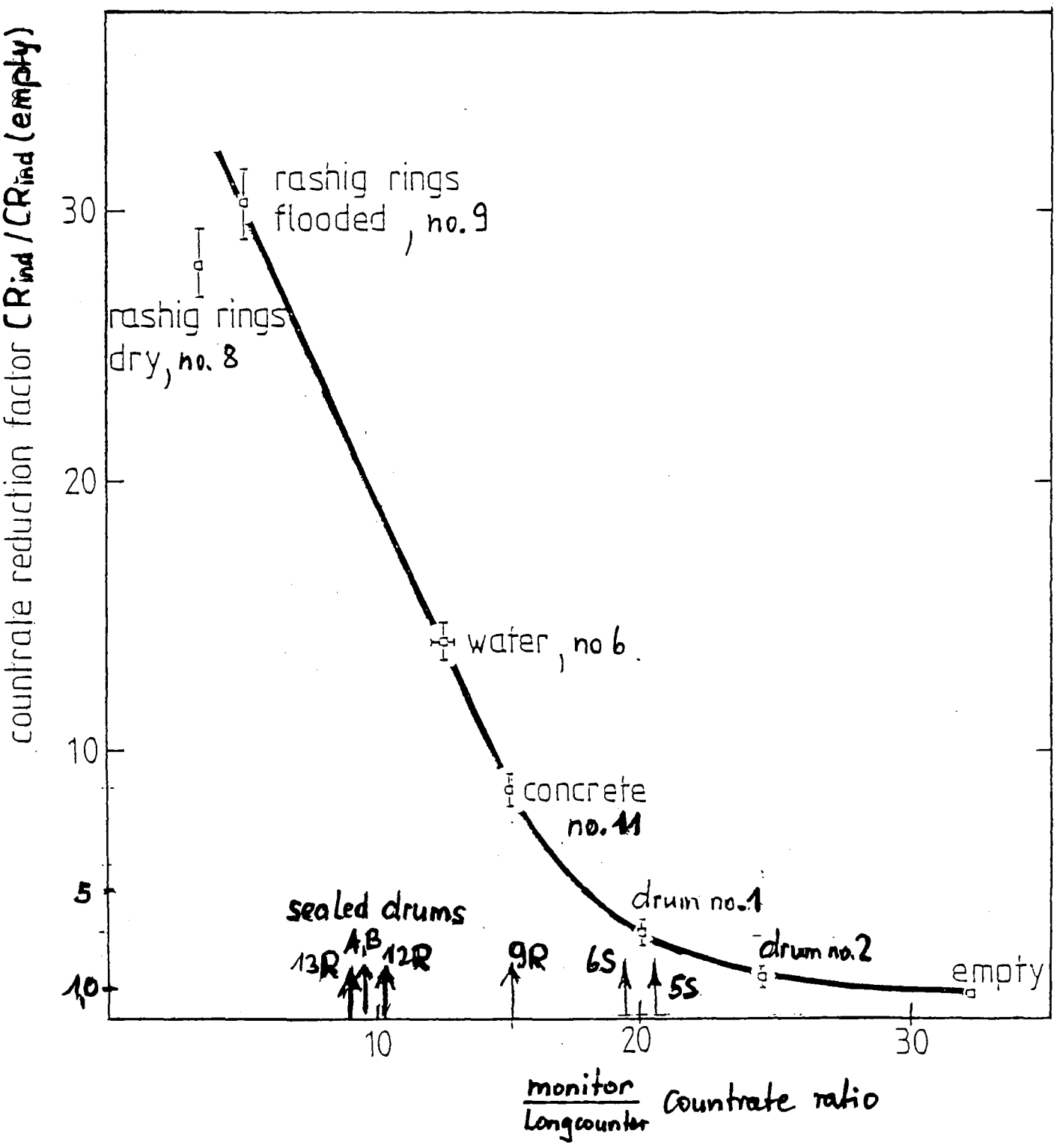

Fig.27

Matrix influence on signal countrate.

Homogeneous Pu distribution. Countrate ratios for the sealed 220 l drums are indicated.

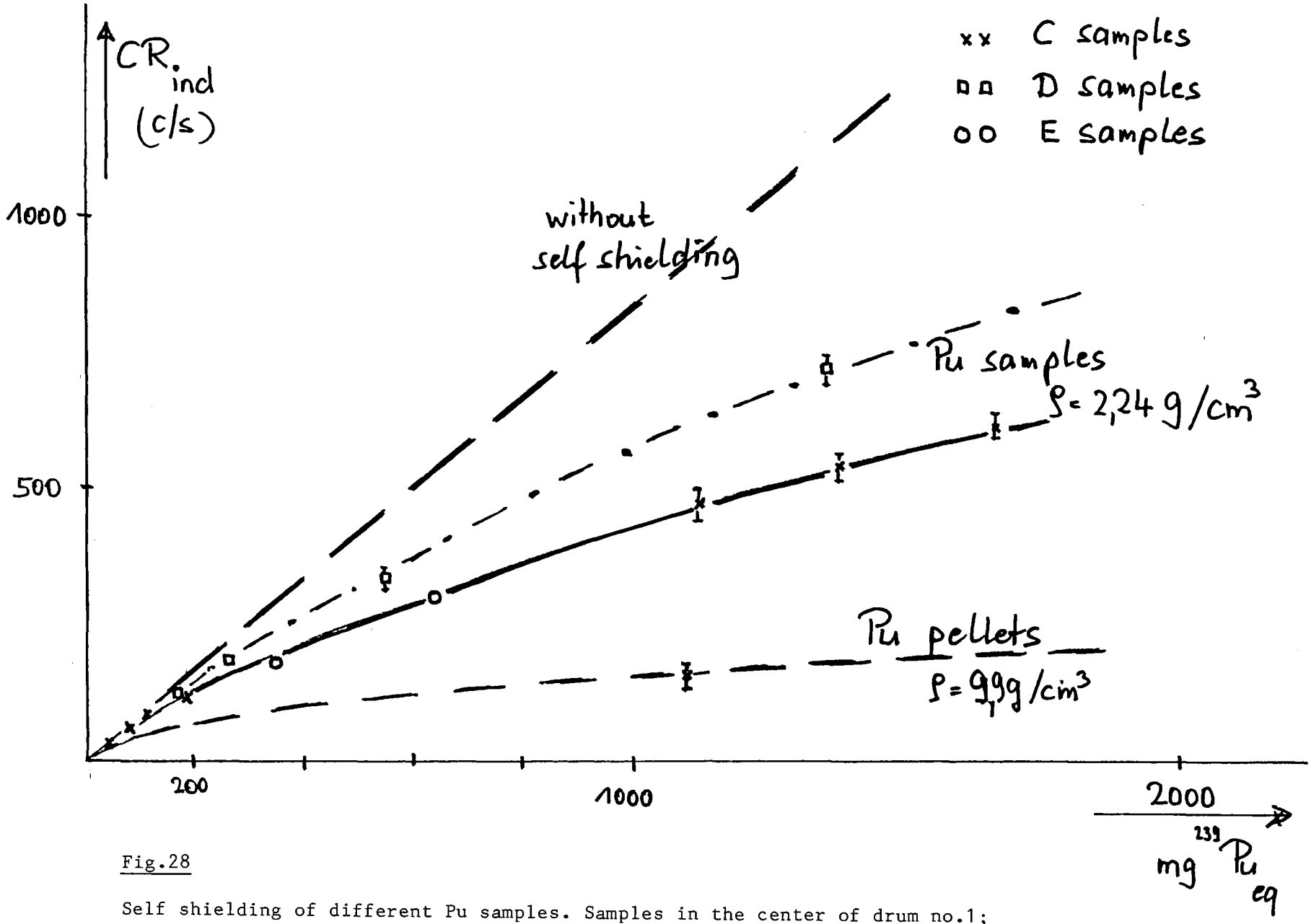

Fig.28

Self shielding of different Pu samples. Samples in the center of drum no.1; n-source rate 2,2 10^{11} n/s.

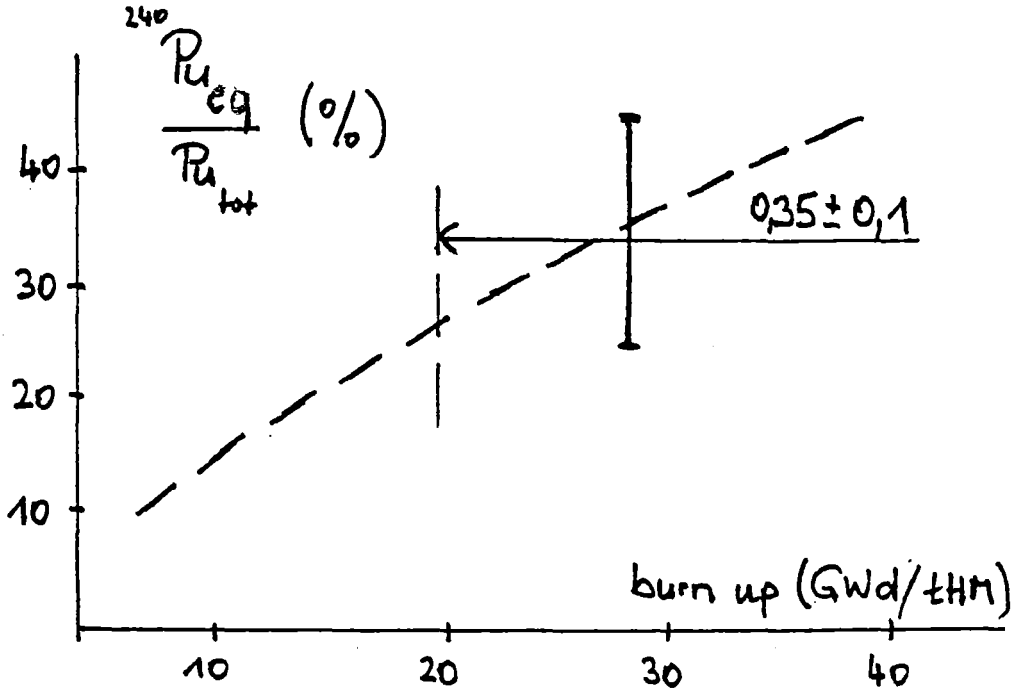

Fig.29

Fraction of $^{240}Pu_{eq}$ and dependence on burn up for LWR fuel.

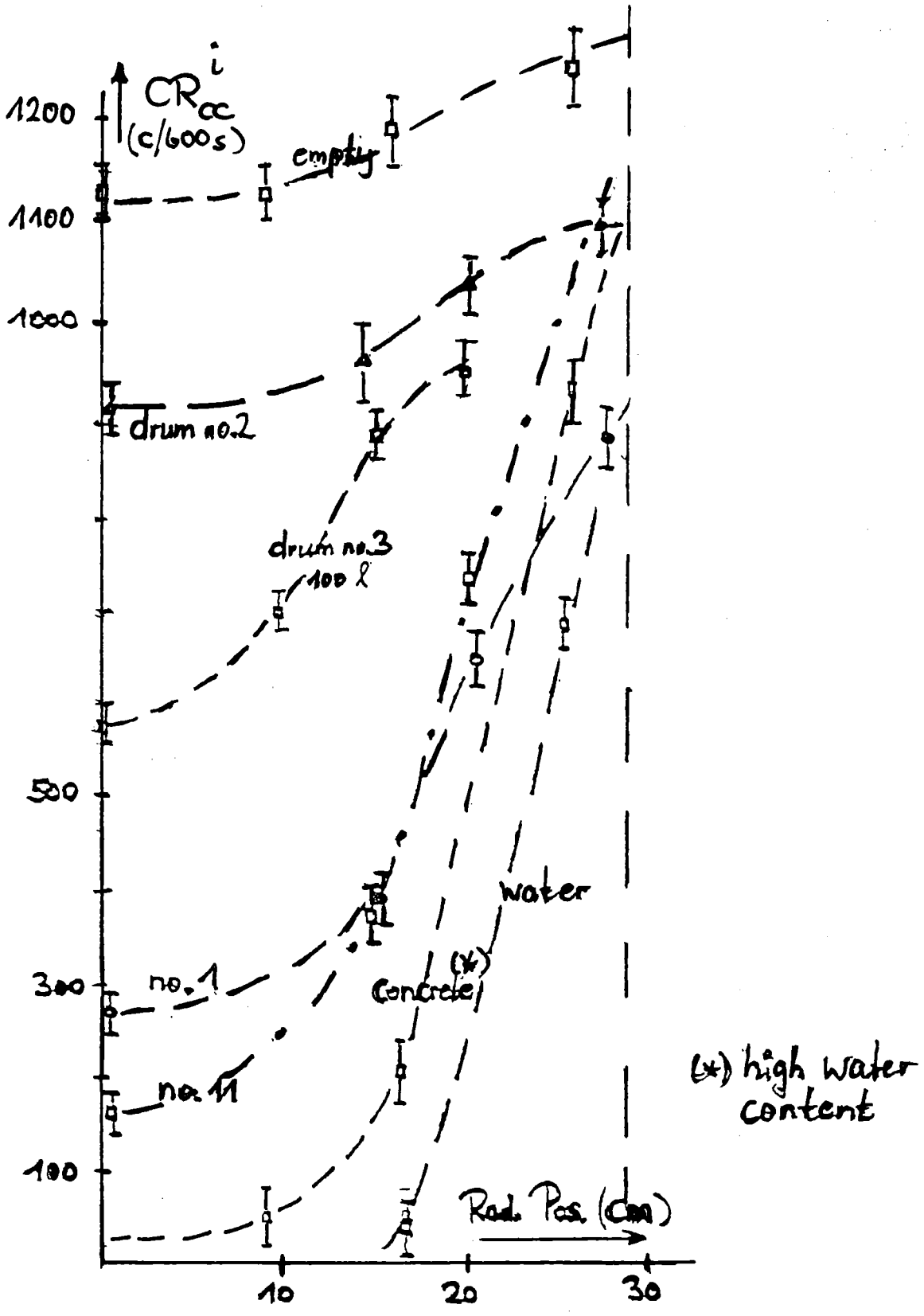

Fig.30

Coincidence countrate for the inner counter layer. Pu sample 269,5 mg $^{240}Pu_{eq}$. Sample at half height.

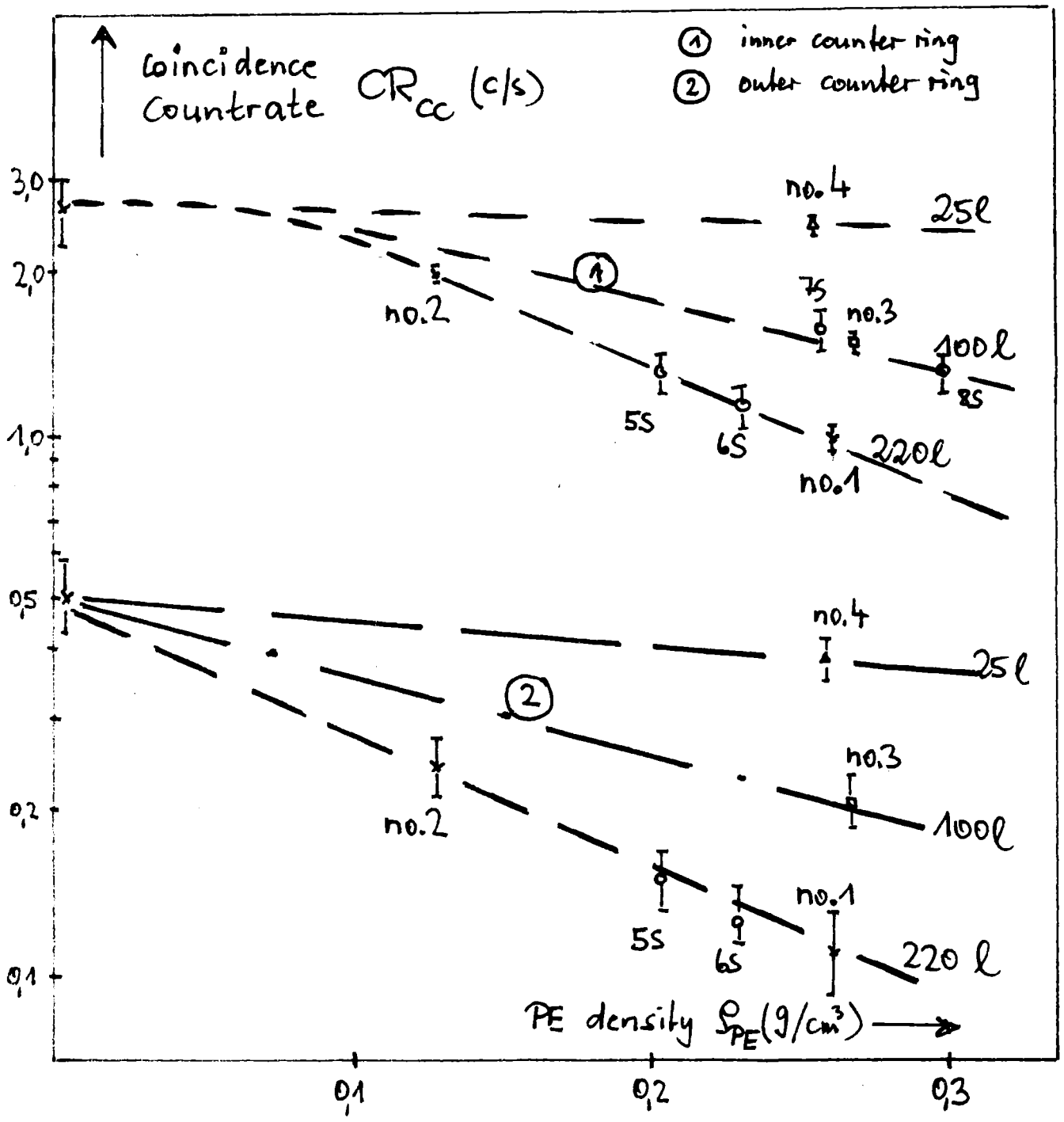

Fig.31

Coincidence countrate versus matrix density. Homogeneous sample distribution, 383 mg $^{240}Pu_{eq}$.

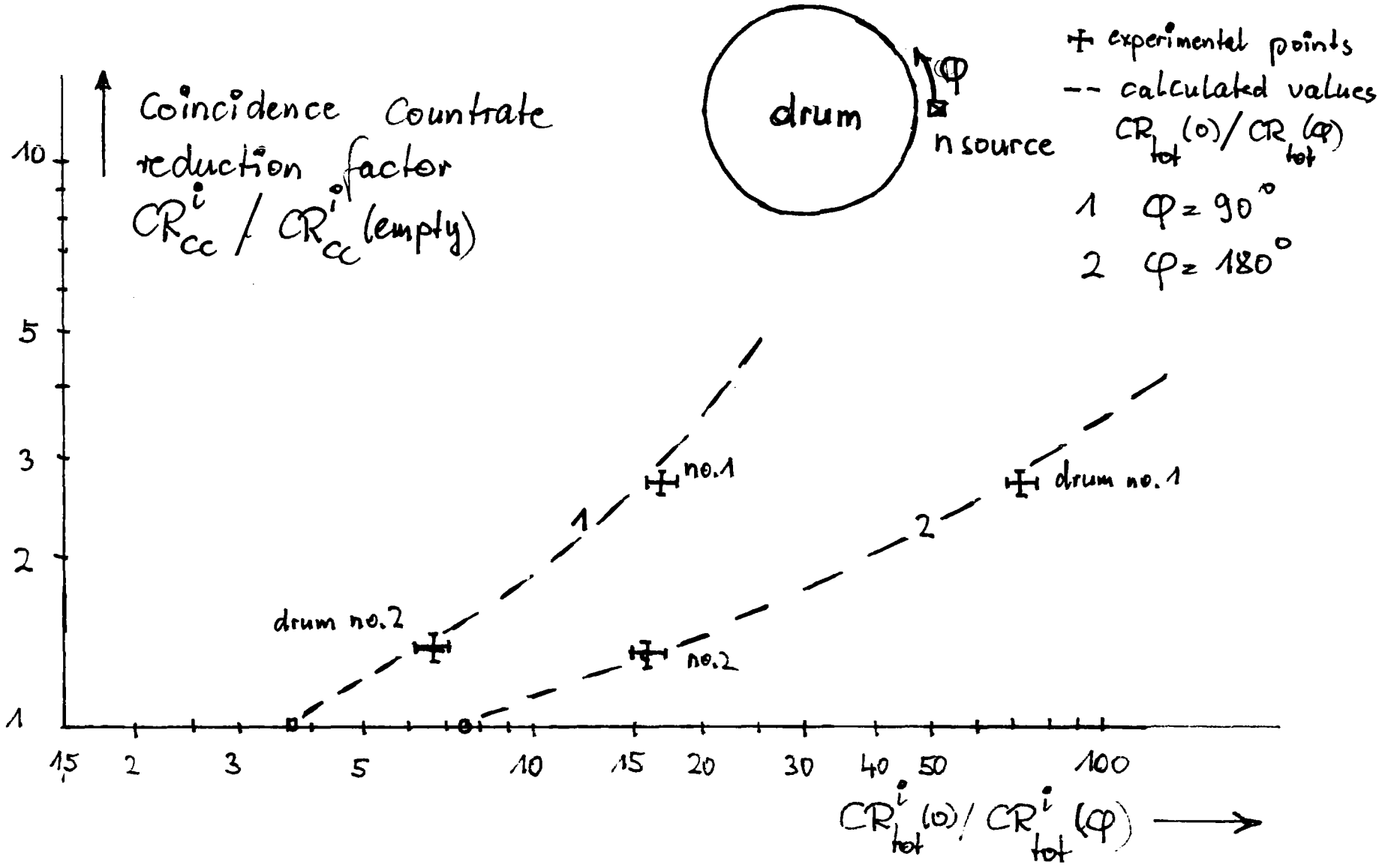

Fig.32

Coincidence countrate reduction factor for homogeneous Pu distribution as function of the totals countrate ratio for hydrogeneous matrix materials. Inner counter layer.